People's Democratic Republic of Algeria
Ministry of Higher Education and Scientific Research

University of Hamma Lakhdar – El Oued

Faculty of Technology

Department of Hydraulics and Civil Engineering

MASTER'S THESIS

To obtain the Degree of Master

Field: Civil Engineering
Option: Materials in Civil Engineering

Structural Study and Design of a Mixed Sports Complex (Steel Structure and Reinforced Concrete) — El Alia, Hadjira, Wilaya of Touggourt

Realized by:

Ahmed Yacine Daikha

Oussama Zerroud

Under supervision of:

Dr. Abdel Aziz Logbi

Academic Year 2025/2026

بسم الله الرحمن الرحيم

Acknowledgments

We praise Allah with abundant, good, and blessed praise for His great gifts and favor upon us, for granting us the success to complete this academic work. We ask the Almighty that it may be of benefit to others. Our hearts overflow with gratitude, and we are honored to commend those who paved the way for this work, offering their support and enlightening our vision with sincere mentorship and true leadership. We extend our deepest thanks to our esteemed professor: Logbi Abdel Aziz, for graciously accepting the supervision of this thesis, and for his continuous support and tireless efforts throughout the entire journey.

We also extend our profound thanks and sincere gratitude to the honorable members of the Examination Committee for graciously accepting to discuss, evaluate, and enrich this thesis with their valuable insights and expertise. We would also like to express our sincere gratitude to ALBENAA for their cooperation and for giving us the opportunity to conduct this field study within the company. We greatly appreciate the facilities, support, and information they provided, which significantly contributed to the successful completion of this work. We wish them continued success and prosperity in all their professional endeavors.

Finally, we extend our heartfelt thanks to everyone who lent a helping hand and contributed, directly or indirectly, to the completion of this academic work.

Dedication

In the Name of Allah, the Most Gracious, the Most s 9e praise is due to Allah, who granted me the strength and guidance to complete this work and helped me overcome the challenges and difficulties along the way.I dedicate this humble work to the dearest people in my life, my beloved parents, who have always been my source of strength and support. Their sacrifices, encouragement, and unconditional love have been the foundation of every achievement in my journey. May Allah bless them with good health, happiness, and abundant rewards.I also dedicate this work to everyone who offered a helping hand, a word of encouragement, or a sincere prayer, and who contributed directly or indirectly to the completion of this work, I express my deepest gratitude.Finally, I dedicate this achievement to myself, in recognition of the effort, patience, and determination invested throughout the years of study. I pray that this success marks the beginning of a future filled with greater accomplishments and continued success.

Abstract

This work presents a structural study of a sports complex located in El Alia, Hadjira, Wilaya of Touggourt, Algeria, carried out as part of a Master's final year project. The complex consists of two main structural systems: a steel structure forming the main sports hall (30.40 m × 21.00 m, height 9.098 m) and two reinforced concrete blocks accommodating changing rooms (Blocks A and B, height 3.23 m). The study covers the structural presentation of the project, seismic site classification according to RPA 2024 (Zone I, A = 0.07, soil category S3), load evaluation for both structural systems using appropriate load transfer methodology, and preliminary dimensioning of structural elements including beams, slabs, and columns in conformity with BAEL91 and Algerian steel structure design rules. Column cross-sections of 30 × 30 cm were adopted for the reinforced concrete blocks, and 40 × 70 cm for the sports hall columns, both verified under the governing combined load cases.

Keywords: Sports hall, steel structure, reinforced concrete, RPA 2024, BAEL 91, load evaluation, preliminary dimensioning, Touggourt.

ملخص

يتناول هذا العمل الدراسة الإنشائية لمجمع رياضي يقع بمنطقة العالية، الحجيرة، ولاية تقرت، وذلك في إطار مشروع التخرج لنيل شهادة الماستر في الهندسة المدنية. يتكون المجمع من منظومتين إنشائيتين: هيكل فولاذي يشكّل قاعة الرياضة الرئيسية بأبعاد 30.40 م × 21.00 م وارتفاع 9.098 م، وكتلتان من الخرسانة المسلحة مخصصتان لغرف تغيير الملابس بارتفاع 3.23 م. تشمل الدراسة تقديم المشروع والتصنيف الزلزالي للموقع وفق RPA 2024 (المنطقة I، A = 0.07، تربة من الصنف S3)، وتقييم الأحمال وفق منهجية نقل الأحمال، والتحديد المسبق لأبعاد العناصر الإنشائية وفق BAEL91 وقواعد تصميم المنشآت الفولاذية. تم اعتماد قسم 30 × 30 سم للأعمدة الخرسانية في الكتلتين A وB، وقسم 40 × 70 سم لأعمدة قاعة الرياضة، مع التحقق من صحة هذه الأقسام تحت مختلف توليفات الأحمال المعتمدة.

الكلمات المفتاحية: قاعة رياضية، هيكل فولاذي، خرسانة مسلحة، BAEL91، RPA 2024، نقل الأحمال، تحديد مسبق للأبعاد، تقرت.

Résumé

Ce travail présente une étude de structure d'un complexe sportif implanté à El Alia, Hadjira, Wilaya de Touggourt, réalisé dans le cadre d'un projet de fin d'études Master. Le complexe comprend deux systèmes structuraux distincts : une structure métallique constituant la salle omnisports principale (30,40 m × 21,00 m, hauteur 9,098 m) et deux blocs en béton armé abritant les vestiaires (Blocs A et B, hauteur 3,23 m). L'étude couvre la présentation du projet, le classement sismique du site selon RPA 2024 (Zone I, A = 0,07, catégorie de sol S3), l'évaluation des charges pour les deux systèmes structuraux selon la méthode de descente des charges, et le prédimensionnement des éléments structuraux (poutres, dalles et poteaux) conformément aux règles BAEL91 et aux règles de calcul des structures métalliques. Des sections de poteaux de 30 × 30 cm ont été retenues pour les blocs en béton armé, et de 40 × 70 cm pour les poteaux de la salle sportive, vérifiées sous les combinaisons d'actions appropriées.

Mots clés: Salle de sport, structure métallique, béton armé, RPA 2024, BAEL91, descente des charges, prédimensionnement, Touggourt.

Table of Contents

List of Figures

List of Tables

General Introduction

Project Background

The construction sector has undergone significant transformations in recent decades, driven by the growing demand for sports facilities that have become an essential component of modern communities' social and public health infrastructure. In Algeria, the development of such facilities requires careful structural design that combines the use of modern materials with strict safety requirements in accordance with national standards and regulations.

This work was carried out as part of a Master's final year project in Civil Engineering, assigned by the design office "El Binaa". The project involves the structural study of a sports complex intended to accommodate various sporting activities, located in El Alia, Hadjira, Wilaya of Touggourt. The complex brings together two distinct structural systems: a reinforced concrete structure housing the changing rooms, and a steel structure forming the main sports hall with a large unobstructed interior space.

Problem

The main challenge of this work lies in how to design a mixed structural facility—combining a steel frame system and a reinforced concrete system—in full compliance with Algerian design codes (RPA 2024, BAEL91), while ensuring the safe behavior of all structural elements under permanent, live, wind, and seismic loads, and verifying the integrity of foundations for a site located in a defined seismic zone.

Proposed Solutions

This study aims to carry out a comprehensive structural analysis and design of the sports complex, covering the following objectives:

- Presenting the project and defining its structural systems;
- Evaluating all loads acting on the structure;
- Performing preliminary dimensioning of structural elements;
- Conducting a full seismic study for the reinforced concrete blocks in accordance with RPA 2024;
- Calculating and verifying all structural elements including reinforced concrete columns, beams, steel members, and connections;
- Designing and verifying the foundations;
- Using recognized engineering software for modeling, analysis, and verification purposes.

Document Plan

This thesis is organized into two main parts comprising seven chapters.

Part I — Bibliographic Study

Part I contains one chapter:

- **Chapter 1 — Steel Hangars and Industrial Buildings**: reviews the general concepts related to steel hangars and industrial buildings, covering their historical development, structural characteristics, main components, environmental and economic advantages, and various fields of application.

Part II — Practical Study

Part II constitutes the applied study and is organized into six chapters:

- **Chapter 2 — Project Presentation**: presents the project, defining its location (El Alia, Hadjira, Wilaya of Touggourt), seismic site classification (Zone I according to RPA 2024), structural dimensions of all blocks, applicable regulations and standards, and the software used.
- **Chapter 3 — Load Evaluation**: addresses the evaluation of permanent and live loads for the reinforced concrete blocks (Blocks A and B) and the steel sports hall block,

using the appropriate load transfer methodology and establishing the governing design load combinations.

- **Chapter 4 — Preliminary Dimensioning**: covers the preliminary sizing of all structural elements including beams, hollow block slabs, and columns for the reinforced concrete blocks and the sports hall block, in conformity with BAEL91 and Algerian steel structure design rules.
- **Chapter 5 — Seismic Study**: presents the seismic analysis of Blocks A and B in accordance with RPA 2024, including quality factor calculation, global behavior factor, seismic force calculation by the equivalent static method, and verification of dynamic behavior, overall stability, and P–Δ effects.
- **Chapter 6 — Calculation and Verification of Structural Elements**: details the calculation and verification of all structural elements, covering reinforced concrete columns and beams (BAEL91), as well as the dimensioning and verification of steel members and connections under ultimate limit state (ULS) conditions.
- **Chapter 7 — Foundation Calculation and Verification**: covers the design and verification of foundations for all blocks, including geotechnical parameters, footing design for Blocks A and B (Footing S02), the sports hall block (Footing S01), and the construction joint footing (Footing SJ02). “‘

Part I

Bibliographic Study

Chapter 1

Steel Hangars and Industrial Buildings

1.1 Introduction

Steel hangars and industrial buildings play an important role in modern construction and in many industrial sectors. Due to their structural strength, flexibility, and ability to cover large spaces, these buildings are widely used for storage, production, logistics, and maintenance activities. Unlike traditional construction materials, steel allows the creation of large spans with fewer structural supports, providing open interior spaces that are highly suitable for industrial operations.

Over the years, the development of steel construction techniques has significantly improved the efficiency and functionality of industrial buildings. Today, steel hangars represent one of the most practical solutions for large-scale buildings because they combine structural reliability, rapid construction, and adaptability to different operational requirements.

1.2 Historical Development of Hangars

The concept of hangars first appeared at the end of the nineteenth century. At that time, these structures were relatively small and mainly used in the agricultural sector. Farmers used them to store tools, machinery, and harvested products. The early hangars were simple structures constructed with locally available materials such as wood and stone. Their main purpose was to provide protection against weather conditions rather than to serve complex industrial functions.

Although the construction techniques were basic and did not require advanced architectural knowledge, these buildings were efficient and economical. As agriculture developed and mechanization increased, the need for larger storage spaces also grew. Hangars gradually became an essential part of agricultural infrastructure.

During the twentieth century, especially after the Second World War, the role of hangars expanded significantly. Industrial development and technological progress led to the introduction of steel structures. Steel frames made it possible to construct larger and more durable buildings capable of supporting heavy equipment and accommodating larger working areas.

As a result, the use of hangars extended beyond agriculture and became common in many industrial sectors, including manufacturing, transportation, and logistics. These structures later evolved into large warehouses and industrial facilities designed to support modern production and distribution systems.

1.3 Structural Characteristics of Steel Hangars

Steel hangars have several structural characteristics that distinguish them from traditional buildings. One of the most important properties of steel is its high mechanical strength. Steel can resist both tension and compression forces, which makes it suitable for large structural elements such as beams, columns, and trusses. This strength allows engineers to design lightweight structures capable of supporting significant loads [1].

Another characteristic is the relatively low weight of steel compared to other construction materials such as reinforced concrete. Because of this reduced weight, the loads transferred to the foundations are lower, which can reduce the overall construction cost.

Steel structures also allow large spans without intermediate columns. This is particularly beneficial for industrial buildings where large open spaces are required for machinery, storage systems, or transportation equipment. In addition, steel structures are usually fabricated in factories and then transported to the construction site for assembly. This prefabrication process improves construction quality and significantly reduces the time required for installation [2, 3].

1.4 Main Structural Components of Steel Hangars

A typical steel hangar consists of several structural elements that ensure stability and load transfer:

- **Columns** are vertical members that transmit loads from the roof and beams to the foundations. They play a fundamental role in supporting the overall structure.
- **Beams and roof trusses** form the main framework of the roof. These elements are responsible for carrying permanent loads such as the weight of the roof covering as well as variable loads including snow and wind.

- **Purlins** are secondary structural elements placed on the main beams or trusses. Their role is to support the roof cladding and distribute loads to the main structural frame.
- **Bracing systems** are used to ensure the stability of the structure against horizontal forces such as wind or seismic loads. They help maintain the structural integrity of the building.
- **Roof cladding and wall panels** protect the building from environmental conditions and contribute to thermal and weather insulation.

1.5 Advantages of Steel Industrial Buildings

Steel hangars offer several advantages that make them highly suitable for industrial applications. One major advantage is the speed of construction. Since many structural components are prefabricated, the assembly process on site is relatively fast. This reduces construction time and allows the building to become operational more quickly.

Another advantage is flexibility in design. Steel structures can easily be adapted to meet the specific needs of different industries. They can be designed for storage facilities, production halls, maintenance workshops, or logistics centers.

Steel buildings are also highly adaptable. If the operational requirements change, the structure can often be extended or modified without major reconstruction. This flexibility is particularly valuable for industries that may expand in the future.

Durability is another important benefit. Steel structures can resist harsh environmental conditions and heavy loads, ensuring a long service life with relatively low maintenance requirements.

1.6 Environmental and Energy Considerations

In recent years, environmental considerations have become increasingly important in construction projects. Steel structures offer several environmental advantages compared to other building systems.

Steel is a recyclable material. After a building reaches the end of its service life, the steel elements can be dismantled and recycled without losing their original mechanical properties. This contributes to the reduction of construction waste and promotes sustainable building practices.

Moreover, steel structures allow the integration of large openings and glazed surfaces, which improves natural lighting inside the building. Increased natural light reduces the need for artificial lighting and contributes to energy savings.

Proper insulation systems can also improve the thermal performance of steel buildings, reducing energy consumption for heating and cooling. As a result, modern steel hangars can achieve high levels of energy efficiency while maintaining their structural performance [4, 5].

1.7 Applications of Steel Hangars

Steel hangars are widely used in various industrial sectors due to their versatility. In the aviation industry, hangars are essential for aircraft storage, maintenance, and repair. These structures provide large unobstructed spaces that allow technicians to work efficiently around aircraft. In the logistics sector, steel warehouses are commonly used for storage and distribution of goods. Their flexible layout allows the installation of shelving systems, loading docks, and efficient circulation areas for transportation equipment. In manufacturing industries, steel buildings are used as production facilities where large machinery and assembly lines require spacious and adaptable working environments. Steel hangars are also used for agricultural storage, industrial workshops, and sometimes sports facilities where large, covered areas are required. A comparable structural configuration — combining a steel-framed sports hall with reinforced concrete changing rooms — was studied by Ouahmed and Mahmoudi for a sports complex in Tlemcen, confirming the suitability of this hybrid approach for Algerian climatic and seismic conditions [1].

1.8 Conclusion

Steel hangars and industrial buildings represent an efficient and reliable solution for large-scale construction projects. Their structural strength, flexibility, and rapid construction make them particularly suitable for industrial and logistical applications.

The evolution of steel construction has transformed traditional storage structures into modern industrial facilities capable of meeting complex operational requirements. In addition to their functional advantages, steel buildings also contribute to sustainable construction through recyclability and improved energy performance.

For these reasons, steel structures continue to play a major role in the development of modern industrial infrastructure.

Part II

Practical Study

CHAPTER 2

Project Presentation

2.1 PROJECT PRESENTATION

As part of our final year project, we were assigned by the design office **"El Binaa"** to study a sports hall intended to accommodate various sporting activities. Such facilities generally require large, unobstructed interior spaces in order to ensure proper functionality and ease of use.

The project consists of two main parts with different structural systems. The first part corresponds to the main sports hall, which is designed using a **steel structural system** with dimensions of 30.40 m × 21.00 m and a total height of 9.098 m. This structural solution makes it possible to cover a large span without intermediate columns.

The second part is located at the front façade of the building and consists of a **reinforced concrete structure** measuring 21.00 m × 10.60 m with a height of 3.23 m. This section accommodates the auxiliary spaces required for the operation of the sports facility.

The main objective of this study is to analyze the structural behavior of the building, determine the loads acting on the structure, and design the structural elements in accordance with the applicable standards and regulations in civil engineering RPA24.

2.1.1 Project Objective

The project aims to **construct a sports complex including a sports hall and changing rooms**, intended to accommodate various sporting activities. The main objective is to provide a **functional, safe, and suitable space for sports practice**, while complying with construction and safety standards.

2.1.2 Project location

EL ALIA EL HADJIRA W. TOUGGOURT.

2.1.3 Site classification

According to the RPA 2024 (Algerian Seismic Regulations) [6], the Wilaya of Touggourt is classified in **Zone I**, with a zone acceleration coefficient of A = 0.07, usage group 1B. In accordance with the geotechnical report, the soil has been classified as category S3.

2.1.4 Structure dimensions

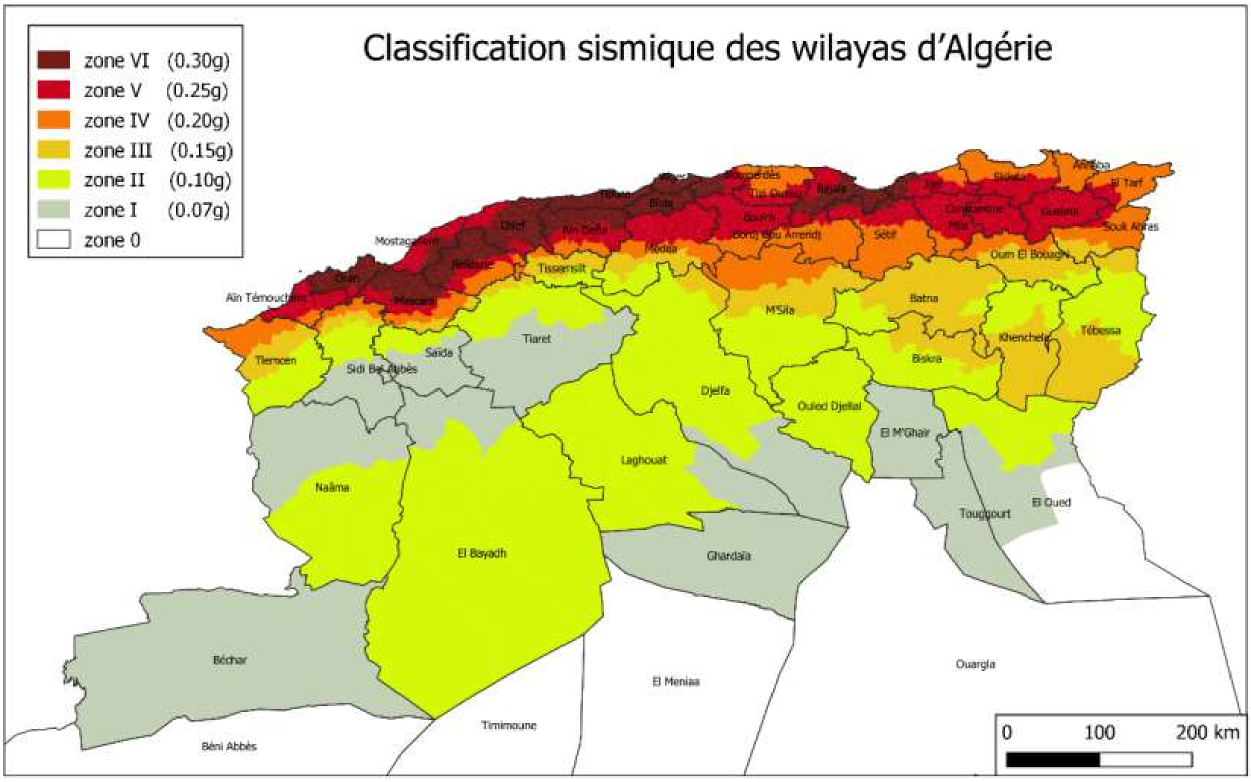

Figure 2.1: Seismic Zoning of Algeria

- Reinforced Concrete Section :
  - Block A: Girls' Sports Changing Room
    - Total building height : 3.23 m
    - Ground floor height : 3.23 m
    - Building length (X) : 14.05 m
    - Building width (Y) : 10.30 m

Figure 2.2: Floor shape block A (m)

    - Building area : 90.425 m^2

  - Block B: Boys' Sports Changing Room:
    - Ground floor height: 3.23 m
    - Total building height: 3.23 m
    - Building length (X): 18.05 m
    - Building width (Y) : 10.30 m
    - Building area : 131.725 m^2

- Steel Structure:
  - Block : Sports Hall
    - Ground floor height: 7.00 m (level of reinforced concrete columns)
    - Total building height: 9.098 m (ridge level)
    - Building length (X) : 30.00 m
    - Building width (Y) : 20.30 m
    - Building area : 609.00 m^2

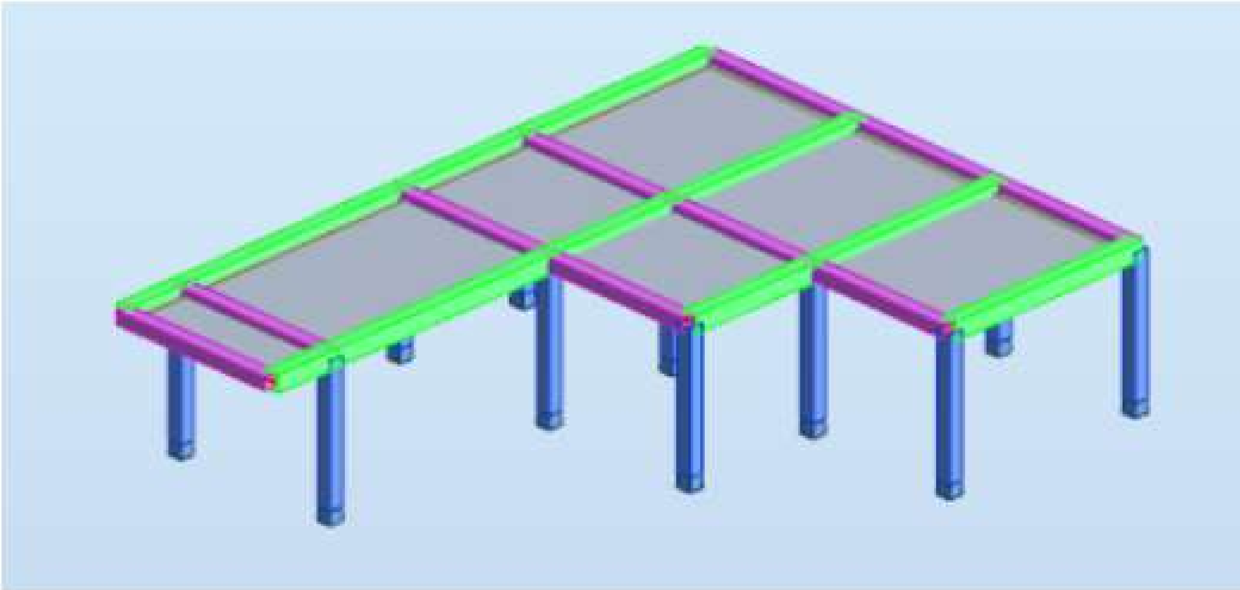

Figure 2.3: 3D VIEW block A

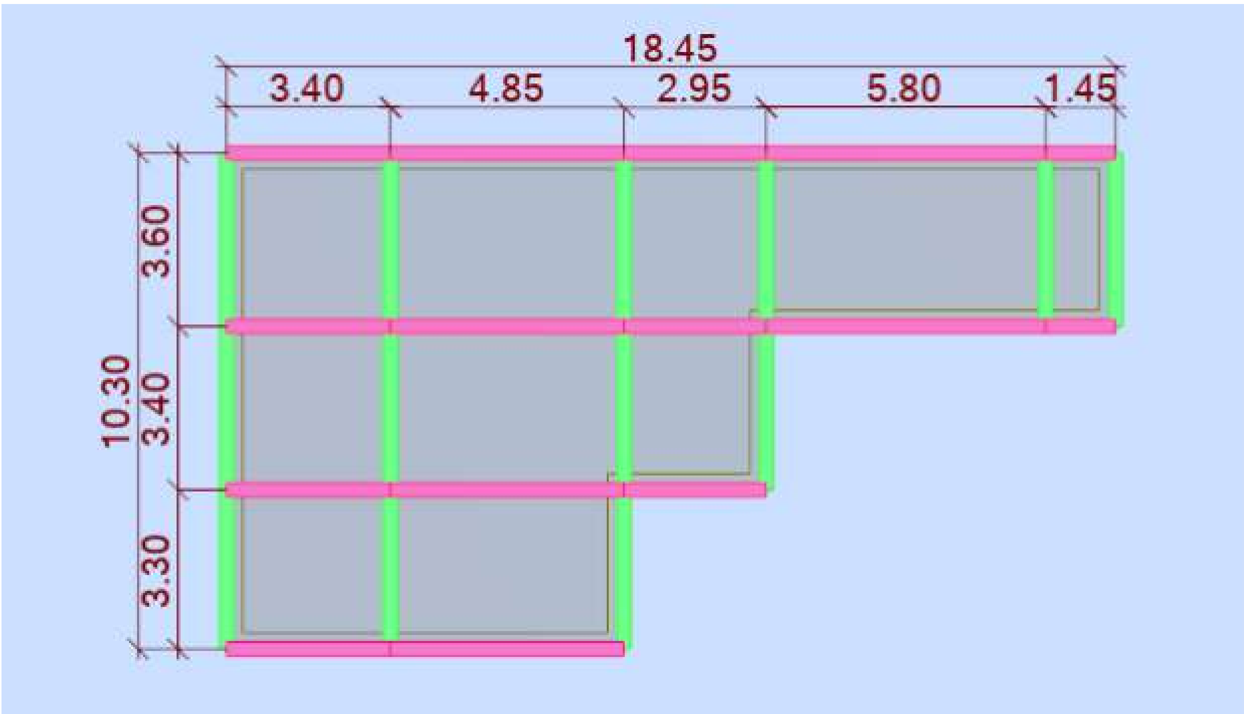

Figure 2.4: Floor shape block B (m)

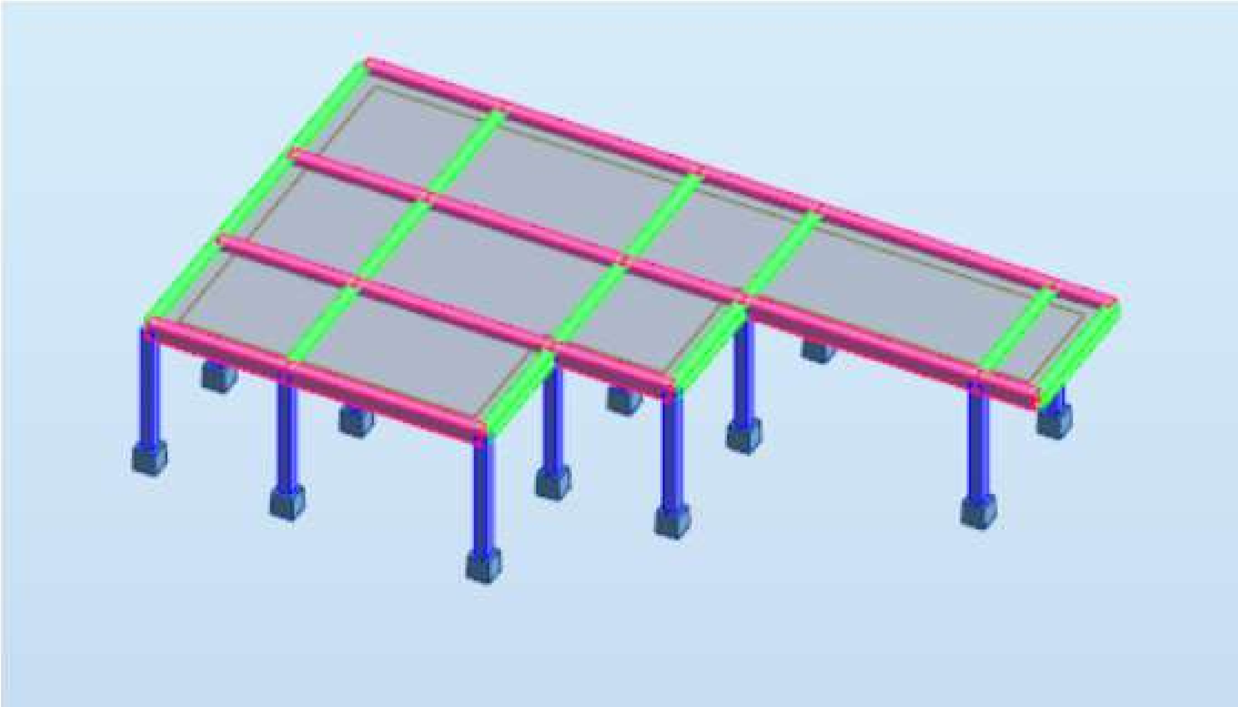

Figure 2.5: 3D VIEW block B

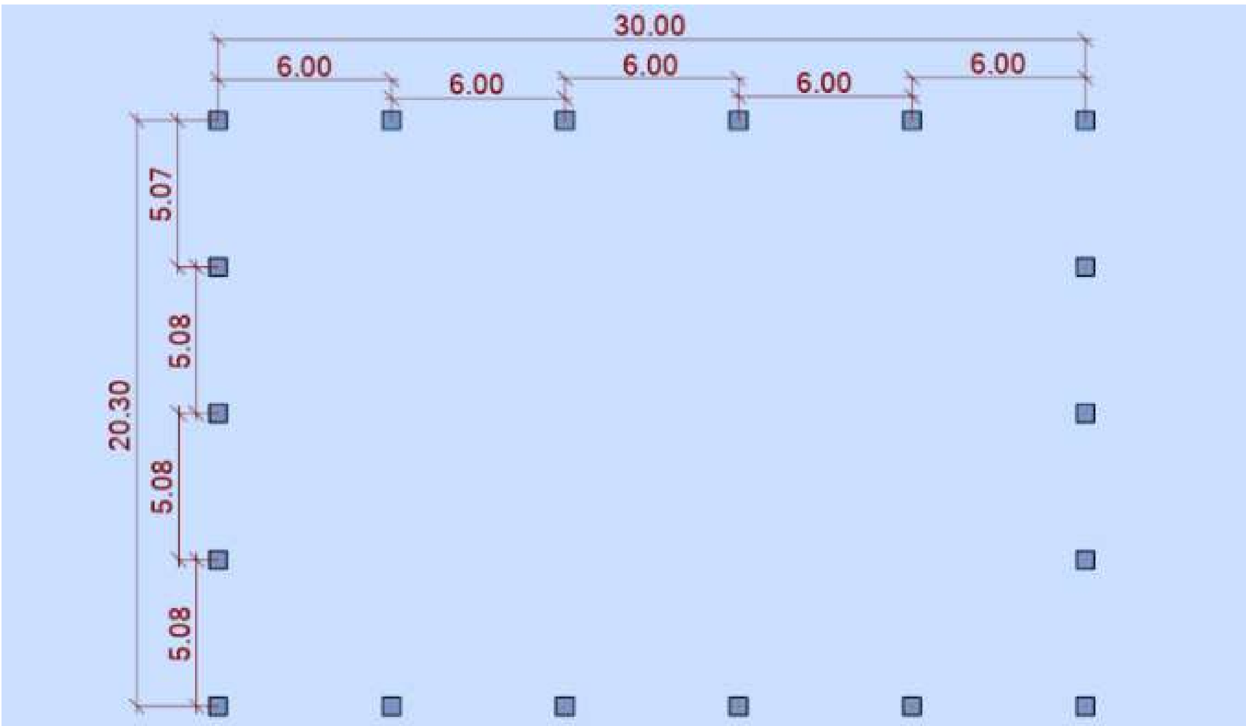

Figure 2.6: Floor shape Sports Hall (m)

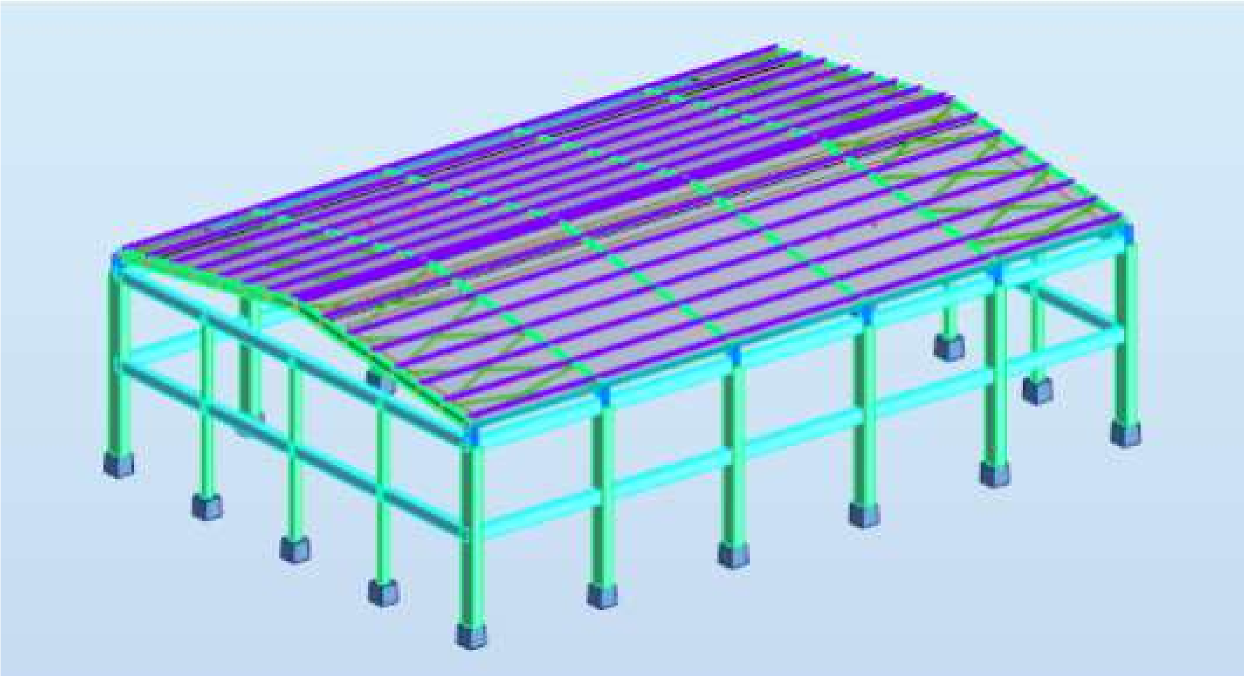

Figure 2.7: 3D VIEW Sports Hall

2.1.5 Study Based on Regulations and Standards

This study is conducted based on the following regulations and standards:

- **Permanent and live loads (**h × f g**)**: For determining the permanent loads and live loads applied to the structure.
- **Snow and wind rules (RNV 2013)**: For determining climatic loads, including the effects of snow and wind.
- **Design and Calculation Rules for Steel Structures (CCM97)**: For verification and sizing of steel structural elements.
- **Eurocode 3 – Design of Steel Structures, Part 1-8 (EN 1993-1-8)**: For verification and sizing of steel connections and assemblies.

2.1.6 Software Used

- Robot Structural Analysis 2024: used for structural analysis and calculations.
- AutoCAD 2021: used for preparing technical drawings and plans.

2.2 STRUCTURAL ELEMENTS

This section describes the structural elements of the sports complex, the materials used, and the load transfer system. The project consists of reinforced concrete columns supporting a metallic roof structure.

2.2.1 Reinforced Concrete Sections

- **Block A (Girls' Changing Room) and Block B (Boys' Changing Room)** are built with reinforced concrete columns, beams, and slabs.
- The RC structure provides **stability for the low-rise auxiliary spaces**, supporting vertical loads from walls and roof, as well as lateral loads such as wind.
- The columns are designed to transfer the loads **directly to the foundation**.

2.2.2 Steel Structure (Sports Hall)

- The main sports hall uses a metallic roof supported by reinforced concrete columns.
- Steel trusses and beams cover the large span, creating a column-free interior ideal for sporting activities.
- Roof loads, including snow and live loads, are transmitted from the metallic structure to the RC columns and then to the foundations.
- This combination ensures strength, durability, and flexibility while meeting all safety and regulatory requirements.

2.3 CALCULATION HYPOTHESES

2.3.1 Concrete

The concrete will be prepared according to a mix design established by the laboratory based on the assumptions of the design office (BET), with fc28= 25MPa for structural elements.

- *fc28 = 25 MPa*: compressive strength
- *ft28 = 2,10 MPa*: tensile strength

The same steel grade was adopted in a multi-storey steel-frame building study conducted at the University of Ouargla under Eurocode 3, where the material properties were verified to be consistent with Algerian standard practice [5].

Ultimate limit state:

$$f_{bu} = \frac{0.85 \times f_{c28}}{\theta \times \gamma_b}$$

$\theta = 1$ (normal situation)
$\theta = 0.85$ (accidental situation)
$\gamma_b = 1.5$ (normal situation)
$\gamma_b = 1.20$ (accidental situation)
$f_{bu} = 14.17$ MPa (normal situation)
$f_{bu} = 20.83$ MPa (accidental situation)

Service limit state:

$$f_{bs} = 0.6 \times f_{c28}$$

$f_{bs} = 15$ MPa

Longitudinal deformation modulus according to the CBA code (Article A.2.1.2.1 and A.2.1.2.2)

$f_{c28} = 25$ MPa
$E_{i28} = 11000\sqrt[3]{f_{c28}}$ (Instantaneous modulus)
$E_{i28} = 32164.195$ MPa
$E_{d28} = 3700\sqrt[3]{f_{c28}}$ (Long-term modulus)
$E_{d28} = 10818.865$ MPa

2.3.2 Steel

Characteristic design strength

- High Bond Reinforcement Steel (FeE500)
  - Internal forces under fundamental load combinations:

$$\sigma_s = \frac{f_e}{\gamma_s} = \frac{500}{1.15} = 434.78 \text{ MPa}$$

  - Internal forces under accidental actions:

$$\sigma_s = \frac{f_e}{\gamma_s} = \frac{500}{1} = 500 \text{ MPa}$$

- The design codes used for structural calculations:
  - Algerian seismic design rules RPA 2024 (h × f g D9HP)
  - Permanent loads & service loads (DTR BC 2.2)
  - BAEL 91 design rules, revised 1999 (DTU P18-702)
  - Design and calculation rules for reinforced concrete structures (CBA 93 – DTR BC 2-41)
- Structural design combinations (superstructure):

Table 2.1: Structural design combinations

Combination	Name	Analysis Type	Comb. Type	Nature of Case
6 (C)	ULS	Linear Combination	ULS	permanent
7 (C)	SLS	Linear Combination	SLS	permanent
8 (C)	G+psiQ	Linear Combination	ACC	permanent
9 (C) (CQC)	Acc.Hor.G+psiQ+Ex+0.3Ey	Linear Combination	ACC	accidental
10 (C) (CQC)	Acc.Hor.G+psiQ+0.3Ex+Ey	Linear Combination	ACC	accidental
11 (C) (CQC)	Acc.Hor.G+psiQ+Ex-0.3Ey	Linear Combination	ACC	accidental
12 (C) (CQC)	Acc.Hor.G+psiQ-Ex+0.3Ey	Linear Combination	ACC	accidental
13 (C) (CQC)	Acc.Hor.G+psiQ-Ex-0.3Ey	Linear Combination	ACC	accidental
14 (C) (CQC)	Acc.Hor.G+psiQ+0.3Ex-Ey	Linear Combination	ACC	accidental
15 (C) (CQC)	Acc.Hor.G+psiQ-0.3Ex-Ey	Linear Combination	ACC	accidental
16 (C) (CQC)	Acc.Hor.G+psiQ-0.3Ex+Ey	Linear Combination	ACC	accidental

The application of loads on the finite element model is illustrated in Appendix A 7.7 for each load case. The appendix figures are direct outputs extracted from Robot Structural Analysis Professional 2024, presented in their original language (French) as generated by the software

Chapter 3

Load Evaluation

3.1 OBJECTIVE OF LOAD EVALUATION

This part of the study aims to identify and evaluate the various loads acting on the structure, whether permanent or variable, in accordance with the applicable standards, particularly RPA 24. It also includes an analysis of the load transfer path through the different structural elements, starting from the steel roof, passing through the secondary and primary members, and reaching the reinforced concrete columns and foundations.

This work also includes a dedicated section for the study of reinforced concrete elements and another for the steel roof, with the objective of ensuring proper load distribution and achieving the required safety and stability conditions in the final structural design.

3.2 LOAD TRANSFER (BLOCK A AND BLOCK B)

Load transfer in Block A and Block B occurs through reinforced concrete elements, where loads move from slabs to beams, then to columns, and finally to the foundations and soil. This path ensures proper load distribution and structural stability.

3.2.1 Permanent and Live Loads for Accessible Terrace Slab (Hollow Block System)

3.2.2 Live load

3.3 LOAD EVALUATION (BLOCK: SPORTS HALL)

The load evaluation of the sports hall is a fundamental step in the structural design process. This section aims to identify and quantify all the loads acting on the steel roof and

Table 3.1: Dead load contributions of the roof slab components

Materials	G **(kN/m^2)**
Reinforced concrete screed (5 cm)	1.25
Gravel 3/8 protective layer (3 cm)	0.51
Thermal insulation in fine sand (12 cm)	2.04
Bastard mortar (3 cm)	0.54
Ribbed slab with cast-in-place joists and concrete hollow blocks, spacing 60 cm center-to-center, with compression topping slab (16+4)	2.80
Cement mortar plaster (2 cm)	0.36
Total	$G = 7.50$

Table 3.2: Live loads for structural elements

Element	Q **(kN/m^2)**
Inaccessible roof terrace	1.00
Parapet wall	2.00
Double-walled partition	2.80

the supporting reinforced concrete elements.

The sports hall is characterized by a large-span steel structure supported by reinforced concrete columns, which requires careful assessment of both permanent loads (dead loads) and variable loads (live loads, wind, etc.). These loads are transmitted from the roof covering to the secondary elements, then to the main structural system, and finally to the foundations.

This analysis ensures the proper distribution of loads and guarantees the safety, stability, and serviceability of the structure in accordance with the applicable standards, particularly **RNV 2013**.

3.3.1 Structural elements of the structure

The sections of the structural elements are organized into distinct families. Each family plays a well-defined role in the overall behavior of the structure and is governed by specific regulatory parameters during the design process.

3.3.1.1 Structural Families

The steel structure in our project consists of 6 families — each one has a specific role:

Table 3.3: Classification of Structural Components of the Steel

Family	Name	Section	Remarks
1	Columns	HEA400	Self-stable frame structure
2	Beams	IPE400	Self-stable frame structure
3	Purlins	HEA140	Frame bracing
4	Roof purlins	IPE140	Roof support
5	Cladding rail	UPN100	Cladding support
6	Bracings	CAE60×6	Roof bracing

- **Columns HEA400**: These are the backbone of the structure. They stand on the existing concrete columns and raise the roof to a height of 7 meters. The HEA400 section means an H-shaped profile with a width of 40 cm — a heavy section because it carries all roof loads.
- **Rafters IPE400**: These are the inclined members forming the triangular shape of the roof. They extend from the top of one column to the top of the opposite column across a span of 20.30 m — therefore requiring a strong section.
- **Longitudinal beam HEA140 (Eave beam / Sablière)**: It runs along the length of the building at the top, connecting the frames together and distributing loads between them. Without it, each frame would act independently.
- **Purlins IPE140**: These are placed perpendicular to the rafters. They directly support the sandwich panels. The smaller the spacing between them, the stronger the roof.
- **Wall girts UPN100 (Cladding rails)**: Similar to purlins but for vertical walls — they support wall panels and distribute wind pressure to the columns.
- **Bracing CAE60×6**: Steel bars arranged in an X-shape in the roof. Their sole role is to prevent horizontal sway of the structure under wind or seismic effects.

The use of HEA and IPE profiles in steel industrial buildings is well established in Algerian practice; similar section families were employed in a large-span hangar study carried out at ENSTP, confirming their structural adequacy under comparable loading conditions [3].

3.3.2 Structural Design

The structural behavior of a steel frame is governed primarily by the nature of the connections between its members and by the lateral stability system adopted to resist horizontal actions. Accordingly, all connections were carefully defined and modeled within Robot Structural Analysis, and an appropriate bracing system was selected and implemented.

Furthermore, the influence of wall openings on wind pressure distribution was taken into account in accordance with RNV 2013, to ensure both the accuracy and the safety of the results obtained.

- **Modeling of Connections in Robot Structural Analysis**
  - Column Bases = Pinned Supports (Articulation): The steel columns are placed on existing concrete columns. However, the connection is modeled as a pinned support, meaning the column is free to rotate at its base and does not transfer bending moments to the foundation. This assumption simplifies the analysis and generally leads to safer design results.
  - - Column–Rafter Joint = Rigid Connection (Encastrement): At the junction between the column and the rafter, the connection is considered fully rigid. This allows the transfer of bending moments between elements, enabling the frame to behave as a rigid portal frame, which improves its resistance to horizontal loads.
  - Haunches (Jarrets) at Connections: Triangular stiffening elements (haunches) are introduced at the column–rafter connections. Their role is to reduce stress concentrations at this critical zone and enhance structural performance.
- **Structural Stability System** The stability of the structure is ensured in two directions:
  - In the X Direction (Transverse – Portal Frame Direction): Stability is provided by the rigid frames themselves. The rigid connections prevent lateral collapse.
  - In the Y Direction (Longitudinal – Along the Building): Stability is ensured by X-bracing (contreventement) in the roof, which resists longitudinal forces and transfers them to the columns.

3.3.2.1 Important Note (RNV 2013 – Wind Classification)

The building is considered enclosed since the openings (doors and windows) represent less than 30% of each façade area, in accordance with RNV 2013 requirements. If this percentage exceeds 30%, internal pressure coefficients will change, resulting in increased wind loads on the structure.

3.3.3 Load Calculation

- **Permanent Loads (G)**
  - Self-weight of all structural steel members constituting the frame.

- Roofing system composed of sandwich panels with a thickness of 40 mm and a distributed load of $0.18\ \text{kN/m}^2$.

- **Live Loads (Q)**
  - Maintenance load for inaccessible roofs equal to 1 kN, applied at one-third and two-thirds of the span length of the roof purlins.

- **Sand Load (D)**
  - Location: Touggourt City.
  - Sand zone: Zone D.
  - Altitude: $H = 80$ m (average altitude of the municipality).
  - Roof slope: $\alpha = 7.85°$.
  - Sand load: To be determined according to the applicable sand loading code.

Table 3.4: Sand Load Values by Wilaya

Wilaya	Commune	Uniformly Distributed Load (N/m^2)	q_1 (kN/m)	q_2 (kN/m)
Ouargla	Ouargla / Touggourt	0.20	0.30	0.40
Ouargla	Rest of the Wilaya	0.25	0.30	0.50

- **Wind Loads (W) Wind Loads (W)**
  - Location: Touggourt City.
  - Wind zone: Zone III.
  - Reference pressure: $q_{\text{ref}} = 50\ \text{kN/m}^2$.
  - Terrain category: II.
  - Reference height: $Z_j = 9.098$ m.
  - Peak pressure: q_p.

Table 3.5: Sand Load Values by Wilaya

Element	Z_j (m)	C_t	C_r	I_v	C_e	q_p (kN/m^2)
Roof	9.1	1.00	0.99	0.192	2.29	114.6

  - Aerodynamic Wind Pressure (W_{z_j}): Wind actions are evaluated for both the roof surfaces and the vertical walls of the structure.
  - Wind parallel to the ridge (Gable End)
    Pignon

Element	E	d	b	H	$2H$
Value	18.2	30	20.3	9.1	18.2

$\theta = 90°$	$e/4$	$e/2$	$e/10$
	4.55	9.1	1.82

- Wind Perpendicular to the Ridge Line (Long Span)
  Longpan

e	d	b	H	$2H$
15.4	20.3	30	7.7	15.4

$\theta = 0°$	$e/4$	$e/2$	$e/10$
	3.85	7.7	1.54

Opening Surface Data

NB: S is the area of openings on the windward face.
S_t is the area of openings where $C_p \leq 0$.

Direction	S (m^2)	S_t (m^2)	Observation	μ_p
Direction V1	9.24	29.16	Non-dominant face	0.76
Direction V2	9.24	29.16	Non-dominant face	0.76
Direction V3	9.96	28.44	Non-dominant face	0.74
Direction V4	9.96	28.44	Non-dominant face	0.74
Totals	**38.40**			

Data for C_{pi}

NB: If the sum of openings is equal to zero, the maximum values of the internal pressure coefficient C_{pi} are adopted, namely 0.35, -0.5, and -0.3, or values obtained by interpolation between -0.5 and -0.3. Otherwise, these data are disregarded.

C_{pi}	Direction V1	Direction V2	Direction V3	Direction V4
Value	-0.18	-0.18	-0.14	-0.14

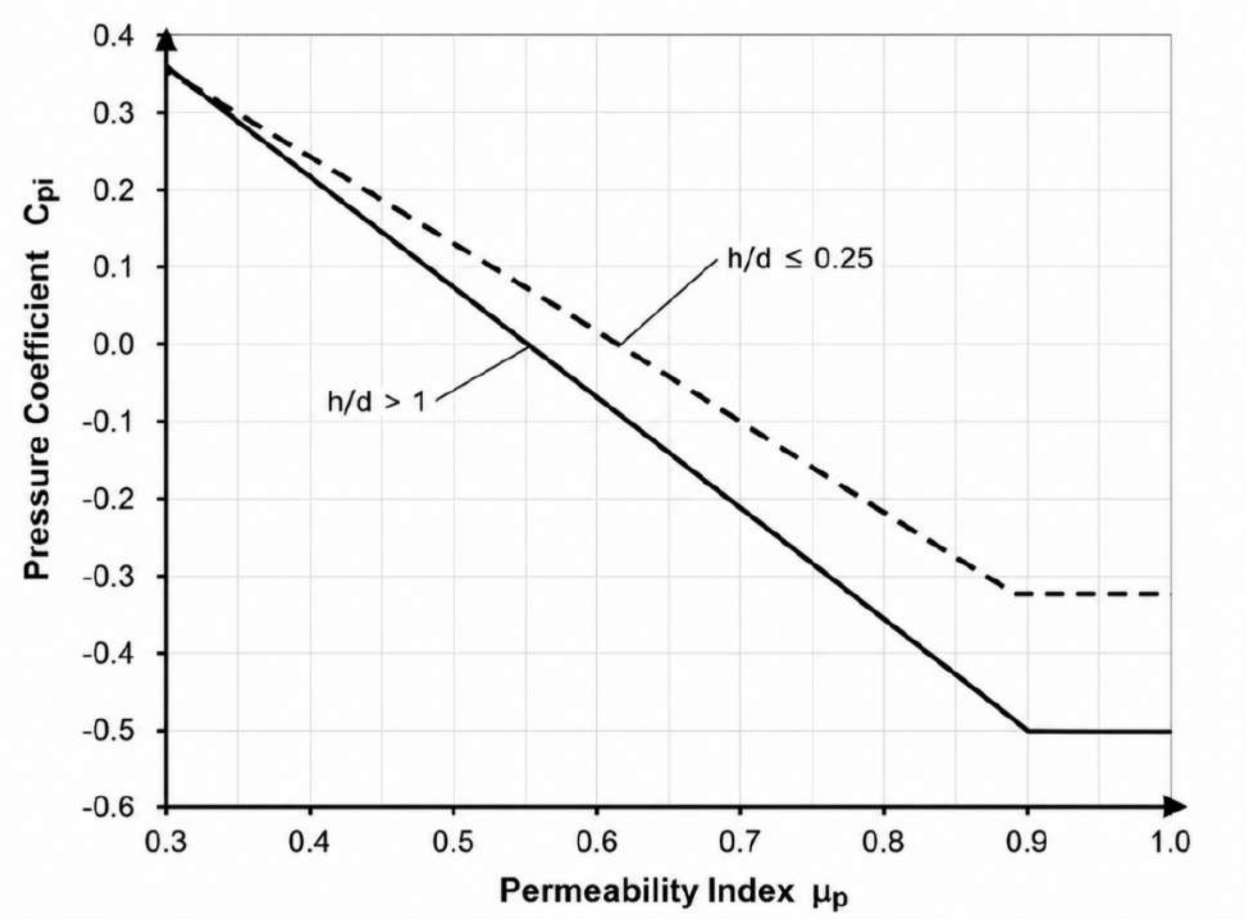

Figure 3.1: Variation of the Internal Pressure Coefficient (Cpi) as a Function of the Wall Permeability Index (μp) — According to RNV 2013

- Calculation of Aerodynamic Pressure $W(Z_j)$

$$W = q_p(Z_e)\ (C_{pe} - C_{pi}) \qquad (\text{daN/m}^2) \qquad [7] \tag{3.1}$$

- Calculation of Peak Dynamic Pressure $q_p(Z_e)$

$$q_p(Z_e) = q_{\text{ref}} \times C_e(Z_e) \qquad (\text{daN/m}^2) \qquad [7] \tag{3.2}$$

Zone	q_{ref} (daN/m^2)
I	37.5
II	43.5
III	50.0
IV	57.5

$$q_{\text{ref}} = 50 \ \textbf{daN/m}^2$$

- Calculation of Exposure Coefficient

$$C_e(z) = C_t^2 \times C_r^2 \times [1 + 7I_v] \qquad [7] \tag{3.3}$$

- Calculation of Site Factors
  C_r: Roughness coefficient [7]
  C_t: Topography coefficient [7]
  Terrain category: 2 [7]

K_r	Z_0 (m)	Z_{min} (m)	ℓ
0.19	0.05	2	0.52

1. **Roughness Coefficient (C_r)**
   The (C_r) is calculated as:

$$C_r(z) = \begin{cases} K_r \ln\left(\frac{z}{z_0}\right), & Z_{\text{min}} \leq z \leq 200\,\text{m}, \\ K_r \ln\left(\frac{Z_{\text{min}}}{z_0}\right), & z < Z_{\text{min}}. \end{cases} \tag{3.4}$$

   The reference height is:

$$z = H = 9.1 \text{ m}$$

   Since:

$$Z_{\text{min}} \leq z \leq 200$$

   the roughness coefficient is calculated as:

$$C_r(z) = K_r \times \ln\left(\frac{z}{Z_0}\right)$$

$$C_r = 0.99$$

For completeness, when:

$$z < Z_{\min}$$

the expression becomes:

$$C_r = K_r \times \ln\left(\frac{Z_{\min}}{Z_0}\right)$$

$$C_r = 0.00$$

Therefore, the adopted value is:

$$\boxed{C_r = 0.99}$$

2. **Topography Coefficient (C_t)** Site category:

$$\text{Site} = 1$$

Hence:

$$\boxed{C_t = 1}$$

3. **Turbulence Intensity (I_v)**
According to RNV [7], the turbulence intensity is calculated as:

$$I_v(z) = \frac{1}{C_r(z) * \ln\left(\frac{z}{Z_0}\right)} \qquad \text{for } z > Z_{\min}$$

$$I_v(z) = \frac{1}{C_r(z)\ln\left(\frac{Z_{\min}}{Z_0}\right)} \qquad \text{for } z \leq Z_{\min}$$

For the considered structure:

$$I_v = 0.192$$

The exposure coefficient is therefore:

$$C_e(z) = C_t^2\, C_r^2\, [1 + 7I_v]$$

$$C_e(z) = 2.29$$

The peak dynamic pressure is calculated as:

$$q_p(z) = q_{\text{ref}} \times C_e(z)$$

$$q_p(z) = 114.6 \text{ daN/m}^2$$

	Z_j **(m)**	C_t	C_r	I_v	C_e	q_p **(daN/m²)**
Roof	9.1	1.00	0.99	0.192	2.29	114.6

- Wind loads (W_x), $(-W_x)$
  Wind on the roof perpendicular to the ridge $(\theta = 0°)$
  Roof 2V $(\theta = 0)$
  $\alpha = 7.85°$

Table 3.6: Positive Pressure (+)

Surface	cpe	cpi	cpe - cpi	qp (daN/m²)	W (daN/m²)
F	0.14	-0.18	0.32	114.6	37.03
G	0.14	-0.18	0.32	114.6	37.03
H	0.14	-0.18	0.32	114.6	37.03
I	-0.17	-0.18	0.01	114.6	1.03
J	-0.17	-0.18	0.01	114.6	1.03

Table 3.7: External Pressure Coefficients (+) – Two Slopes

Surface	$+5°$	$15°$	$7.85°$
F	0	0.2	0.14
G	0	0.2	0.14
H	0	0.2	0.14
I	-0.6	0	-0.17
J	-0.6	0	-0.17

- Wind on Roof Parallel to the Ridge Line $(\theta = 90°)$
  ROOF 2V, $\theta = 90°$
  $\alpha = 7.85°$
- Load cases and load combinations
  - Simple cases
  - ULS and SLS Load Combinations

Table 3.8: Negative Pressure (-)

Surface	cpe	cpi	cpe - cpi	qp (daN/m^2)	W (daN/m^2)
F	-1.13	-0.18	-0.95	114.6	-108.67
G	-0.91	-0.18	-0.73	114.6	-84.14
H	-0.39	-0.18	-0.21	114.6	-23.56
I	-0.46	-0.18	-0.28	114.6	-31.75
J	-0.66	-0.18	-0.48	114.6	-54.80

Table 3.9: External Pressure Coefficients (-) – Two Slopes

Surface	5°	15°	7.85°
F	-1.7	-0.9	-1.13
G	-1.2	-0.8	-0.91
H	-0.6	-0.3	-0.39
I	-0.6	-0.4	-0.46
J	0.2	-1.0	-0.66

Table 3.10: t v 384

Surface	cpe	cpi	cpe - cpi	qp (daN/m^2)	W (daN/m^2)
F	-1.39	-0.14	-1.2455	114.6	-142.78
G	-1.30	-0.14	-1.16	114.6	-132.98
H	-0.63	-0.14	-0.4885	114.6	-56.00
I	-0.53	-0.14	-0.3885	114.6	-44.54

Table 3.11: External Pressure Coefficients (-) – Two Slopes

Surface	5°	15°	7.85°
F	-1.6	-1.3	-1.39
G	-1.3	-1.3	-1.30
H	-0.7	-0.6	-0.63
I	-0.6	-0.5	-0.53

Table 3.12: 1st case (wind perpendicular to the long-span face) — List of defined cases

No.	Case Name	Type
1	PP	dead load
2	MAINTENANCE	live load
3	CLADDING	permanent
4	SAND	snow load
5	W-	wind load
6	W+	wind load

Table 3.13: 2^{nd} case (Wind facing the gable) — List of defined cases

Nº	Case Name	Nature
1	DL (Self-weight)	Dead load
2	CLADDING	Permanent load
3	MAINTENANCE	Live load
4	SAND	Snow load
5	W	Wind load

Table 3.14: 1^{st} Case (Wind fronting the long-span wall)

Combination	Name	Analysis Type	Limit State Type	Case Nature	Definition
6 (C)	1.35G+1.5Q	Linear combination	ULS	Structural	1*1.35+2*1.50

Table 3.15: 2^{nd} case (Wind Facing Gable)

Combination	Name	Analysis Type	Limit State Type	Case Nature	Definition
6 (C)	1.35G+1.5Q	Linear combination	ULS	Structural	1*1.35+2*1.50
7 (C)	1.35G+1.5S	Linear combination	ULS	Structural	1*1.35+3*1.50
8 (C)	G+1.5WL	Linear combination	ULS	Structural	1*1.00+4*1.50
9 (C)	1.35G+1.5W+	Linear combination	ULS	Structural	1*1.35+5*1.50
10 (C)	1.35G+1.35Q+1.35S	Linear combination	ULS	Structural	(1+2+3)*1.35
11 (C)	1.35G+1.35S+1.35WL	Linear combination	ULS	Structural	(1+3+4)*1.35
12 (C)	1.35G+1.35S+1.35W+	Linear combination	ULS	Structural	(1+3+5)*1.35
13 (C)	G+Q	Linear combination	SLS	Structural	(1+2)*1.00
14 (C)	G+S	Linear combination	SLS		(1+3)*1.00
15 (C)	G+0.9Q+0.9S	Linear combination	SLS		(1+3)*0.90+2*1.00
16 (C)	G+WL	Linear combination	SLS		(1+4)*1.00
17 (C)	G+W+	Linear combination	SLS		(1+5)*1.00

Chapter 4

Preliminary Dimensioning

4.1 Pre-dimensioning

This chapter aims to carry out the preliminary sizing of the different structural elements of the building according to the applicable standards and regulations while respecting the required resistance and stability conditions.

The preliminary dimensions of the different structural resisting elements were determined while respecting certain conditions, particularly the deflection condition for the preliminary sizing of beams (load-bearing and non-load-bearing), and the buckling condition for the preliminary sizing of columns according to (BAEL 91). These dimensions must also satisfy the requirements imposed by the Algerian seismic code RPA 2024 [6].

4.2 Beam Pre-Dimensioning Calculation

Deflection criterion :

The beam height must satisfy the following dimensioning conditions:

$$\frac{L}{15} \leq h \leq \frac{L}{10} \tag{4.1}$$

Where:

- L: Beam length.
- h: Beam height.
- b: Beam width.

$$\begin{cases} b \geq 20\,\text{cm} & \text{for zones I, II and III} \\ b \geq 25\,\text{cm} & \text{for zones IV, V and VI} \\ h \geq 30\,\text{cm} \\ \dfrac{h}{b} \leq 4.0 \\ b_{\text{max}} \leq 1.5h + b_c \end{cases}$$

Formwork

Beams must satisfy structural limits. The height h in structures braced by shear walls. According to the Algerian seismic code **RPA 2024**, the Wilaya of Touggourt is classified in seismic **Zone I**.

4.2.1 Block A

Main Beams (30×40)

Given $L_{\text{max}} = 580cm$:

$$\frac{525}{15} \leq h \leq \frac{525}{10} \;\Rightarrow\; 35.00 \leq h \leq 52.50 \;\Rightarrow\; h = 40.00 \text{ cm}$$

Verification of the conditions imposed by RPA 2024:

$$\begin{cases} \bullet \quad b = 30 \text{ cm} \geq 20 \text{ cm} \\ \bullet \quad h = 40 \text{ cm} \geq 30 \text{ cm} \\ \bullet \quad \dfrac{h}{b} = \dfrac{40}{30} = 1.33 \leq 4 \end{cases} \Rightarrow \text{Conditions verified}$$

Secondary Beams (30×30)

Given $L_{\text{max}} = 360cm$:

$$\frac{360}{15} \leq h \leq \frac{360}{10} \;\Rightarrow\; 24.00 \leq h \leq 36.00 \;\Rightarrow\; \text{We take } h = 30.00 \text{ cm}$$

Verification of the conditions imposed by RPA 2024:

$$\begin{cases} \bullet \quad b = 30 \text{ cm} \geq 20 \text{ cm} \\ \bullet \quad h = 30 \text{ cm} \geq 30 \text{ cm} \\ \bullet \quad \dfrac{h}{b} = \dfrac{30}{30} = 1.00 \leq 4 \end{cases} \Rightarrow \text{Conditions verified}$$

4.2.2 Block B

Main Beams (30×40**)**

Given $L_{\text{max}} = 580cm$:

$$\frac{525}{15} \leq h \leq \frac{585}{10} \;\Rightarrow\; 38.66 \leq h \leq 58.00 \;\Rightarrow\; h = 40.00 \text{ cm}$$

Verification of the conditions imposed by RPA 2024:

$$\begin{cases} \bullet \quad b = 30 \text{ cm} \geq 20 \text{ cm} \\ \bullet \quad h = 40 \text{ cm} \geq 30 \text{ cm} \\ \bullet \quad \dfrac{h}{b} = \dfrac{40}{30} = 1.33 \leq 4 \end{cases} \Rightarrow \text{Conditions verified}$$

Secondary Beams (30×30**)**

Given $L_{\text{max}} = 360cm$:

$$\frac{360}{15} \leq h \leq \frac{360}{10} \;\Rightarrow\; 24.00 \leq h \leq 36.00 \;\Rightarrow\; \text{We take } h = 40.00 \text{ cm}$$

Verification of the conditions imposed by RPA 2024:

$$\begin{cases} \bullet \quad b = 30 \text{ cm} \geq 20 \text{ cm} \\ \bullet \quad h = 30 \text{ cm} \geq 30 \text{ cm} \\ \bullet \quad \dfrac{h}{b} = \dfrac{30}{30} = 1.00 \leq 4 \end{cases} \Rightarrow \text{Conditions verified}$$

4.2.3 SPORT HALL BLOCK

Main Beams (X-direction – Y-direction) (30×40**)**

Given $L_{\text{max}} = 600cm$:

$$\frac{600}{15} \leq h \leq \frac{600}{10} \;\Rightarrow\; 40.00 \leq h \leq 60.00 \;\Rightarrow\; \text{We take } h = 50.00 \text{ cm}$$

Verification of the conditions imposed by RPA 2024:

$$\begin{cases} \bullet \quad b = 30 \text{ cm} \geq 20 \text{ cm} \\ \bullet \quad h = 50 \text{ cm} \geq 30 \text{ cm} \\ \bullet \quad \dfrac{h}{b} = \dfrac{50}{30} = 1.66 \leq 4 \end{cases} \Rightarrow \text{Conditions verified}$$

4.3 Preliminary Sizing of Slabs

In this project, two types of slabs were adopted according to the structural and architectural requirements of the building, including hollow block slabs, which are widely used due to their ability to reduce self-weight while maintaining the required strength.

4.3.1 Hollow Block Slab

Since the different floors are not heavily loaded, hollow block slabs were adopted (the hollow blocks are used as permanent formwork), as they are economical and provide good thermal and acoustic insulation. The hollow block slab consists of a compression slab and hollow blocks. To determine the thickness of hollow block slabs, the following deflection condition is used:

$$\frac{L}{25} \leq h \leq \frac{L}{20}$$

- $ht = h$: Total height (thickness) of the slab.
- h_0: Thickness of the compression slab.
- h_1: Thickness of the hollow block.
- L: Largest span between the faces of supports of the joist.

4.3.2 Blocks A And B

Given Rib N1 $L_{\max} = 360cm$:

$$\frac{360}{25} \leq h \leq \frac{360}{20} \;\Rightarrow\; 14.40 \leq h \leq 18.00 \;\Rightarrow\; \text{We take } h = 20.00 \text{ cm} \;\Rightarrow\; \text{Slab } 16+4$$

4.4 Preliminary Sizing of Columns

The column cross-section dimensions must satisfy the following conditions:

$$\begin{cases} Min(b_c, h_c) \geq 25 \text{ cm : in zones I,II, and III} \\ Min(b_c, hc) \geq 30 \text{ cm : in zones IV,V, and VI} \\ Min(b_c, h_c) \geq \dfrac{l_k}{20} \text{ : in any zone} \\ \dfrac{1}{4} < \dfrac{b_c}{h_c} < \dfrac{1}{4} \text{ : in any zone} \end{cases}$$

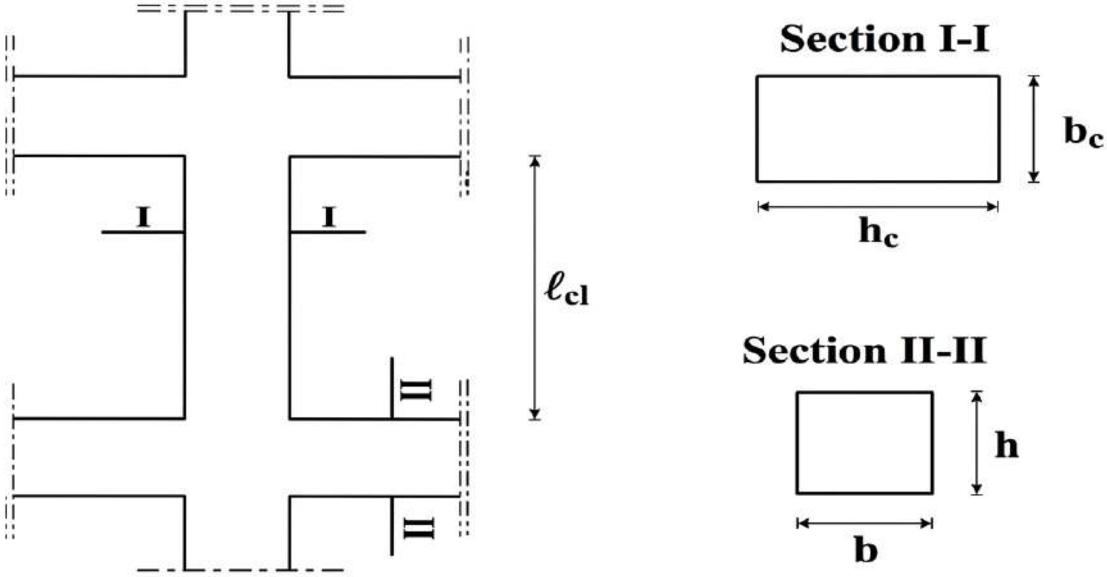

Figure 4.1: Formwork of the column

According to RPA2024, the Wilaya of Touggourt is classified in Zone I.
According to BAEL91 [8] rules: the theoretical value of the resistant axial force is:

$$N_{\text{res.th}} \leq (B_r \times \sigma_b + A \times \sigma_s)$$

Where:

- B_r: Reduced cross-section of the column, obtained by subtracting 1 cm thickness from its actual cross-section along its entire perimeter, such that:
- $B_r = (a-2)(b-2)$, where a and b are dimensions in [cm].

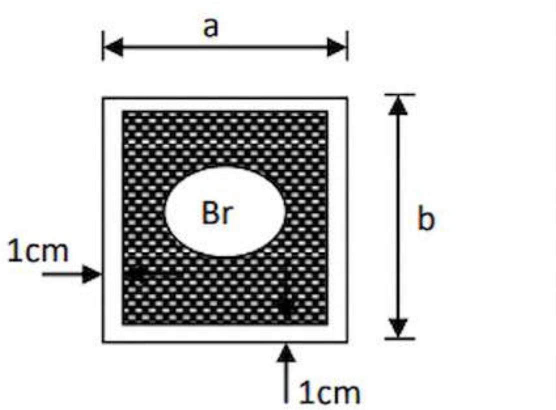

Figure 4.2: Reduced g Section

Compressive strength of concrete: $\sigma_b = 14.17$ **MPa**

$$\text{For : } \lambda \leq 50 : \alpha = \frac{0.85}{1 + 0.2\left(\frac{\lambda}{35}\right)^2} = \frac{0.85}{\beta}$$

With :

$$\beta = 1 + 0.2\left(\frac{\lambda}{35}\right)^2$$

With these corrections, the ultimate resistant axial force becomes:

$$N_u = \alpha[(B_r \times f_{c28})/(0.9 \times \gamma_b) + (A.f_e/\gamma_s)]$$

- γ_b: Concrete safety factor = 1.5
- γ_s: Steel safety factor = 1.15
- fe: Steel grade (yield strength; $fe = 400$ MPa)
- A: Reinforcement area to be provided
- α: Coefficient depending on slenderness λ

The general formula gives:

$$B_r \geq \frac{\beta.N_u}{\frac{\sigma_b}{0.9} + 0.85\left(\frac{A}{B_r}\right).\frac{f_e}{\gamma_s}}$$

We take :

$$\frac{A}{B_r} = 1\% = \frac{1}{100} \quad \text{[BAEL91]}$$

- σ_s : Steel stress ; $\sigma_s = \frac{fe}{\gamma_s} = 348$ MPa
- σ_b : Design compressive strength of concrete : $\sigma_b = \frac{0.85 \times f_{c28}}{\gamma_b} = 14.17$ MPa

According to BAEL91 rules: for a rectangular column ($a \leq b$), it is preferable to take $\lambda \leq 35$.

$$\beta = 1 + 0.2\left(\frac{35}{35}\right)^2 = 1.2$$

By substituting these values into inequality (*), we obtain:

$$B_r \geq \frac{1{,}2N_u}{\left[\frac{14{,}17}{0{,}9} + 0{,}85\left(\frac{1}{100}\right)\frac{400}{1{,}15}\right] * 10} = 0{,}0064N_u \Rightarrow B_r \geq 0{,}0064N_u$$

We can determine a and b knowing that:

$$B_r = (a-2) \times (b-2) \quad [\text{cm}^2]$$

- A column cross-section of 30×30 cm^2 is adopted for Blocks A and B.
- For the sports hall block, a 40×70 cm^2 section is adopted, subject to verification of the reduced axial force.

Chapter

5

Seismic Study

5.1 INTRODUCTION

This chapter presents the seismic study of the proximity sports complex located in El Alia El Hadjira, Wilaya of Touggourt, in accordance with the Algerian Seismic Regulations RPA 2024 (DTR BC 2.48). The study aims to verify the stability and resistance of the structure against seismic actions prior to the dimensioning of structural elements.

The seismic analysis is performed using Autodesk Robot Structural Analysis Professional 2024, applying the Modal Response Spectrum Analysis (MRSA) method. This dynamic approach, required by RPA 2024 for structures in which the equivalent static method is insufficient, provides a more accurate representation of the building's seismic response by combining the contributions of all significant vibration modes. According to RPA 2024, the project site is classified in Seismic Zone I, corresponding to the lowest level of seismic hazard, with a zone acceleration coefficient $A = 0.07$. The foundation soil is classified as Category S3 (medium dense sand), as established by the geotechnical investigation report. The structure is assigned to Usage Group 1B (sports and recreational facilities). These parameters govern the shape and ordinates of the design response spectrum applied in the analysis.

The seismic study covers two reinforced concrete blocks: Block A (Girls' Locker Room, $14.05m$×$10.30m$) and Block B (Boys' Locker Room, $18.45m$×$10.30m$). Both blocks are single-storey structures (RDC) with a floor height of $3.23m$, founded on isolated footings anchored at $1.20m$ depth. The Sports Hall block is a mixed reinforced-concrete and steel structure whose seismic behaviour is governed by the metal framework design and is therefore treated separately within the steel structure chapter.

The following verifications are performed in accordance with RPA 2024 for each block:

1. Dynamic behaviour verification — ART. 4.3.3
2. Base shear force verification — ART. 4.3.5

3. Inter-storey drift verification — ART. 5.10
4. Overall stability against overturning — ART. 5.5
5. $P - \Delta$ second-order effect verification — ART. 5.9

All results are presented and discussed in the sections that follow.

5.2 SEISMIC STUDY – BLOCK A

This section of the calculation report presents the seismic study of the building in accordance with the requirements of DTR BC 2.48 (RPA 2024). The analysis was carried out using Robot Structural Analysis software by applying a modal spectral analysis. All regulatory verifications according to RPA 2024 were performed to ensure compliance of the structure with current standards.

Table 5.1: Seismic Calculation Parameters

Seismic Zone	Usage Group	Site
I	Group 1B	S3

5.2.1 Quality Factor Calculation

The quality factor Q is determined using the following expression:

$$Q = 1 + \sum_{q=1}^{6} P_q \tag{5.1}$$

where P_q represents the penalty associated with quality criterion q, depending on whether the criterion is satisfied or not.

Table 5.2: Quality Factor Evaluation in the X Direction

Criterion	Penalty	Condition
Plan regularity	0.05	Not verified
Elevation regularity	0.20	Verified
Minimum conditions on number of stories	0.20	Not verified
Minimum conditions on spans	0.10	Verified

$$Q_{fX} = 1.25 \tag{5.2}$$

Table 5.3: Quality Factor Evaluation in the Y Direction

Criterion	Penalty	Condition
Plan regularity	0.05	Not verified
Elevation regularity	0.20	Verified
Minimum conditions on number of stories	0.20	Not verified
Minimum conditions on spans	0.10	Verified

$$Q_{fY} = 1.25 \tag{5.3}$$

5.2.2 Global Behavior Factor of the Structure (R)

Table 5.4 presents the distribution of the base shear forces between columns and shear walls.

Table 5.4: Distribution of Base Shear Forces

Floor	F_X on Columns (kN)	F_X on Shear Walls (kN)	F_Y on Columns (kN)	F_Y on Shear Walls (kN)
Floor 1	73.11	0.00	73.64	0.00

5.2.2.1 X Direction

- Percentage of base shear carried by frames: 100.00%.
- Percentage of base shear carried by shear walls: 0.00%.

Therefore, the adopted structural system is a **Frame System**. The behavior factor is $R_X = 5.5$ corresponding to Category (a).

5.2.2.2 Y Direction

- Percentage of base shear carried by frames: 100.00%.
- Percentage of base shear carried by shear walls: 0.00%.

Therefore, the adopted structural system is a **Frame System**. The behavior factor is $R_Y = 5.5$ corresponding to Category (a).

5.2.3 Calculation of Seismic Force

The seismic actions are calculated using the Modal Response Spectrum Dynamic Analysis Method. The seismic action is represented by the following design response spectrum:

$$\frac{S_{ad}(T)}{g} = \begin{cases} AIS\left[\frac{2}{3} + \frac{T}{T_1}\left(2.5\frac{Q_F}{R} - \frac{2}{3}\right)\right], & 0 \leq T < T_1, \\ AIS\left(2.5\frac{Q_F}{R}\right), & T_1 \leq T < T_2, \\ AIS\left(2.5\frac{Q_F}{R}\right)\frac{T_2}{T}, & T_2 \leq T < T_3, \\ AIS\left(2.5\frac{Q_F}{R}\right)\frac{T_2 T_3}{T^2}, & T_3 \leq T < 4\,s. \end{cases} \tag{5.4}$$

Table 5.5: Values Characterizing the Design Response Spectrum

Parameter	Value
Zone acceleration coefficient A	0.07
Importance coefficient I	1.20
Site coefficient S	1.55
Lower period limit T_1 (s)	0.10
Lower period limit T_2 (s)	0.40
Beginning of constant spectral displacement branch T_3 (s)	1.20

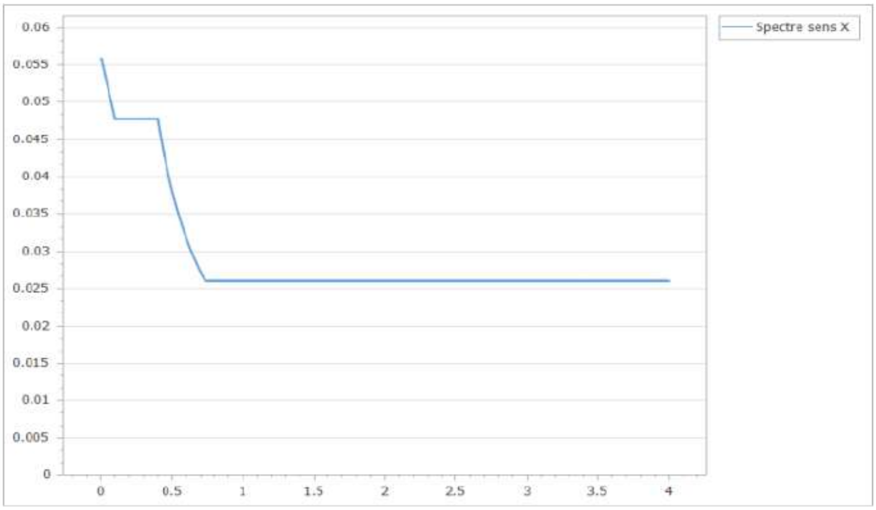

Figure 5.1: Response spectrum in X direction

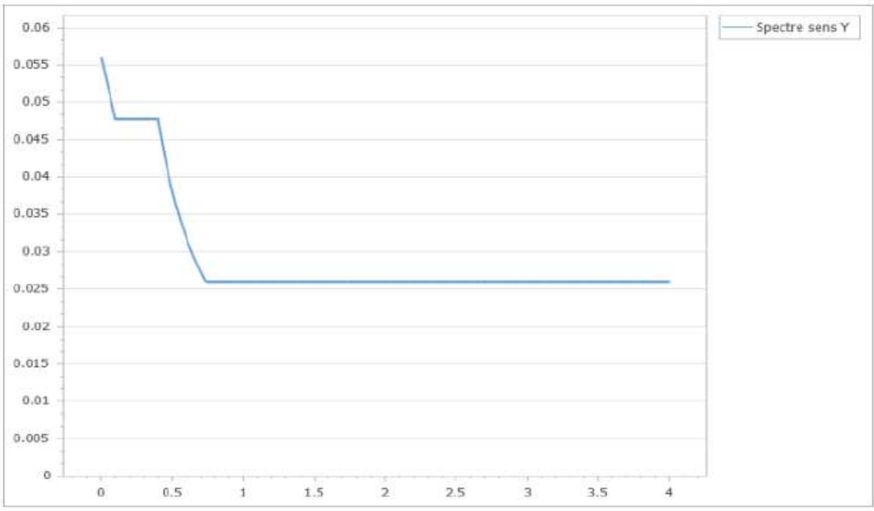

Figure 5.2: Response spectrum in Y direction

5.2.4 Verification of Dynamic Behavior

Table 5.6: Modal Analysis Results

Mode	Period (s)	Cum. Mass UX (%)	Cum. Mass UY (%)	Modal Mass UX (%)	Modal Mass UY (%)	Total Mass UX (kg)
1	0.241	2.25	85.97	2.25	85.97	110210.79
2	0.227	84.45	91.57	82.20	5.60	110210.79
3	0.206	96.18	96.44	11.73	4.86	110210.79
4	0.072	96.47	96.44	0.30	0.00	110210.79
5	0.057	96.47	96.44	0.00	0.00	110210.79
6	0.057	96.48	96.44	0.01	0.00	110210.79
7	0.053	96.48	96.45	0.00	0.01	110210.79
8	0.052	96.58	96.45	0.10	0.00	110210.79
9	0.050	96.58	96.45	0.00	0.00	110210.79

Table 5.7: Interpretation of the Dominant Modes

Mode	Behavior	Period (s)
1	Translation in Y direction	0.241
2	Translation in X direction	0.227
3	Torsional mode	0.206

Verification According to RPA 2024, Article 4.3.3

According to Article 4.3.3 of RPA 2024, the number of retained modes in each excitation direction shall be such that the sum of the effective modal masses reaches at least 90% of the total mass of the structure.

- X direction: cumulative mass participation = 96.58%.
- Y direction: cumulative mass participation = 96.45%.

The cumulative modal mass exceeds the minimum requirement of 90% in both directions. Therefore, the modal analysis satisfies the requirements of Article 4.3.3 of RPA 2024.

Verification ART 4.3.5 RPA 2024

The resultant of seismic forces at the base obtained by combining modal values must not be less than 80% of the resultant of seismic forces determined by the equivalent static method for a value of the fundamental period T_0.

5.2.5 Calculation of Seismic Force by the Equivalent Static Method

According to Article 4.2.3 of RPA 2024, the total seismic force V applied to the base of the structure shall be calculated successively in two orthogonal horizontal directions according to the following formula:

$$V = \lambda \cdot \frac{S_{ad}}{g}(T_0) \cdot W$$

Where:

- $\frac{S_{ad}(T_0)}{g}$: Ordinate of the design spectrum for period T_0
- λ: Correction coefficient
  - $\lambda = 0.85$: if $T_0 \leq 2 \cdot T_2$ and if the building has more than 2 levels
  - $\lambda = 1$: otherwise $\rightarrow$ For our case, $\lambda = 1$
- T_0: Fundamental vibration period of the building

Estimation of the fundamental period:

- Empirical: $T_{\text{empirical}} = C_T \cdot h_N^{3/4} = 0.12\,\text{s}$

Analytical periods obtained by Robot software:

- $T_{\text{analytical-x}} = 0.241\,\text{s}$
- $T_{\text{analytical-y}} = 0.227\,\text{s}$

Table 5.8: Value of the period T_0 used for the calculation of the base shear force V.

Case	Period Used
$T_{\text{calc}} < 1.3\,T_{\text{emp}}$	$T_0 = T_{\text{calc}}$
$T_{\text{calc}} \geq 1.3\,T_{\text{emp}}$	$T_0 = 1.3\,T_{\text{emp}}$

5.2.5.1 Spectral Acceleration Values

According to Table 4.4 of RPA 2024, the spectral acceleration values corresponding to the fundamental periods are:

$$\left(\frac{S_a}{g}\right)_{T_{0X}} = 0.074 \tag{5.5}$$

$$\left(\frac{S_a}{g}\right)_{T_{0Y}} = 0.074 \tag{5.6}$$

5.2.5.2 Calculation of Total Seismic Weight

According to Article 4.2.3 of RPA 2024, the total seismic weight W of the structure is equal to the sum of the seismic weights calculated at each level:

$$W = \sum_{i=1}^{n} W_i \tag{5.7}$$

where

$$W_i = W_{Gi} + \psi W_{Qi} \tag{5.8}$$

with:

- W_{Gi}: weight due to permanent loads and fixed equipment;
- W_{Qi}: live load at level i;
- ψ: live-load participation coefficient (Table 4.2 of RPA 2024);
- n: total number of levels.

For the studied structure:

$$W = 1081.17 \text{ kN} \tag{5.9}$$

5.2.5.3 Seismic Forces Computed by the Equivalent Static Method

The base shear forces obtained using the equivalent static method are:

$$V_X = 80.01 \text{ kN} \tag{5.10}$$

$$V_Y = 80.01 \text{ kN} \tag{5.11}$$

Table 5.9: Verification of Base Shear Force

Direction	V (kN)	$0.8V$ (kN)	E_x, E_y (kN)	Verification
X	80.01	64.01	73.11	Condition verified
Y	80.01	64.01	73.64	Condition verified

5.2.5.4 Verification of Inter-Story Drifts – RPA 2024 Article 5.10

Relative lateral displacements of one story with respect to the one below must not exceed the limits prescribed by RPA 2024.

$$\Delta_k < \bar{\Delta}_k$$

The allowable inter-story drift $\bar{\Delta}_k$ is determined according to the structural type using Equations (5.11), (5.12), and (5.13) of RPA 2024.

Table 5.10: Inter-Story Drift Limits According to RPA 2024

Structure Type	Drift Limit $\bar{\Delta}_k$
Reinforced Concrete Buildings without Fragile or Ductile Elements	$\Delta_k \leq 0.0150\, h_k$

Table 5.11: Verification of Inter-Story Drifts

Floor	Height (m)	$\Delta_{k,\text{lim}}$ (cm)	$\Delta_{k,x}$ (cm)	$\Delta_{k,y}$ (cm)	$\Delta_k \leq \Delta_{k,\text{lim}}$
Floor 1	3.23	4.85	0.40	0.46	Verified

5.2.6 Verification of Overall Stability – RPA 2024 Article 5.5

Verification of structural overturning is performed through application of the following formula:

$$Moment_{\text{Stabilisant}} > 1.3 * Moment_{\text{renversant}}$$

Table 5.12: Stabilizing Moment Calculation

W (kN)	$W_{i,\text{addtnl}}$ (kg)	X_g (m)	Y_g (m)	$M_{\text{stab},x}$ (kN.m)	$M_{\text{stab},y}$ (kN.m)
1081.17	0.00	8.53	6.29	9222.38	6800.56

Overturning Moment Calculation:
$M_{\text{Renversement}}$: le moment de renversement de la structure = $\sum F_k * H_k$
where:

- F_k: seismic force applied at level k;
- H_k: height of level k measured from the base.

Table 5.13: Overturning Moment Calculation

Floor	**Level (m)**	V_x **(kN)**	F_x **(kN)**	V_y **(kN)**	F_y **(kN)**	$M_{\text{ren},x}/M_{\text{ren},y}$ **(kN.m)**
Floor 1	3.23	73.11	73.11	73.64	73.64	236.15 / 237.86

Table 5.14: Overall Stability Verification in the X Direction (Block A)

$M_{\text{ren},x}$ **(kN.m)**	$M_{\text{stab},x}$ **(kN.m)**	**Condition:** $M_{\text{stab}} > 1.30\, M_{\text{ren}}$
236.15	9222.38	Verified

Table 5.15: Overall Stability Verification in the Y Direction (Block A)

$M_{\text{ren},y}$ **(kN.m)**	$M_{\text{stab},y}$ **(kN.m)**	**Condition:** $M_{\text{stab}} > 1.30\, M_{\text{ren}}$
237.86	6800.56	Verified

5.2.7 Verification of P-Δ Effect – RPA 2024 Article 5.9

The effects of second order (or P-Δ effect) may be neglected in buildings if the following condition is satisfied at all levels:

$$\left(\theta_k = \frac{P_k \cdot \Delta_k}{V_k \cdot h_k}\right) \leq 0.10$$

where:

- P_k : total weight of the structure and live loads, above level "k".

$$P_k = \sum_{i=k}^{n} (G_i + \psi \cdot Q_i)$$

- V_k : storey shear force at level "k" : $V_k = \sum_{i=k}^{n} F_i$
- Δ_k : relative displacement of level "k" with respect to level "$k-1$"
- h_k : height of level "k".

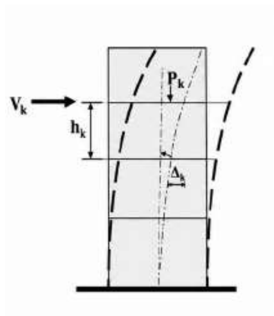

Figure 5.3: Schematic representation of the second-order P-Δ effect on a multi-story building frame.

Verification of ≤ 8u i ×ve DBDHe MR

Table 5.16: Verification of the Stability Coefficient Θ

Floor	H (m)	P (kN)	$\Delta_{k,x}$ (cm)	$\Delta_{k,y}$ (cm)	V_x (kN)	V_y (kN)	Θ_x	Θ_y
1	3.23	1089.84	0.40	0.46	73.11	73.64	0.0185	0.0183

The stability coefficient Θ shall satisfy the following condition:

$$\theta \leq 0.10$$

For the studied structure:

$$\Theta_x = 0.0185 < 0.10, \tag{5.12}$$

$$\Theta_y = 0.0183 < 0.10. \tag{5.13}$$

Therefore, the stability condition is satisfied in both directions and second-order effects may be neglected according to the provisions of RPA 2024.

5.3 SEISMIC STUDY – BLOCK B

This section of the calculation report presents the seismic analysis of Block B in accordance with the requirements of DTR BC 2.48 (RPA 2024). The analysis was performed using Robot Structural Analysis software through the Modal Response Spectrum Method. All verifications required by RPA 2024 were carried out to assess the seismic behavior of the structure and to ensure compliance with the applicable regulatory provisions.

5.3.1 Seismic Calculation Parameters

Table 5.17: Seismic Calculation Parameters

Seismic Zone	Usage Group	Site
I	Group 1B	S3

5.3.2 Quality Factor Calculation

The quality factor (Q) is determined according to the following expression:

$$Q = 1 + \sum_{q=1}^{6} P_q \tag{5.14}$$

where (P_q) represents the penalty associated with quality criterion (q), depending on whether the corresponding requirement is satisfied or not. The values of these penalties are determined according to the provisions of RPA 2024.

(P_q) is the penalty applied depending on whether quality criterion (q) is satisfied or not.

5.3.2.1 Direction X

Table 5.18: Quality Factor Evaluation in the X Direction

Criterion	Penalty	Condition
Plan regularity	0.05	Not verified
Elevation regularity	0.20	Verified
Minimum conditions on number of stories	0.20	Not verified
Minimum conditions on spans	0.10	Verified

$$Q_{fX} = 1.25$$

5.3.2.2 Direction Y

Table 5.19: Quality Factor Evaluation in the Y Direction

Criterion	Penalty	Condition
Plan regularity	0.05	Not verified
Elevation regularity	0.20	Verified
Minimum conditions on number of stories	0.20	Not verified
Minimum conditions on spans	0.10	Verified

$$Q_{fY} = 1.25$$

5.3.3 Global Structural Behavior Factor (R)

The following table presents the distribution of shear forces in columns and shear walls at the base level.

5.3.3.1 Direction X

- Percentage of base shear carried by frames: 100.00
- Percentage of base shear carried by shear walls: 0.00

Table 5.20: Distribution of Base Shear Forces

Floor	F_X on Columns (kN)	F_X on Walls (kN)	F_Y on Columns (kN)	F_Y on Walls (kN)
Floor 1	99.12	0.00	96.43	0.00

- Structural system: Frame system.

$$R_X = 5.5 \tag{5.15}$$

The structure belongs to Category (a).

5.3.3.2 Direction Y

- Percentage of base shear carried by frames: 100.00
- Percentage of base shear carried by shear walls: 0.00
- Structural system: Frame system.

$$R_Y = 5.5 \tag{5.16}$$

The structure belongs to Category (a).

5.3.4 Calculation of Seismic Force (RPA 2024 Art. 3.3.3)

Seismic actions are calculated using the modal spectral dynamic analysis method. The seismic action is represented by the following design spectrum:

$$\frac{S_{ad}}{g}(T) = \begin{cases} A \cdot I \cdot S \cdot \left[\frac{2}{3} + \frac{T}{T_1} \cdot \left(2.5\,\frac{Q_F}{R} - \frac{2}{3}\right)\right] & \text{if } 0 \leq T < T_1 \\ A \cdot I \cdot S \cdot \left[2.5\,\frac{Q_F}{R}\right] & \text{if } T_1 \leq T < T_2 \\ A \cdot I \cdot S \cdot \left[2.5\,\frac{Q_F}{R}\right] \cdot \left[\frac{T_2}{T}\right] & \text{if } T_2 \leq T < T_3 \\ A \cdot I \cdot S \cdot \left[2.5\,\frac{Q_F}{R}\right] \cdot \left[\frac{T_2 T_3}{T^2}\right] & \text{if } T_3 \leq T < 4\,\mathrm{s} \end{cases}$$

Values Characterizing the Design Response Spectrum:

Table 5.21: Parameters of the Design Response Spectrum

Parameter	Value
Zone acceleration coefficient A	0.07
Importance coefficient I	1.2
Site coefficient S	1.55
Lower period limit T_1 (s)	0.1
Upper period limit T_2 (s)	0.4
Start of constant spectral displacement branch T_3 (s)	1.2

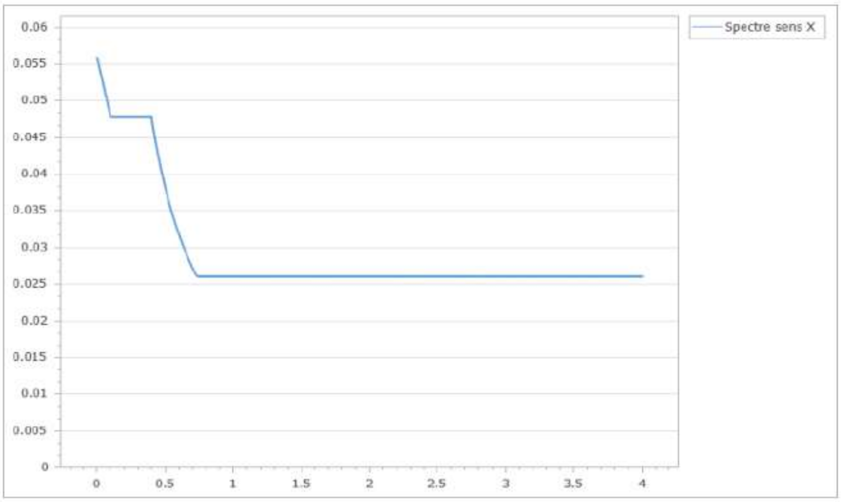

Figure 5.4: Response spectrum in X direction: obtained from Robot Structural Analysis software.

5.3.5 Verification Against Algerian Seismic Code RPA 2024

5.3.5.1 Verification of Dynamic Behavior

Modal Analysis Results:

Interpretation:

Verification ART 4.3.3 RPA 2024

The number of modes to be retained in each excitation direction shall be such that the sum of effective modal masses for retained modes equals at least 90% of the total structural mass:

- Direction X: Cumulative mass = 96.74%
- Direction Y: Cumulative mass = 96.63%

[✓] *Cumulative mass at the last mode exceeded 90% in both directions X and Y.*

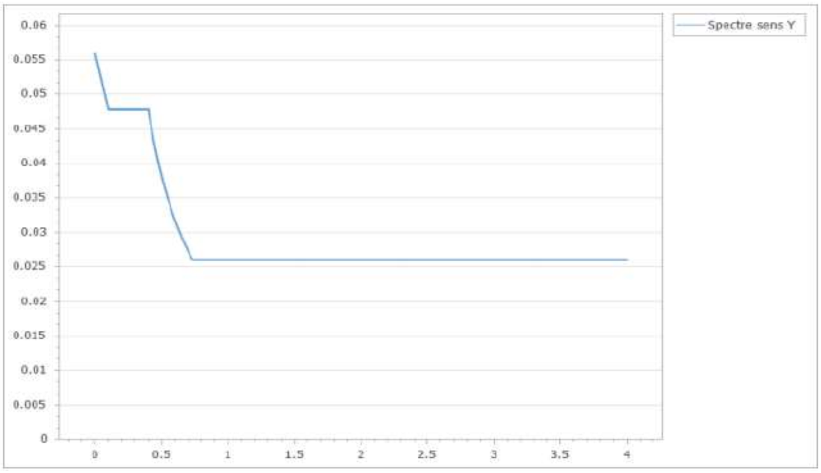

Figure 5.5: Response spectrum in Y direction: obtained from Robot Structural Analysis software.

Table 5.22: Modal Analysis Results and Mass Participation Factors

Mode	Period (s)	Cum. UX (%)	Cum. UY (%)	Modal UX (%)	Modal UY (%)	Total Mass UX (kg)
1	0.247	0.64	86.81	0.64	86.81	151 334.47
2	0.228	90.14	89.10	89.51	2.29	151 334.47
3	0.212	96.42	96.63	6.28	7.53	151 334.47
4	0.079	96.73	96.63	0.31	0.00	151 334.47
5	0.062	96.73	96.63	0.00	0.00	151 334.47
6	0.061	96.73	96.63	0.00	0.00	151 334.47
7	0.059	96.73	96.63	0.00	0.00	151 334.47
8	0.054	96.73	96.63	0.00	0.00	151 334.47
9	0.052	96.74	96.63	0.00	0.00	151 334.47

Table 5.23: Dynamic Behavior Interpretation of Primary Modes

Mode	Behavior	Period (s)
1	Translation in Y direction	0.247
2	Translation in X direction	0.228
3	Torsion	0.212

Verification ART 4.3.5 RPA 2024

The resultant of seismic forces at the base obtained by combining modal values must not be less than 80% of the resultant determined by the equivalent static method for period T_0.

Calculation of Seismic Force – Equivalent Static Method (Block B)

According to Article 4.2.3 of RPA 2024, the total seismic force V applied at the base of the structure shall be calculated successively in two orthogonal horizontal directions using the following formula:

$$V = \lambda \cdot \frac{S_{ad}}{g}(T_0) \cdot W$$

For our case, $\lambda = 1$.
Estimation of the fundamental period: Empirical: $T_{\text{empirical}} = C_T \cdot h_N^{3/4} = 0.12\,\text{s}$

Where:

- Empirical: $T_0 = C_T \cdot h_N^{3/4} = 0.12\,\text{s}$
- $T_{\text{analytical-x}} = 0.247\,\text{s}$
- $T_{\text{analytical-y}} = 0.228\,\text{s}$

Case	Period to use
$T_{\text{calcul}} < 1.3\,T_{\text{empirique}}$	$T_0 = T_{\text{calcul}}$
$T_{\text{calcul}} \geq 1.3\,T_{\text{empirique}}$	$T_0 = 1.3\,T_{\text{empirique}}$

Table 5.24: Value for the period (T_0) used to calculate the base shear force V

From Table 5.24 of RPA 2024:

- $\frac{S_a}{g}(T_{0\text{-}x}) = 0.074$
- $\frac{S_a}{g}(T_{0\text{-}y}) = 0.074$

For our case: $W = 1\,484.59\,\text{kN}$

- $V_x = 109.86\,\text{kN}$
- $V_y = 109.86\,\text{kN}$

Verification of Base Shear Force – Block B

Table 5.25: Base Shear Force Verification Against Equivalent Static Method

Dir.	V **(kN)**	$80\% \times V$ **(kN)**	E_x, E_y **(kN)**	**Verification**
X	109.86	87.89	103.25	Condition verified
Y	109.86	87.89	100.45	Condition verified

Verification of Inter-Story Drift – RPA 2024, Article 5.10

The relative lateral displacements of a story with respect to the story immediately below shall not exceed the allowable limits specified in the following table:

Table 5.26: Inter-Story Drift Limit According to Structure Type

Structure Type	Drift Limit $\bar{\Delta}_k$
RC Buildings without Fragile or Ductile Elements	$\Delta_k \leq 0.0150 \times h_k$

Table 5.27: Inter-Story Drift Calculations and Verification

Floor	Height (m)	$\Delta_{k,\text{lim}}$ (cm)	Δ_{k-x} (cm)	Δ_{k-y} (cm)	$\Delta_k \leq \Delta_{k,\text{lim}}$
Floor 1	3.23	4.85	0.42	0.48	[✓] Verified

$$\Delta_k < \bar{\Delta}_k$$

Where: $\bar{\Delta}_k$ is determined according to the type of structure based on Equations (5.11), (5.12), and (5.13) of RPA 2024.

Verification of Overall Stability – RPA 2024 Art. 5.5 (Block B)

The verification of the structure against overturning is carried out using the following equation:

$$Moment_{stabilizing} > 1.3 * Moment_{overturning}$$

Stabilizing Moment Calculation

Table 5.28: Stabilizing Moment Calculation Data

W (kN)	W_i addtnl (kg)	X_g (m)	Y_g (m)	$M_{\text{stab-x}}$ (kN·m)	$M_{\text{stab-y}}$ (kN·m)
1 484.59	0.00	7.28	5.93	10 807.82	8 803.62

Overturning Moment Calculation

$M_{\text{Overturning}}$: the overturning moment of the structure = $\sum F_k \cdot H_k$

- F_k: seismic force applied at level k;
- H_k: height of level k measured from the base.

Table 5.29: Overturning Moment Calculations per Story

Floor	Level (m)	V_x (kN)	F_x (kN)	V_y (kN)	F_y (kN)	$M_{\text{ren-x}}/M_{\text{ren-y}}$ (kN·m)
Floor 1	3.23	103.25	103.25	100.45	100.45	333.50 / 324.45

Summary Table – Block B:

Table 5.30: Overturning Stability Verification (X Direction)

$M_{\text{ren-x}}$ (kN·m)	$M_{\text{stab-x}}$ (kN·m)	Condition: $M_{\text{stab}} > 1.30 \times M_{\text{ren}}$
333.50	10 807.82	[✓] Verified

Table 5.31: Overturning Stability Verification (Y Direction)

$M_{\text{ren-y}}$ (kN·m)	$M_{\text{stab-y}}$ (kN·m)	Condition: $M_{\text{stab}} > 1.30 \times M_{\text{ren}}$
324.45	8 803.62	[✓] Verified

5.3.6 Verification of P-Δ Effect – RPA 2024 Article 5.9

The effects of second order (or P-Δ effect) may be neglected in buildings if the following condition is satisfied at all levels:

$$\left(\theta_k = \frac{P_k \cdot \Delta_k}{V_k \cdot h_k}\right) \leq 0.10$$

where:

- P_k : total weight of the structure and live loads, above level "k".

$$P_k = \sum_{i=k}^{n} (G_i + \psi \cdot Q_i)$$

- V_k : storey shear force at level "k" : $V_k = \sum_{i=k}^{n} F_i$
- Δ_k : relative displacement of level "k" with respect to level "$k - 1$"
- h_k : height of level "k".

Table 5.32: Verification of the Stability Coefficient Θ

Floor	H (m)	P (kN)	$\Delta_{k,x}$ (cm)	$\Delta_{k,y}$ (cm)	V_x (kN)	V_y (kN)	Θ_x	Θ_y
1	3.23	1496.89	0.42	0.48	103.25	100.45	0.0188	0.0193

Verification of ≤ 8u i ×ve DBDHe MR

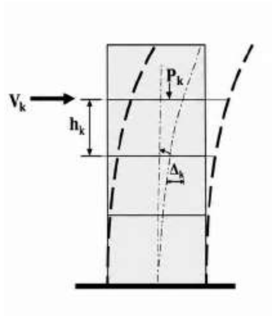

Figure 5.6: Schematic representation of the second-order P-Δ effect on a multi-story building frame.

The stability coefficient Θ shall satisfy the following condition:

$$\theta \leq 0.10$$

For the studied structure:

$$\Theta_x = \text{B9BCPP} < 0.10, \quad (5.17)$$

$$\Theta_y = \text{B9BCRE} < 0.10. \quad (5.18)$$

Therefore, the stability condition is satisfied in both directions and second-order effects may be neglected according to the provisions of RPA 2024.

5.4 CONCLUSION

This chapter has presented the complete seismic analysis of the reinforced concrete blocks constituting the proximity sports complex at El Alia El Hadjira, Wilaya of Touggourt, in full compliance with the Algerian ≤ Regulations RPA 2024 (DTR BC 2.48). The analysis was conducted using the Modal Response Spectrum Analysis method implemented in Robot Structural Analysis Professional 2024.

The seismic context of the project is characterised by a low level of hazard: Seismic Zone $I(A = 0.07)$, Usage Group 1B, Site Category S3 (site coefficient $S = 1.55$, importance coefficient $I = 1.2$). Under these conditions, the design response spectrum yields a normalised spectral acceleration Sa/g = 0.074, which is among the lowest values applicable under RPA 2024.

Both Block A and Block B adopt a pure frame structural system (Ossature portique) with a behaviour factor R = 5.5 and a quality factor $Q = 1.25$, reflecting minor penalties related to plan irregularity and the single-storey configuration. The seismic weight of Block A is $W = 1\,081.17\ kN$, and that of Block B is $W = 1\,484.59\ kN$.

All five regulatory verifications required by RPA 2024 have been satisfied for both blocks, as summarised in the Table 5.33.

Table 5.33: Summary of Regulatory Verifications and Compliance Under RPA 2024

Verification	**Article**	**Block A**	**Block B**
Dynamic behaviour	ART. 4.3.3	[✓] Verified	[✓] Verified
Base shear force	ART. 4.3.5	[✓] Verified	[✓] Verified
Inter-story drifts	ART. 5.10	[✓] Verified	[✓] Verified
Overall stability	ART. 5.5	[✓] Verified	[✓] Verified
P-Δ effect	ART. 5.9	[✓] Verified	[✓] Verified

The maximum inter-story drift recorded is $\Delta k = 0.48\ cm$ (Block B, Y direction), well below the allowable limit of $4.85\ cm$ imposed by RPA 2024, confirming the high lateral stiffness of the structure. The $P - \Delta$ stability index remains below 0.02 for both blocks, indicating that second-order effects are negligible and do not require amplification of the computed seismic forces.

It should be noted that the Sports Hall block, which incorporates a steel moment-resisting frame (portal frames with HEA 400 columns and IPE 400 rafters) resting on reinforced concrete columns, is not subject to a conventional seismic analysis under RPA 2024 within this chapter. The seismic resistance of the steel superstructure is addressed through the capacity design principles applied in the steel structure dimensioning chapter, in accordance with CCM 97 and Eurocode 3.

In conclusion, both reinforced concrete blocks satisfy all seismic requirements of RPA 2024 with comfortable safety margins. The structural design is deemed adequate with respect to seismic performance, and the selected structural system and member dimensions may be retained for the final dimensioning presented in the following chapters.

Chapter

6

Calculation and Verification of Structural Elements

6.1 CALCULATION AND VERIFICATION OF REINFORCED CONCRETE ELEMENTS

6.1.1 Calculation and verification of columns

6.1.1.1 RPA 2024 Requirements for Columns

Columns are the primary vertical load-bearing members of a reinforced concrete structure. They transmit combined axial forces and bending moments from the floor slabs and beams down to the foundations. In a seismic context, columns must also resist horizontal forces generated by earthquake ground motion and must exhibit sufficient ductility to dissipate seismic energy without premature failure.

The design of columns in this project is carried out in accordance with two complementary references: the French concrete design code BAEL 91 revised 99 (Béton Armé aux États Limites), which governs the dimensioning of longitudinal and transverse reinforcement under gravity load combinations at Ultimate and Serviceability Limit States; and the Algerian $\leq$ Regulations RPA 2024 (DTR BC 2.48), which imposes additional detailing requirements and checks specific to seismic zones, including minimum reinforcement ratios, confinement of the concrete core, and control of the normalised axial force.

Three column types are addressed in this chapter: the $30\ cm \times 30\ cm$ section used in Block A (Girls' Locker Room) and Block B (Boys' Locker Room), and the $40\ cm \times 70\ cm$ section used in the Sports Hall block. For each section, the following verifications and designs are performed: (1) normalised axial force ν — RPA 2024 Art. 7.4.3; (2) shear stress — CBA 93 A.5.1.1 and RPA 2024 Eq. 7.6; (3) longitudinal reinforcement — combined bending, governed by RPA 2024 Art. 7.4.2 minimum; (4) transverse reinforcement — RPA 2024 Art. 7.4.2

with zone-dependent spacing limits.

The minimum reinforcement requirements imposed by RPA 2024 for seismic Zone I are recalled below, prior to the detailed calculations.

Longitudinal reinforcement bars must be high-bond, straight and without hooks:

- Their minimum percentage shall be: $0.8\% \rightarrow$ Zone I
- Their maximum percentage shall be:
  - 4% in the current zone
  - 8% in the lap splice zone
- Minimum bar diameter is $12\,\text{mm}$
- Minimum lap splice length is:
  - 50ϕ in Zones I, II and III
- Spacing between vertical bars on one face of a column shall not exceed $20\,\text{cm}$ in Zones I, II and III.

6.1.1.2 BLOCK A – GIRLS LOCKER ROOM:

Column 30×30

1. **Material Properties:**
   - Concrete: $f_{c28} = 25.00\,\text{MPa}$
   - Steel: $f_e = 500\,\text{MPa}$
2. **Cross-Section Dimensions**
   - $b = 30.00\,\text{cm}$
   - $h = 30.00\,\text{cm}$

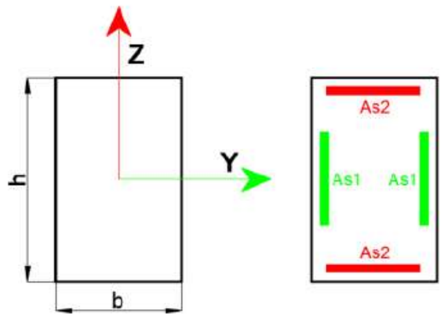

Figure 6.1: Cross-Section Dimensions

3. **Load Combinations**

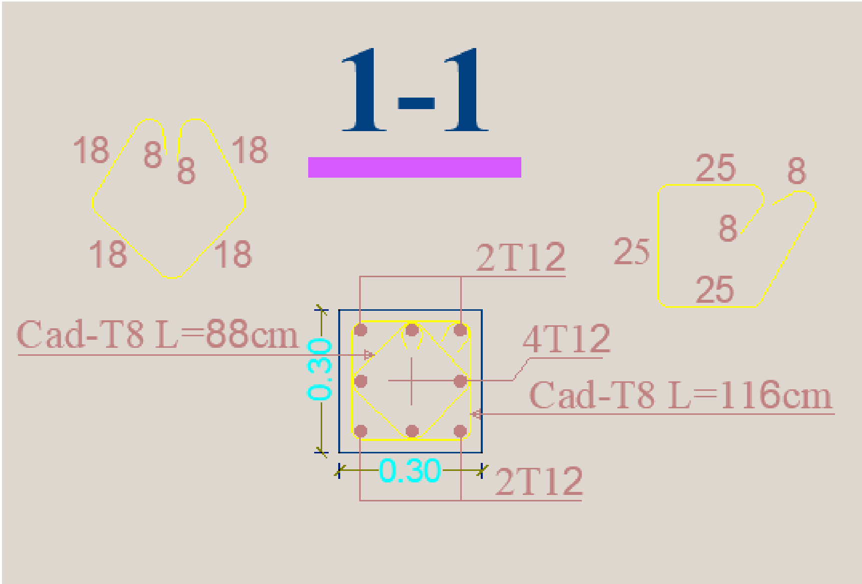

Figure 6.2: Reinforcement Detail of Column.

- Ultimate Limit States (ULS): $1.35G + 1.5Q \quad (\gamma_b = 1.5\,;\ \gamma_s = 1.15)$
- Accidental Limit States (ALS): $G + \psi Q \pm E \quad (\gamma_b = 1.2\,;\ \gamma_s = 1)$

4. **Design Forces**

Table 6.1: Load Cases for Column 30×30 (Block A)

Load Cases	Column 30X30		
	N (kN)	My (kN.m)	Mz (kN.m)
ELU (Nmax; Mycorr; Mzcorr)	**198.78**	10.52	0.04
ACC1 (Mymax; Ncorr; Mzcorr)	78.72	**27.93**	0.62
ACC2 (Mzmax; Ncorr; Mycorr)	102.17	9.40	**15.37**
ACC3 (Nmin; Mycorr; Mzcorr)	**17.34**	5.41	0.68

5. Verification of Reduced Axial Force

The design compressive axial force is limited by the condition of RPA 2024 Article 7.4.3:

$$v = \frac{N_d}{B_c f_{c28}} \leq 0.35$$

Where:

ν: the reduced axial force.

N_d: design axial force acting on a cross-section.

B_c: column cross-sectional area.

F_{c28}: characteristic compressive strength of concrete.

Parameter	Value
N_d (KN)	136.76
B_c (cm^2)	900.00
F_{c28} (MPa)	25.00
ν	0.06
Condition	**Condition Verified**

6. Verification of Shear Stresses Verification of ultimate shear stress limit per CBA93 A.5.1.1

$$\tau_{bu} = \frac{V_u}{b \cdot d}$$

Where:

- V_u: Shear force at the Ultimate Limit State.
- τ_{bu}: Shear stress in MPa.
- b: beam width, d: Effective depth $h - (h/10)$.

The conventional design shear stress in concrete, τ_{bu}, under seismic combination shall not exceed the following limit value:

$$\tau_{bu} \leq \overline{\tau_{bu}} = \rho_d \times f_{c28} \qquad \text{(RPA 2024 Eqn(7.6))}$$

where: ρ_d equals 0.075 if the geometric slenderness, in the direction considered, is greater than or equal to 5; it equals 0.04, otherwise.

In the case of masonry infill, not extending over the full column height (e.g. transom windows), the design height for the geometric slenderness shall equal the opening height.

$$\lambda_g = \left(\frac{l_f}{a} \text{ or } \frac{l_f}{b} \right)$$

Where:

λ_g: is the geometric slenderness ratio of the column.

a and b: dimensions of the column cross-section in the direction of deformation considered.

l_f: buckling length of the column $l_f = 0.7L$ (general building case).

Calculation Results

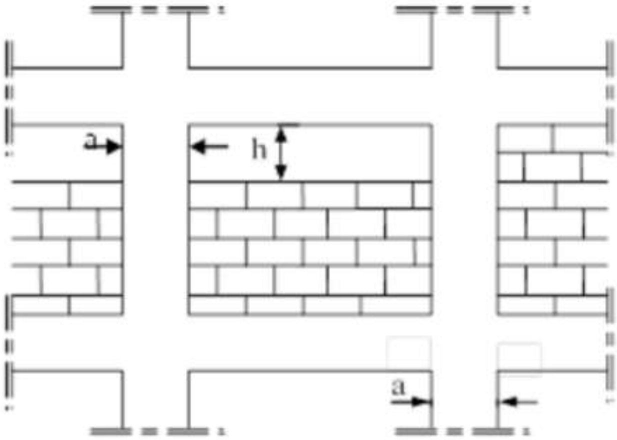

Figure 6.3: Influence of masonry infill and opening height h on columns.

Table 6.2: Shear Verification (Block A)

Y-Y Direction		Z-Z Direction	
λ_g	7.53	λ_g	7.53
ρ_d	0.075	ρ_d	0.075
τ_{bu} (MPa)	1.88	τ_{bu} (MPa)	1.88
T_y (kN)	9.02	T_z (kN)	14.46
$\tau = \dfrac{T_y}{b \times 0.9h}$ (MPa)	0.11	$\tau = \dfrac{T_z}{h \times 0.9b}$ (MPa)	0.18
Condition	Condition Verified ✓	Condition	Condition Verified ✓

7. Longitudinal Reinforcement Design

Table 6.3: Longitudinal Reinforcement Results – Combined Bending

As1 [cm^2]	As2 [cm^2]	As Total [cm^2]
0.08	1.34	2.83

Table 6.4: Reinforcement Conditions per RPA 2024 Art. 7.4.2

bc (cm)	hc (cm)	Seismic Zone	As-min (%)	As-min (cm^2)
30.00	30.00	I	0.80	7.20

Table 6.5: Additional Reinforcement Requirements

ϕ_{min} (mm)	As-max ZC (%)	As-max ZR (%)	Min. Lap Length	Max. Bar Spacing (cm)
12	4	8	50ϕ	20

Reinforcement Selection	Actual A_s (cm^2)	Condition $A_s > \max(A_{s\text{-min}}, A_{s\text{ tot}})$
8 HA 12	9.04	Condition Verified ✓

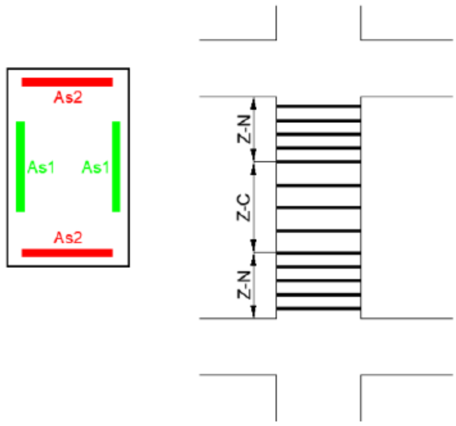

Figure 6.4: Column cross-section reinforcement layout and longitudinal confinement zones.

8. Transverse Reinforcement Design

   According to RPA 2024 Article 7.4.2, column transverse reinforcement is calculated using the formula:

$$\frac{A_t}{t} = \rho_a \frac{V_u}{h_1 \cdot f_e} \tag{6.1}$$

A_t: straight or equivalent cross-section of the transverse reinforcement links.

V_u: design shear force at the ULS in kN.

h_1: total height of the gross section in the direction considered.

f_e: yield strength of the transverse reinforcement steel.

t: spacing of transverse reinforcement.

ρ_a: corrective coefficient accounting for the brittle shear failure mode:

- $\rho_a = 2.5$ if $\lambda_g \geq 5$
- $\rho_a = 3.75$ otherwise.

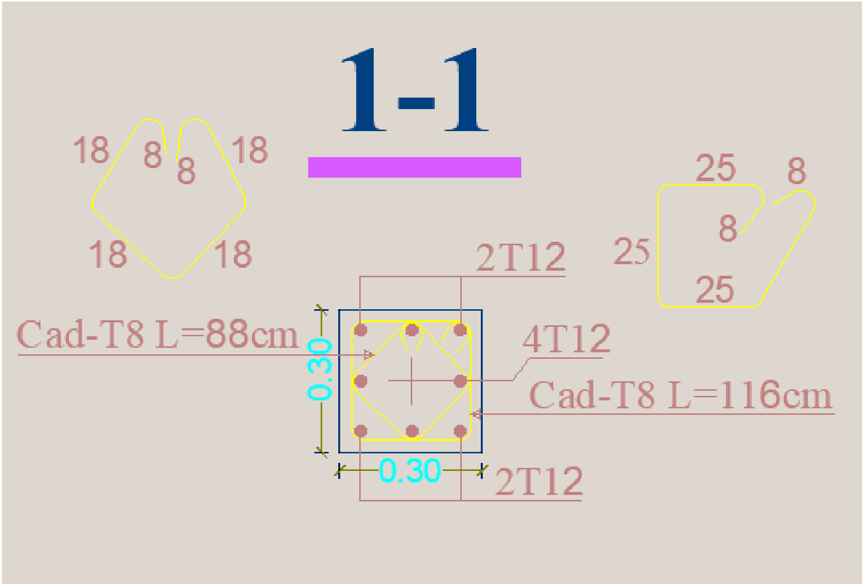

Figure 6.5: Cross-Section Dimensions

Maximum Spacing

The maximum spacing is given by the following expression:

Seismic Zone	I, II and III	IV, V and VI
Nodal Zone	$\min(10\phi_l, 12.5\text{ cm})$	$\min(b_0/3, 6\phi_l, 10\text{ cm})$
Current Zone	$15\phi_l$	$\min(b_c/2, h_c/2, 10\phi_l)$

Where:

ϕ_l: the minimum diameter of longitudinal column reinforcement.

b_0: minimum dimension of the concrete core (inside the confinement reinforcement).

6.1.1.3 BLOCK B – BOYS LOCKER ROOM

Column 30×30

1. Material Properties:
   - **Concrete:** $f_{c28} = 25.00$ MPa
   - **Steel:** $f_e = 500$ MPa (FeE 500)
2. Cross-Section Dimensions:
   - **Section width (b):** $b = 30.00$ cm
   - **Section height (h):** $h = 30.00$ cm

Table 6.6: Transverse Reinforcement Verification

Direction	Y-Y Direction	Z-Z Direction
Transverse Reinforcement ϕ (mm)	8.00	
Number of Stirrups	2.00	
At (cm2)	2.01	
Fe (MPa)	500	
ρ_a	2.5	2.5
V_u (kN)	9.02	14.46
Max. Spacing – RPA (cm)	Current Zone	18.00
	Nodal Zone	12.00
Spacing Chosen (cm)	Current Zone	15.00
	Nodal Zone	10.00

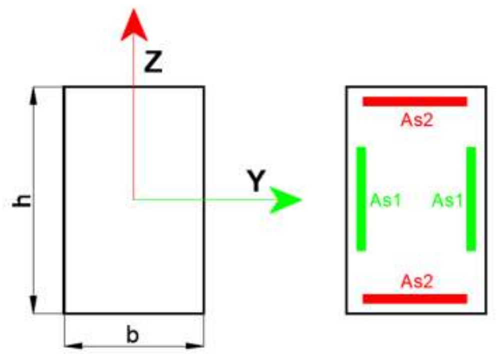

Figure 6.6: Column local axes and longitudinal reinforcement layout.

3. Load Combinations
   - **Ultimate Limit States (ULS):** $1.35G + 1.5Q \quad \gamma_b = 1.5 \quad \gamma_s = 1.15$
   - **Accidental Limit States (ALS):** $G + \psi Q \pm E \quad \gamma_b = 1.2 \quad \gamma_s = 1.0$
4. Design Forces
5. Verification of Reduced Axial Force

   The design compressive axial force is limited by the condition of RPA 2024 Article 7.4.3:

$$v = \frac{N_d}{B_c f_{c28}} \leq 0.35$$

Where:

ν: the reduced axial force.

N_d: design axial force acting on a cross-section.

Table 6.7: Load Cases for Column 30×30 (Block B)

Load Cases	Column 30X30		
	N (kN)	My (kN.m)	Mz (kN.m)
ELU (Nmax; Mycorr; Mzcorr)	**219.86**	4.97	-0.20
ACC1 (Mymax; Ncorr; Mzcorr)	86.89	**23.30**	3.01
ACC2 (Mzmax; Ncorr; Mycorr)	104.28	9.51	**16.50**
ACC3 (Nmin; Mycorr; Mzcorr)	**15.89**	7.96	0.47

B_c: column cross-sectional area.

F_{c28}: characteristic compressive strength of concrete.

Parameter	Value
N_d (KN)	153.47
B_c (cm^2)	900.00
F_{c28} (MPa)	25.00
ν	0.07
Condition	**Condition Verified**

6. Verification of Shear Stresses Verification of ultimate shear stress limit per CBA93 A.5.1.1

$$\tau_{bu} = \frac{V_u}{b \cdot d}$$

Where:

- V_u: Shear force at the Ultimate Limit State.
- τ_{bu}: Shear stress in MPa.
- b: beam width, d: Effective depth $h - (h/10)$.

The conventional design shear stress in concrete, τ_{bu}, under seismic combination shall not exceed the following limit value:

$$\tau_{bu} \leq \overline{\tau_{bu}} = \rho_d \times f_{c28} \qquad \text{(RPA 2024 Eqn(7.6))}$$

where: ρ_d equals 0.075 if the geometric slenderness, in the direction considered, is greater than or equal to 5; it equals 0.04, otherwise.

In the case of masonry infill, not extending over the full column height (e.g. transom windows), the design height for the geometric slenderness shall equal the opening height.

$$\lambda_g = \left(\frac{l_f}{a} \text{ or } \frac{l_f}{b}\right)$$

Where:

λ_g: is the geometric slenderness ratio of the column.

a and b: dimensions of the column cross-section in the direction of deformation considered.

l_f: buckling length of the column $l_f = 0.7L$ (general building case).

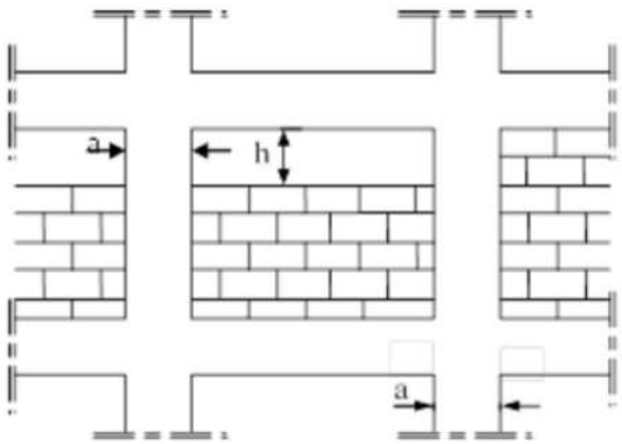

Figure 6.7: Influence of masonry infill and opening height h on columns.

Calculation Results

Table 6.8: ≤ 3≤ m f 4

Y-Y Direction		Z-Z Direction	
λ_g	7.53	λ_g	7.53
ρ_d	0.075	ρ_d	0.075
τ_{bu} (MPa)	1.88	τ_{bu} (MPa)	1.88
T_y (kN)	9.60	T_z (kN)	12.85
$\tau = \dfrac{T_y}{b \times 0.9h}$ (MPa)	0.12	$\tau = \dfrac{T_z}{h \times 0.9b}$ (MPa)	0.16
Condition	Condition Verified ✓	Condition	Condition Verified ✓

7. Longitudinal Reinforcement Design

Table 6.9: Longitudinal Reinforcement Results – Combined Bending

As1 [cm^2]	As2 [cm^2]	As Total [cm^2]
0.51	0.88	2.05

Table 6.10: Reinforcement Conditions per RPA 2024 Art. 7.4.2

bc (cm)	hc (cm)	Seismic Zone	As-min (%)	As-min (cm^2)
30.00	30.00	I	0.80	7.20

Table 6.11: Additional Reinforcement Requirements

$\phi_{\min}$ (mm)	As-max ZC (%)	As-max ZR (%)	Min. Lap Length	Max. Bar Spacing (cm)
12	4	8	50ϕ	20

Reinforcement Selection	Actual A_s (cm^2)	Condition $A_s > \max(A_{s\text{-min}}, A_{s\,\text{tot}})$
8 HA 12	9.04	Condition Verified ✓

8. Transverse Reinforcement Design
According to RPA 2024 Article 7.4.2, column transverse reinforcement is calculated using the formula:

$$\frac{A_t}{t} = \rho_a \frac{V_u}{h_1 \cdot f_e} \tag{6.2}$$

A_t: straight or equivalent cross-section of the transverse reinforcement links.

V_u: design shear force at the ULS in kN.

h_1: total height of the gross section in the direction considered.

f_e: yield strength of the transverse reinforcement steel.

t: spacing of transverse reinforcement.

ρ_a: corrective coefficient accounting for the brittle shear failure mode:

- $\rho_a = 2.5$ if $\lambda_g \geq 5$
- $\rho_a = 3.75$ otherwise.

Maximum Spacing

The maximum spacing is given by the following expression:
Where:

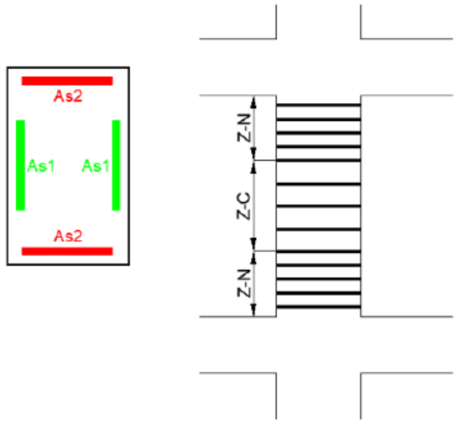

Figure 6.8: Column cross-section reinforcement layout and longitudinal confinement zones.

Seismic Zone	I, II and III	IV, V and VI
Nodal Zone	$\min(10\phi_l, 12.5\text{ cm})$	$\min(b_0/3, 6\phi_l, 10\text{ cm})$
Current Zone	$15\phi_l$	$\min(b_c/2, h_c/2, 10\phi_l)$

ϕ_l: the minimum diameter of longitudinal column reinforcement.

b_0: minimum dimension of the concrete core (inside the confinement reinforcement).

Table 6.12: Transverse Reinforcement Verification

Direction	Y-Y Direction	Z-Z Direction
Transverse Reinforcement ϕ (mm)	8.00	
Number of Stirrups	2.00	
At (cm2)	2.01	
Fe (MPa)	500	
ρ_a	2.5	2.5
V_u (kN)	9.02	14.46
Max. Spacing – RPA (cm)	Current Zone	18.00
	Nodal Zone	12.00
Spacing Chosen (cm)	Current Zone	15.00
	Nodal Zone	10.00

6.1.1.4 SPORTS HALL BLOCK

Column 40×70

1. Material Properties:
   - **Concrete:** $f_{c28} = 25.00$ MPa
   - **Steel:** $f_e = 500$ MPa (FeE 500)
2. Cross-Section Dimensions:
   - **Section width (b):** $b = 40.00$ cm
   - **Section height (h):** $h = 70.00$ cm

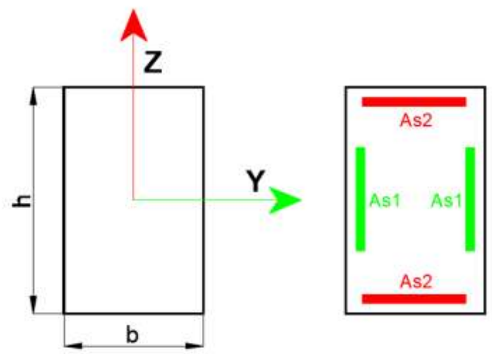

Figure 6.9: Column local axes and longitudinal reinforcement layout.

3. Load Combinations
   - **Ultimate Limit States (ULS):** $1.35G + 1.5Q \quad \gamma_b = 1.5 \quad \gamma_s = 1.15$
   - **Accidental Limit States (ALS):** $G + \psi Q \pm E \quad \gamma_b = 1.2 \quad \gamma_s = 1.0$
4. Design Forces

Table 6.13: Load Cases for Column ĦB ŒB3≤ m f 4

Load Cases	Column 30X30		
	N (kN)	My (kN.m)	Mz (kN.m)
ELU (Nmax; Mycorr; Mzcorr)	**267.02**	165.21	0.78
ACC1 (Mymax; Ncorr; Mzcorr)	183.03	**96.80**	0.09
ACC2 (Mzmax; Ncorr; Mycorr)	44.06	3.38	**9.41**
ACC3 (Nmin; Mycorr; Mzcorr)	**43.69**	3.34	9.41

5. Verification of Reduced Axial Force

   The design compressive axial force is limited by the condition of RPA 2024 Article 7.4.3:

$$v = \frac{N_d}{B_c f_{c28}} \leq 0.35$$

   Where:

   ν: the reduced axial force.

   N_d: design axial force acting on a cross-section.

   B_c: column cross-sectional area.

   F_{c28}: characteristic compressive strength of concrete.

Parameter	**Value**
N_d (KN)	185.43
B_c (cm^2)	2800.00
F_{c28} (MPa)	25.00
ν	0.03
Condition	**Condition Verified**

6. Verification of Shear Stresses Verification of ultimate shear stress limit per CBA93 A.5.1.1

$$\tau_{bu} = \frac{V_u}{b \cdot d}$$

   Where:

   - V_u: Shear force at the Ultimate Limit State.
   - τ_{bu}: Shear stress in MPa.
   - b: beam width, d: Effective depth $h - (h/10)$.

   The conventional design shear stress in concrete, τ_{bu}, under seismic combination shall not exceed the following limit value:

$$\tau_{bu} \leq \overline{\tau_{bu}} = \rho_d \times f_{c28} \qquad \text{(RPA 2024 Eqn(7.6))}$$

   where: ρ_d equals 0.075 if the geometric slenderness, in the direction considered, is greater than or equal to 5; it equals 0.04, otherwise.

   In the case of masonry infill, not extending over the full column height (e.g. transom windows), the design height for the geometric slenderness shall equal the opening height.

$$\lambda_g = \left(\frac{l_f}{a} \text{ or } \frac{l_f}{b} \right)$$

   Where:

λ_g: is the geometric slenderness ratio of the column.

a and b: dimensions of the column cross-section in the direction of deformation considered.

l_f: buckling length of the column $l_f = 0.7L$ (general building case).

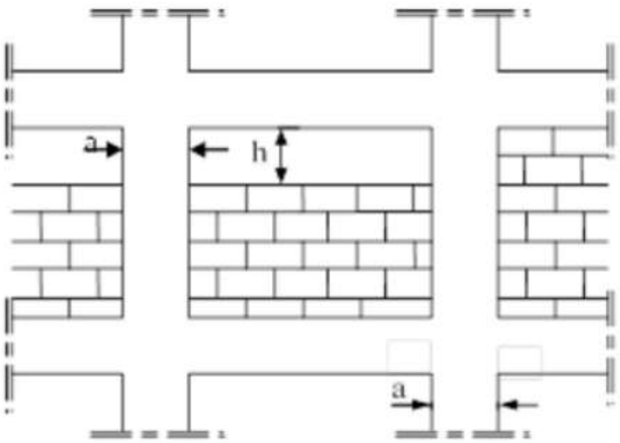

Figure 6.10: Influence of masonry infill and opening height h on columns.

Calculation Results

Table 6.14: Shear Verification (Block B)

Y-Y Direction		Z-Z Direction	
λ_g	12.25	λ_g	7.00
ρ_d	0.075	ρ_d	0.075
τ_{bu} (MPa)	1.88	τ_{bu} (MPa)	1.88
T_y (kN)	7.49	T_z (kN)	23.18
$\tau = \dfrac{T_y}{b \times 0.9h}$ (MPa)	0.03	$\tau = \dfrac{T_z}{h \times 0.9b}$ (MPa)	0.09
Condition	Condition Verified ✓	Condition	Condition Verified ✓

7. Longitudinal Reinforcement Design

Table 6.15: Longitudinal Reinforcement Results – Combined Bending

As1 [cm^2]	As2 [cm^2]	As Total [cm^2]
0.04	1.94	3.96

Table 6.16: Reinforcement Conditions per RPA 2024 Art. 7.4.2

bc (cm)	hc (cm)	Seismic Zone	As-min (%)	As-min (cm^2)
40.00	70.00	I	0.80	22.40

Table 6.17: Additional Reinforcement Requirements

ϕ_{min} (mm)	As-max ZC (%)	As-max ZR (%)	Min. Lap Length	Max. Bar Spacing (cm)
12	4	8	50ϕ	20

Reinforcement Selection	Actual A_s (cm^2)	Condition $A_s > \max(A_{s\text{-min}}, A_{s\text{ tot}})$
6 16+6 16	24.12	Condition Verified ✓

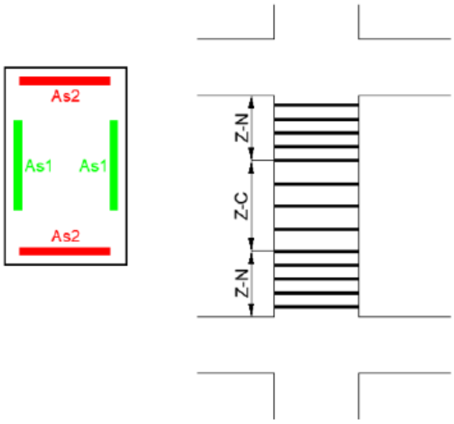

Figure 6.11: Column cross-section reinforcement layout and longitudinal confinement zones.

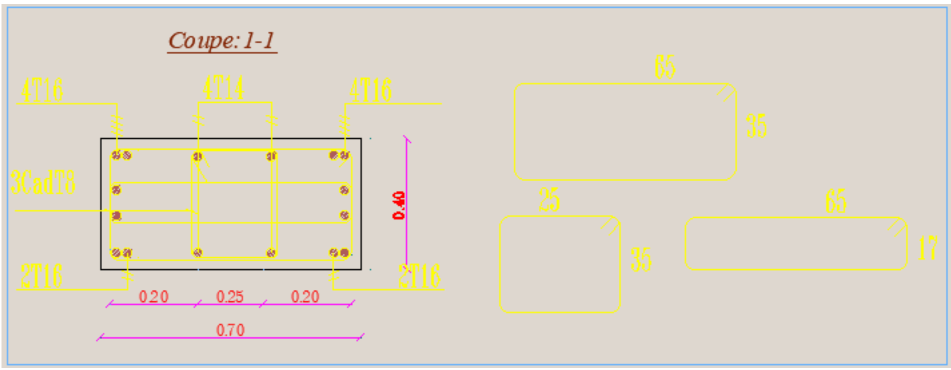

Figure 6.12: Reinforcement Detail of Column.

8. Transverse Reinforcement Design

According to RPA 2024 Article 7.4.2, column transverse reinforcement is calculated using the formula:

$$\frac{A_t}{t} = \rho_a \frac{V_u}{h_1 \cdot f_e} \tag{6.3}$$

A_t: straight or equivalent cross-section of the transverse reinforcement links.

V_u: design shear force at the ULS in kN.

h_1: total height of the gross section in the direction considered.

f_e: yield strength of the transverse reinforcement steel.

t: spacing of transverse reinforcement.

ρ_a: corrective coefficient accounting for the brittle shear failure mode:

- $\rho_a = 2.5$ if $\lambda_g \geq 5$
- $\rho_a = 3.75$ otherwise.

Maximum Spacing

The maximum spacing is given by the following expression:

Seismic Zone	I, II and III	IV, V and VI
Nodal Zone	$\min(10\phi_l, 12.5\text{ cm})$	$\min(b_0/3, 6\phi_l, 10\text{ cm})$
Current Zone	$15\phi_l$	$\min(b_c/2, h_c/2, 10\phi_l)$

Where:

- ϕ_l: the minimum diameter of longitudinal column reinforcement.
- b_0: minimum dimension of the concrete core (inside the confinement reinforcement).

Table 6.18: Transverse Reinforcement Verification

<table>
<tr><th>Direction</th><th>Y-Y Direction</th><th>Z-Z Direction</th></tr>
<tr><td>Transverse Reinforcement ϕ (mm)</td><td colspan="2">8.00</td></tr>
<tr><td>Number of Stirrups</td><td colspan="2">3.00</td></tr>
<tr><td>At (cm2)</td><td colspan="2">3.01</td></tr>
<tr><td>Fe (MPa)</td><td colspan="2">500</td></tr>
<tr><td>ρ_a</td><td>2.5</td><td>2.5</td></tr>
<tr><td>V_u (kN)</td><td>7.49</td><td>23.18</td></tr>
<tr><td rowspan="2">Max. Spacing – RPA (cm)</td><td>Current Zone</td><td>24.00</td></tr>
<tr><td>Nodal Zone</td><td>12.50</td></tr>
<tr><td rowspan="2">Spacing Chosen (cm)</td><td>Current Zone</td><td>15.00</td></tr>
<tr><td>Nodal Zone</td><td>10.00</td></tr>
</table>

Conclusion and Results

This section has presented the complete design of the reinforced concrete columns for the three structural blocks of the sports complex at El Alia El Hadjira, Wilaya of Touggourt. The calculations were carried out in accordance with BAEL 91 revised 99 for the dimensioning of reinforcement under gravity load combinations, and with the Algerian ≤ Regulations RPA 2024 (DTR BC 2.48) for the seismic detailing requirements and additional verifications.

Two cross-sectional types were designed: the 30 cm × 30 cm section adopted for the single-storey blocks (Block A — Girls' Locker Room, and Block B — Boys' Locker Room), and the 40 cm × 70 cm section required by the greater load demands and height of the Sports Hall block. The results of all verifications are summarised in the Table 6.19.

Table 6.19: Summary of Column Design and Verification Results

Parameter	Block A 30×30 cm	Block B 30×30 cm	Sports Hall 40×70 cm	Status
Section	30 cm × 30 cm	30 cm × 30 cm	40 cm × 70 cm	–
B_c (cm^2)	900	900	2800	–
Normalised axial force ν	0.06	0.07	0.03	B9EM ✓
Slenderness λ_g (Y-Y / Z-Z)	7.53 / 7.53	7.53 / 7.53	7.00 / 12.25	$\lambda_g \geq 5 \Rightarrow \rho_d = 0.075$
τ_{bu} limit (MPa)	1.88	1.88	1.88	RPA 2024 Eq. 7.6
$\tau_{\max}$ applied (MPa)	0.18	0.16	0.09	≤ 1.88 ✓
A_s calc (cm^2)	2.83	2.05	3.96	Governed by RPA minimum
$A_{s,\min}$ RPA (cm^2)	7.20	7.20	22.40	Art. 7.4.2
Adopted reinforcement	8 HA 12	8 HA 12	6 HA 16 + 6 HA 16	–
A_s provided (cm^2)	9.04	9.04	24.12	$\geq A_{s,\min}$ ✓
Stirrups	2×ϕ8 / 4 legs	2×ϕ8 / 4 legs	3×ϕ8 / 6 legs	–
A_t provided (cm^2)	2.01	2.01	3.01	Art. 7.4.2 ✓
Nodal spacing (cm)	10	10	10	$\leq$ limit ✓
Current spacing (cm)	15	15	15	$\leq$ limit ✓
All verifications	✓	✓	✓	Compliant

The normalised axial force ν remains well within the RPA 2024 B9EM for all three column types (maximum value: 0.07 for Block B), confirming that the sections are not overstressed under seismic loading. The shear stress verification is equally satisfactory, with applied stresses not exceeding 10% of the allowable $\overline{\tau_{bu}} = 1.88$ MPa in any case.

In all three cases, the longitudinal reinforcement computed by combined bending analysis is smaller than the minimum area imposed by RPA 2024 Article 7.4.2 (0.8% of the gross cross-sectional area for Seismic Zone I). The adopted reinforcement is therefore governed by the RPA minimum rather than by strength demand, which is characteristic of low-seismicity zones (Zone I, $A = 0.07$). The selected bars — 8 HA 12 for the 30 cm $\times$ 30 cm sections and 6 HA 16 + 6 HA 16 for the 40 cm $\times$ 70 cm section — provide adequate cover to all RPA detailing rules regarding minimum bar diameter, maximum spacing, and lap splice length.

Transverse reinforcement consists of closed stirrups of $\phi 8$ mm, providing two-legged confinement for the square sections and three-stirrup confinement for the rectangular section. The chosen spacings — 10 cm in the nodal zone and 15 cm in the current zone — satisfy the RPA 2024 limits in all cases and are more restrictive than the computed minimum, ensuring adequate confinement of the concrete core under seismic reversals.

In conclusion, all column designs comply fully with the requirements of BAEL 91 and RPA 2024. The adopted sections and reinforcement arrangements are retained for execution.

6.1.2 Calculation and verification of beams

Beams are the primary horizontal load-carrying members of a reinforced concrete structure. They receive loads from floor slabs and transfer them to the supporting columns in the form of bending moments and shear forces. In seismic regions, beams must also provide sufficient ductility to ensure adequate energy dissipation during earthquake excitation and to prevent brittle failure mechanisms.

The design of beams in this project is carried out in accordance with two complementary standards:

- **BAEL 91 Revised 99** (*Béton Armé aux États Limites*), which governs the design of longitudinal and transverse reinforcement under gravity load combinations at the Ultimate Limit State (ULS) and Serviceability Limit State (SLS);
- **RPA 2024** (DTR BC 2.48), which introduces additional seismic detailing requirements, including minimum reinforcement ratios, maximum stirrup spacing in critical and current zones, and minimum lap splice lengths.

Three beam types are considered in the present project, corresponding to the different structural blocks and functional requirements of the complex:

- **PP 30×40** – Primary beam (*Poutre Principale*), with a cross-section of 30×40 cm, used in Blocks A and B (locker rooms). This beam carries the highest loads and governs the design of the reinforced concrete blocks.
- **PS 30×30** – Secondary beam (*Poutre Secondaire*), with a cross-section of 30×30 cm, used in Blocks A and B. These beams support lighter loads and transfer forces to the primary beams.

- **PS 30×50** – Secondary beam (*Poutre Secondaire*), with a cross-section of 30×50 cm, used in the Sports Hall block. The increased depth is required to accommodate the longer spans and higher loads associated with the sports hall floor system.

For each beam type, the following verifications are performed:

1. Pre-dimensioning verification according to BAEL 91 and RPA 2024;
2. Design of longitudinal reinforcement under simple bending according to CBA 93;
3. Design and verification of transverse reinforcement spacing according to RPA 2024, Article 7.5.2;
4. Verification of serviceability limit state stresses in concrete and reinforcement;
5. Verification of shear stresses according to CBA 93, Article A.5.

Pre-Dimensioning Requirements

The preliminary dimensions of the beam cross-section shall satisfy the following requirements.

6.1.2.1 BAEL 91 Requirements

The beam depth must satisfy:

$$\frac{L_{\max}}{15} \leq h \leq \frac{L_{\max}}{10}$$

and the beam width must satisfy:

$$\frac{h}{3} \leq b \leq \frac{h}{2}$$

where:

- $L_{\max}$ is the maximum beam span;
- h is the beam depth;
- b is the beam width.

6.1.2.2 RPA 2024 Requirements

The minimum geometric requirements imposed by RPA 2024 are:

$$b \geq 20 \text{ cm}$$

$$h \geq 30 \text{ cm}$$

$$\frac{h}{b} \leq 4$$

Longitudinal Reinforcement Requirements

According to RPA 2024, the total longitudinal reinforcement ratio shall satisfy the following limits:

- Minimum reinforcement ratio:

$$\rho_{\text{min}} = 0.5\%$$

  applicable over the entire beam length.
  The maximum reinforcement ratio is limited to:

- 4% in the current zone;
- 6% in the lap splice zone.

Lap Splice Requirements

The minimum lap splice length prescribed by RPA 2024 is:

$$L_r = 50\phi$$

for seismic Zones I, II, and III,
where:

- L_r is the lap splice length;
- ϕ is the diameter of the reinforcing bar.

6.1.2.3 BLOCK A-B - Most critically loaded primary beam is in the Boys Locker Room block.

Beam Design: PP 30X40

1. Material Properties
   - **Concrete:** Fc28 = 25 MPa
   - **Steel:** FeE 500 MPa
2. Cross-Section Dimensions
   - $b = 30\,\text{cm}$
   - $h = 40\,\text{cm}$
3. Load Combinations

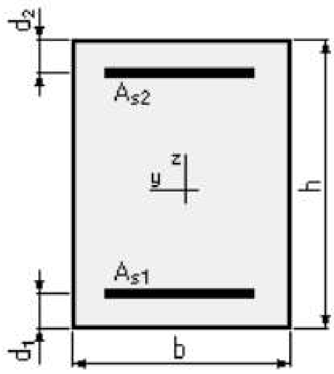

Figure 6.13: Beam cross-section layout and reinforcement nomenclature (SECONDARY BEAM DESIGN: PS 30×40).

- Ultimate Limit States: $1.35G + 1.5Q$; $\gamma_b = 1.5$; $\gamma_s = 1.15$
- Accidental Limit States: $G + \psi Q \pm E$; $\gamma_b = 1.2$; $\gamma_s = 1$

4. Design Forces

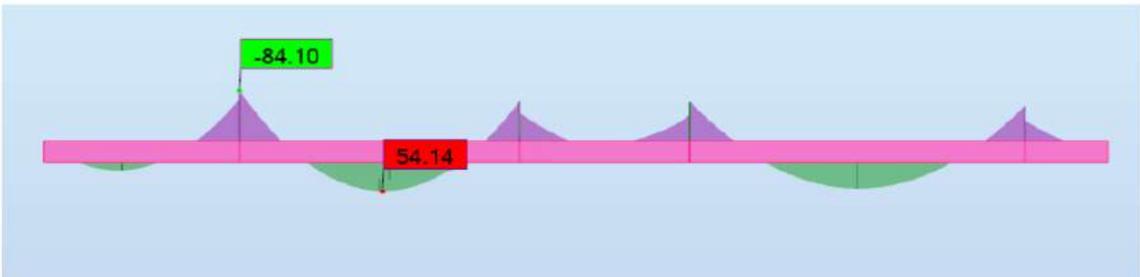

Figure 6.14: ELU (SECONDARY BEAM DESIGN: PS 30×30)

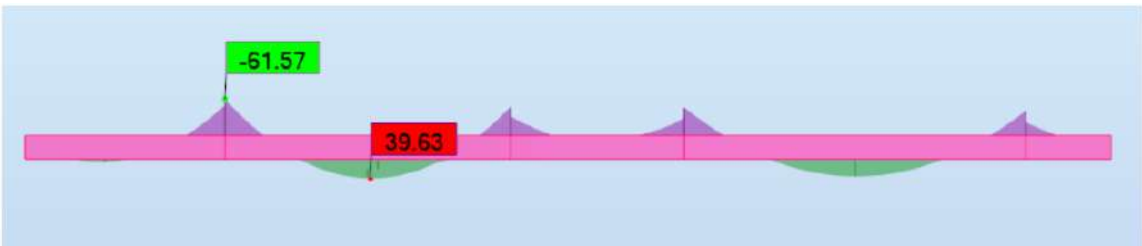

Figure 6.15: ELS (SECONDARY BEAM DESIGN: PS 30×40)

Figure 6.16: ELA (SECONDARY BEAM DESIGN: PS 30×40)

Bending Moment Table

Table 6.20: Design bending moments at supports and spans under different limit states.

Section	Bending Moment (kN·m)			
	ELU	ELS	ELA (min)	ELA (max)
Support	-84.1	-61.57	22.61	-60.85
Span	54.14	39.64	36.97	-21.28

Shear Force Table

Table 6.21: Design shear forces at supports under ELU and ELA limit states.

Section	Shear Force (kN)	
	ELU	ELA
Support	111.12	76.92

5. Longitudinal Reinforcement Design – Simple Bending
   Reinforcement is calculated according to CBA93; results are given below:

Table 6.22: Calculated and minimum required reinforcement areas at supports and spans.

Section	A_{s1} (cm^2)	A_{s2} (cm^2)	$A_{\text{min RPA}}$ (cm^2)	$A_{\text{min CBA}}$ (cm^2)
Support	1.6	7.33	6	1.3
Span	4.56	1.5	6	1.3

Table 6.23: Longitudinal reinforcement selection and actual steel areas at supports and spans.

Section	As1		As2	
Support	3 HA 14	4.62 cm^2	3 HA 14+3 HA 12	8.01 cm^2
Span	3 HA 14	4.62 cm^2	3 HA 14	4.62 cm^2

The minimum lap splice length is: ($L_r = 50 \times \phi$)

6. Transverse Reinforcement Design
   The maximum diameter of transverse reinforcement is limited by the following condition:
   Maximum Diameter $= \min\left[\frac{b}{10}; \frac{h}{35}; \phi_{l,\min}\right]$

Table 6.24: Transverse reinforcement diameter selection and calculated steel area.

Maximum Diameter (mm)	Selected Diameter ϕ (mm)	Number of Bars	Calculated A_t (cm^2)
11.43	8	4	2.01

Transverse Reinforcement Area Calculation per CBA93

The web reinforcement area with its spacing is determined by the following formulas:

- CBA93 A.5.1.2.3

$$\frac{A_t}{b_0 S_t} \geq \frac{\gamma_s(\tau_u - 0.3 f_{tjk})}{0.9 f_e(\cos\alpha + \sin\alpha)} \tag{6.4}$$

- CBA93 A.5.1.2.2

$$S_t \leq \text{Min}\left(0.9d\ ;\ 40\text{cm}\ ;\ \frac{A_t \times f_e}{0.4 \times b'}\ ;\ \right) \tag{6.5}$$

Maximum Spacing per RPA 2024 : The maximum spacing of transverse reinforcement is determined as follows:

- In critical zones:

$$S = \text{Min}\left(\frac{h}{4}\ ;\ 24\Phi_t\ ;\ 17.5\text{cm}\ ;\ 6\Phi_{l,\text{min}}\right) \tag{6.6}$$

- Outside critical zones:

$$\begin{aligned} s' &\leq \frac{h}{2} \\ s' &= \min\left(\frac{h}{4}\ ;\ 12\phi_l\right)^* \end{aligned} \tag{6.7}$$

*if compressed reinforcement is required

Where:

h: beam height.

ϕ_t: diameter of confinement reinforcement.

ϕ_l: minimum diameter of longitudinal reinforcement bars.

Table 6.25: Maximum and selected spacing for nodal and current zones.

Nodal Zone Spacing		**Current Zone Spacing**	
Maximum Spacing (cm)	**Selected Spacing (cm)**	**Maximum Spacing (cm)**	**Selected Spacing (cm)**
7.2	7	14.4	14

Minimum Transverse Reinforcement Verification – RPA 2024 Art. 7.5.2

The minimum transverse reinforcement quantity is given by:

$$A_t = 0.003 \cdot s \cdot b \tag{6.8}$$

A_t/s (RPA) $= 0.09$ cm^2/cm

A_t/s (zone nodale) $= 0.29$ cm^2/cm .... Condition Verified ✓

A_t/s (zone courante) $= 0.14$ cm^2/cm .... Condition Verified ✓

7. Serviceability Limit State Stress Verification
   - Concrete Compression Limit State – CBA93 Art. A.5.4.2 The allowable compressive stress in concrete is:

$$\sigma_{\text{adm}} = 0.6 \cdot f_{c28} \tag{6.9}$$

The compressive stress in concrete is calculated by the following formula:

$$\sigma_{bc} = \frac{M_{\text{ser}} \cdot Y}{I} \tag{6.10}$$

Table 6.26: Concrete serviceability compressive stress verification.

σ_{bc} (MPa)	σ_{adm} (MPa)	Condition
8.34	15.00	Condition Verified ✓

   - Crack Width Limit State – CBA93 Art. A.5.4.3

Cracking: Non-prejudicial The tensile stress in the steel is calculated by the following formula:

$$\sigma_{st} = \frac{M_{\text{ser}}}{I}(d - y) \tag{6.11}$$

Table 6.27: Steel serviceability tensile stress verification.

σ_{st} (MPa)	$\sigma_{st\text{-adm}}$ (MPa)	Condition
263.26	267	Condition Verified ✓

8. Shear Stress Verification – CBA93 Article A.5
   - Verification of Ultimate Shear Stress Limit – CBA93 Article A.5.1.21 $\tau_u < \tau_{\text{adm}}$

τ_u (MPa)	τ_{adm} (MPa)	Condition
0.13	3.33	Condition Verified ✓

   - Verification of Compressive Stress – CBA93 Article A.5.1.313

$$V_u < 0.267 \cdot b \cdot a \cdot f_{c28} \tag{6.12}$$

V_u (N)	$0.267 \times b \times a \times f_{c28}$ (N)	Condition
111.12	720.90	Condition Verified ✓

- Verification of Bottom Support Reinforcement – CBA93 Article A.5.1.312

$$A_{s1} \geq \frac{V_u}{f_e/\gamma_s} \tag{6.13}$$

Table 6.28: Support reinforcement verification under ultimate shear force.

A_{s1} (cm^2)	$V_u/(f_e/\gamma_s)$ (cm^2)	Condition
4.62	3.19	Condition Verified ✓

- Verification of Average Compressive Stress – CBA93 Article A.5.1.322

$$\sigma_{mb} < \frac{1.3 \cdot f_{c28}}{\gamma_b} \tag{6.14}$$

σ_{mb} (MPa)	$1.3 \times f_{c28}/\gamma_b$ (MPa)	Condition
2.47	21.68	Condition Verified ✓

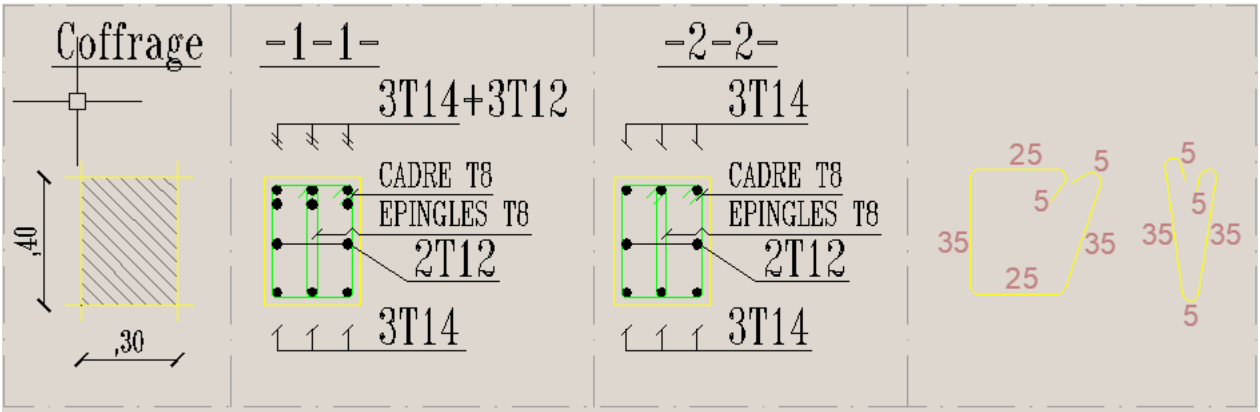

Figure 6.17: Reinforcement Detail of Beams.

6.1.2.4 BLOCK A-B - Most critically loaded secondary beam is in the Boys Locker Room block.

Beam Design: PS 30X30

1. Material Properties

   - **Concrete:** Fc28 = 25 MPa
   - **Steel:** FeE 500 MPa

2. Cross-Section Dimensions

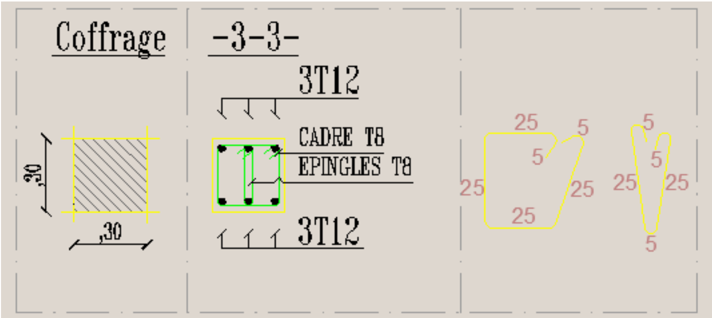

Figure 6.18: Reinforcement Detail of Beams.

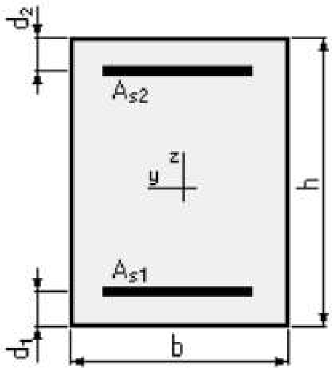

Figure 6.19: Beam cross-section layout and reinforcement nomenclature (SECONDARY BEAM DESIGN: PS 30×30).

- $b = 30\,\text{cm}$
- $h = 30\,\text{cm}$

3. Load Combinations

- Ultimate Limit States: $1.35G + 1.5Q$; $\gamma_b = 1.5$; $\gamma_s = 1.15$
- Accidental Limit States: $G + \psi Q \pm E$; $\gamma_b = 1.2$; $\gamma_s = 1$

4. Design Forces

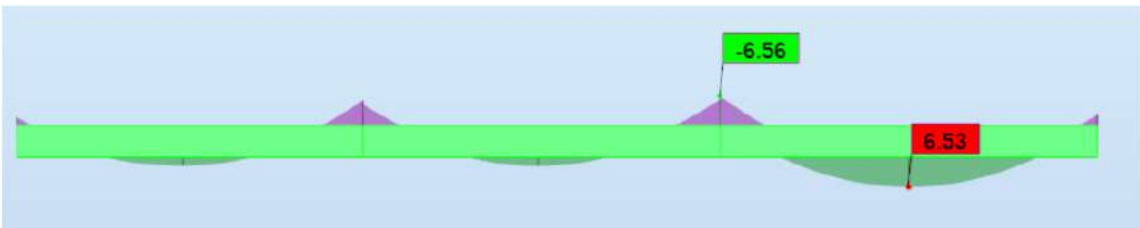

Figure 6.20: ELU (SECONDARY BEAM DESIGN: PS 30×30)

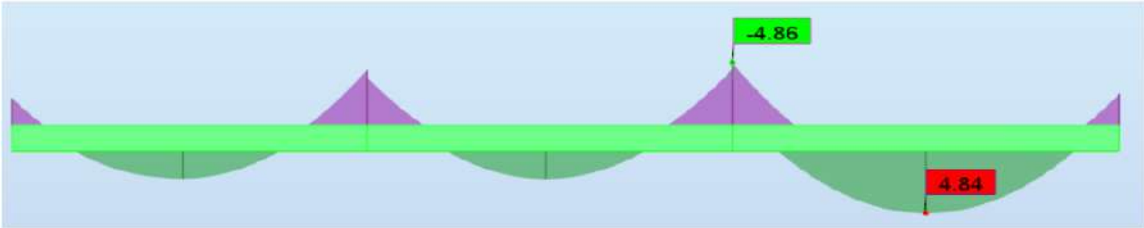

Figure 6.21: ELS (SECONDARY BEAM DESIGN: PS 30×30)

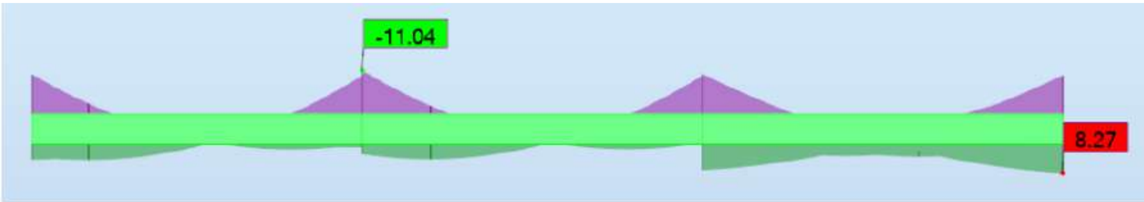

Figure 6.22: ELA (SECONDARY BEAM DESIGN: PS 30×30)

Bending Moment Table

Table 6.29: Design bending moments at supports and spans under different limit states.

Section	Bending Moment (kN·m)			
	ELU	ELS	ELA (min)	ELA (max)
Support	-6.56	-4.86	8.27	-11.04
Span	6.53	4.84	6.25	-3.34

Shear Force Table

Table 6.30: Design shear forces at supports under ELU and ELA limit states.

Section	Shear Force (kN)	
	ELU	ELA
Support	10.96	11.57

5. Longitudinal Reinforcement Design – Simple Bending

   Reinforcement is calculated according to CBA93; results are given below:

Table 6.31: Calculated and minimum required reinforcement areas at supports and spans.

Section	A_{s1} (cm^2)	A_{s2} (cm^2)	$A_{\text{min RPA}}$ (cm^2)	$A_{\text{min CBA}}$ (cm^2)
Support	0.62	0.83	4.5	0.78
Span	0.56	0.25	4.5	0.78

Table 6.32: Longitudinal reinforcement selection and actual steel areas at supports and spans.

Section	As1		As2	
Support	3 HA 12	3.39 cm^2	3 HA 12	3.39 cm^2
Span	3 HA 12	3.39 cm^2	3 HA 12	3.39 cm^2

   The minimum lap splice length is: ($L_r = 50 \times \phi$)

6. Transverse Reinforcement Design

   The maximum diameter of transverse reinforcement is limited by the following condition:

   Maximum Diameter $= \min\left[\frac{b}{10}; \frac{h}{35}; \phi_{l,\min}\right]$

Table 6.33: Transverse reinforcement diameter selection and calculated steel area.

Maximum Diameter (mm)	Selected Diameter ϕ (mm)	Number of Bars	Calculated A_t (cm^2)
8.57	8	4	2.01

Transverse Reinforcement Area Calculation per CBA93

The web reinforcement area with its spacing is determined by the following formulas:

- CBA93 A.5.1.2.3

$$\frac{A_t}{b_0 S_t} \geq \frac{\gamma_s(\tau_u - 0.3 f_{tjk})}{0.9 f_e(\cos\alpha + \sin\alpha)} \tag{6.15}$$

- CBA93 A.5.1.2.2

$$S_t \leq \text{Min}\left(0.9d\ ;\ 40\text{cm}\ ;\ \frac{A_t \times f_e}{0.4 \times b'}\ ;\right) \tag{6.16}$$

Maximum Spacing per RPA 2024 : The maximum spacing of transverse reinforcement is determined as follows:

- In critical zones:

$$S = \text{Min}\left(\frac{h}{4}\ ;\ 24\Phi_t\ ;\ 17.5\text{cm}\ ;\ 6\Phi_{l,\min}\right) \tag{6.17}$$

- Outside critical zones:

$$\begin{aligned} s' &\leq \frac{h}{2} \\ s' &= \min\left(\frac{h}{4}\ ;\ 12\phi_l\right)^* \end{aligned} \tag{6.18}$$

*if compressed reinforcement is required

Where:

h: beam height.

ϕ_t: diameter of confinement reinforcement.

ϕ_l: minimum diameter of longitudinal reinforcement bars.

Table 6.34: Maximum and selected spacing for nodal and current zones.

Nodal Zone Spacing		Current Zone Spacing	
Maximum Spacing (cm)	Selected Spacing (cm)	Maximum Spacing (cm)	Selected Spacing (cm)
7.2	7	14.4	14

Minimum Transverse Reinforcement Verification – RPA 2024 Art. 7.5.2

The minimum transverse reinforcement quantity is given by:

$$A_t = 0.003 \cdot s \cdot b \tag{6.19}$$

A_t/s (RPA) $= 0.09$ cm^2/cm

A_t/s (zone nodale) $= 0.29$ cm^2/cm .... Condition Verified ✓

A_t/s (zone courante) $= 0.14$ cm^2/cm ....Condition Verified ✓

7. Serviceability Limit State Stress Verification

   - Concrete Compression Limit State – CBA93 Art. A.5.4.2 The allowable compressive stress in concrete is:

$$\sigma_{\text{adm}} = 0.6 \cdot f_{c28} \tag{6.20}$$

The compressive stress in concrete is calculated by the following formula:

$$\sigma_{bc} = \frac{M_{\text{ser}} \cdot Y}{I} \tag{6.21}$$

Table 6.35: Concrete serviceability compressive stress verification.

σ_{bc} **(MPa)**	σ_{adm} **(MPa)**	**Condition**	
1.43	15.00	Condition Verified	✓

- Crack Width Limit State – CBA93 Art. A.5.4.3

  Cracking: Non-prejudicial The tensile stress in the steel is calculated by the following formula:

$$\sigma_{st} = \frac{M_{\text{ser}}}{I}(d - y) \tag{6.22}$$

Table 6.36: Steel serviceability tensile stress verification.

σ_{st} **(MPa)**	$\sigma_{st\text{-adm}}$ **(MPa)**	**Condition**	
MP9NC	DNO	Condition Verified	✓

8. Shear Stress Verification – CBA93 Article A.5

- Verification of Ultimate Shear Stress Limit – CBA93 Article A.5.1.21 $\tau_u < \tau_{\text{adm}}$

τ_u **(MPa)**	τ_{adm} **(MPa)**	**Condition**	
0.14	3.33	Condition Verified	✓

- Verification of Compressive Stress – CBA93 Article A.5.1.313

$$V_u < 0.267 \cdot b \cdot a \cdot f_{c28} \tag{6.23}$$

V_u **(N)**	$0.267 \times b \times a \times f_{c28}$ **(N)**	**Condition**	
11.57	520.65	Condition Verified	✓

- Verification of Bottom Support Reinforcement – CBA93 Article A.5.1.312

$$A_{s1} \geq \frac{V_u}{f_e/\gamma_s} \tag{6.24}$$

Table 6.37: Support reinforcement verification under ultimate shear force.

A_{s1} (cm^2)	$V_u/(f_e/\gamma_s)$ (cm^2)	Condition
3.39	0.27	Condition Verified ✓

- Verification of Average Compressive Stress – CBA93 Article A.5.1.322

$$\sigma_{mb} < \frac{1.3 \cdot f_{c28}}{\gamma_b} \tag{6.25}$$

σ_{mb} (MPa)	$1.3 \times f_{c28}/\gamma_b$ (MPa)	Condition
0.26	21.68	Condition Verified ✓

6.1.2.5 Sports Hall Block.

Beam Design: PP 30X50

1. Material Properties
   - **Concrete:** Fc28 = 25 MPa
   - **Steel:** FeE 500 MPa
2. Cross-Section Dimensions
   - $b = 30\,\text{cm}$
   - $h = 50\,\text{cm}$

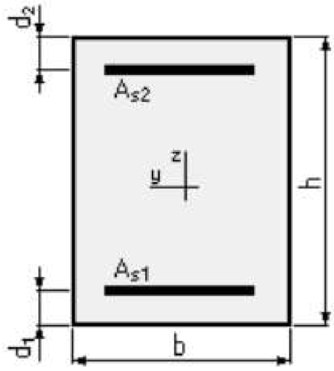

Figure 6.23: Beam cross-section layout and reinforcement nomenclature (BEAM DESIGN: PS 30×50).

3. Load Combinations
   - Ultimate Limit States: $1.35G + 1.5Q$; $\gamma_b = 1.5$; $\gamma_s = 1.15$
   - Accidental Limit States: $G + \psi Q \pm E$; $\gamma_b = 1.2$; $\gamma_s = 1$
4. Design Forces

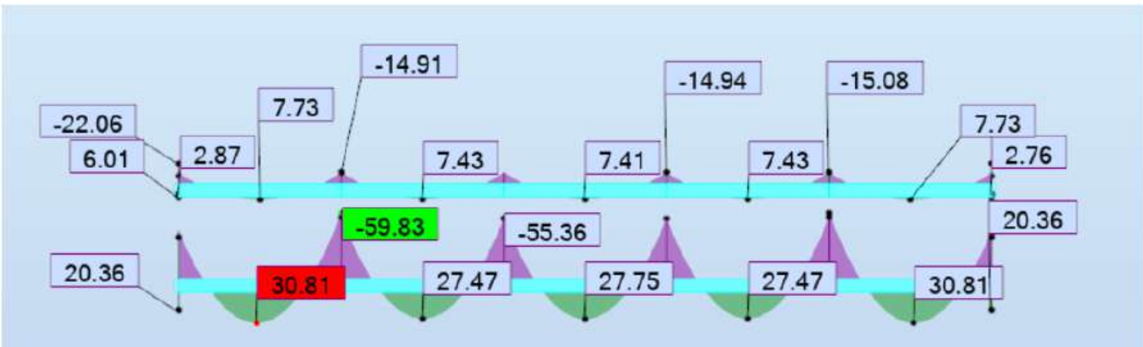

Figure 6.24: ELU (BEAM DESIGN: PS 30×50)

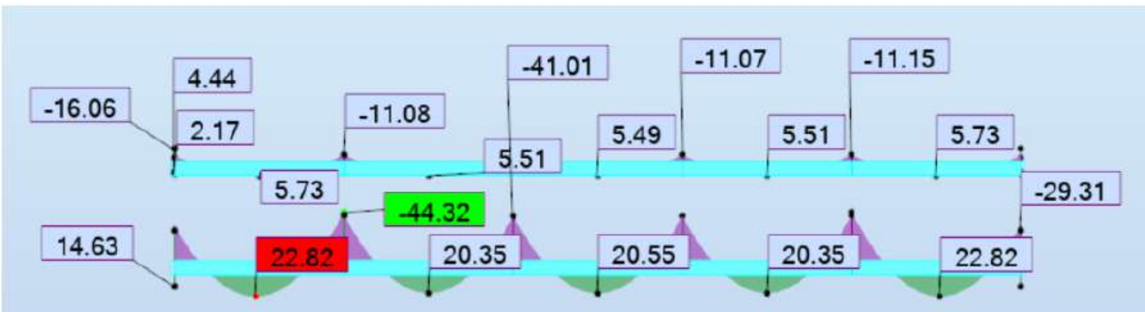

Figure 6.25: ELS (BEAM DESIGN: PS 30×50)

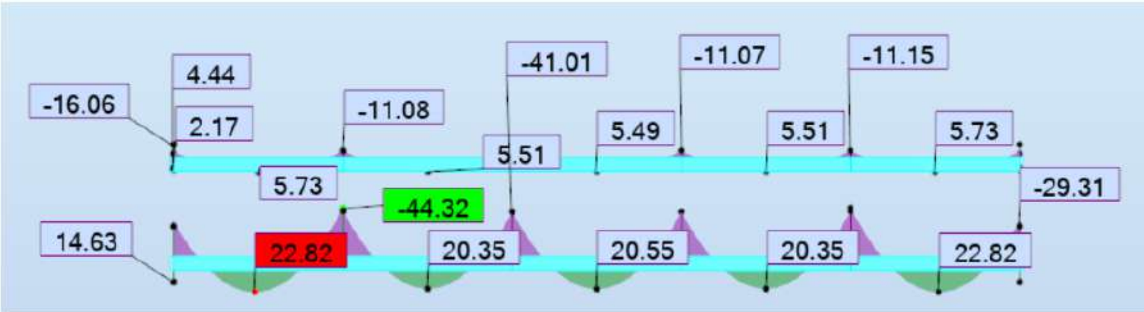

Figure 6.26: ELA (BEAM DESIGN: PS 30×50)

Bending Moment Table

Table 6.38: Design bending moments at supports and spans under different limit states.

Section	Bending Moment (kN·m)			
	ELU	ELS	ELA (min)	ELA (max)
Support	-59.83	-44.32	10.31	-44.34
Span	30.81	22.82	22.81	-3.65

Shear Force Table

Table 6.39: Design shear forces at supports under ELU and ELA limit states.

Section	Shear Force (kN)	
	ELU	ELA
Support	57.86	42.86

5. Longitudinal Reinforcement Design – Simple Bending

   Reinforcement is calculated according to CBA93; results are given below:

Table 6.40: Calculated and minimum required reinforcement areas at supports and spans.

Section	A_{s1} (cm^2)	A_{s2} (cm^2)	$A_{\text{min RPA}}$ (cm^2)	$A_{\text{min CBA}}$ (cm^2)
Support	0.46	3.17	7.5	1.3
Span	1.6	0.16	7.5	1.3

Table 6.41: Longitudinal reinforcement selection and actual steel areas at supports and spans.

Section	As1		As2	
Support	3 HA 14	4.62 cm^2	3 HA 14	4.62 cm^2
Span	3 HA 14	4.62 cm^2	3 HA 14	4.62 cm^2

   The minimum lap splice length is: ($L_r = 50 \times \phi$)

6. Transverse Reinforcement Design

   The maximum diameter of transverse reinforcement is limited by the following condition:

   Maximum Diameter $= \min\left[\frac{b}{10}; \frac{h}{35}; \phi_{l,\min}\right]$

Table 6.42: Transverse reinforcement diameter selection and calculated steel area.

Maximum Diameter (mm)	Selected Diameter ϕ (mm)	Number of Bars	Calculated A_t (cm^2)
14	8	4	2.01

Transverse Reinforcement Area Calculation per CBA93

The web reinforcement area with its spacing is determined by the following formulas:

- CBA93 A.5.1.2.3

$$\frac{A_t}{b_0 S_t} \geq \frac{\gamma_s(\tau_u - 0.3 f_{tjk})}{0.9 f_e(\cos\alpha + \sin\alpha)} \tag{6.26}$$

- CBA93 A.5.1.2.2

$$S_t \leq \text{Min}\left(0.9d\ ;\ 40\text{cm}\ ;\ \frac{A_t \times f_e}{0.4 \times b'}\ ;\right) \tag{6.27}$$

Maximum Spacing per RPA 2024 : The maximum spacing of transverse reinforcement is determined as follows:

- In critical zones:

$$S = \text{Min}\left(\frac{h}{4}\ ;\ 24\Phi_t\ ;\ 17.5\text{cm}\ ;\ 6\Phi_{l,\min}\right) \tag{6.28}$$

- Outside critical zones:

$$\begin{aligned} s' &\leq \frac{h}{2} \\ s' &= \min\left(\frac{h}{4}\ ;\ 12\phi_l\right)^* \end{aligned} \tag{6.29}$$

  *if compressed reinforcement is required

Where:

h: beam height.

ϕ_t: diameter of confinement reinforcement.

ϕ_l: minimum diameter of longitudinal reinforcement bars.

Table 6.43: Maximum and selected spacing for nodal and current zones.

Nodal Zone Spacing		Current Zone Spacing	
Maximum Spacing (cm)	Selected Spacing (cm)	Maximum Spacing (cm)	Selected Spacing (cm)
8.4	7	16.8	15

Minimum Transverse Reinforcement Verification – RPA 2024 Art. 7.5.2

The minimum transverse reinforcement quantity is given by:

$$A_t = 0.003 \cdot s \cdot b \tag{6.30}$$

A_t/s (RPA) $= 0.09$ cm^2/cm

A_t/s (zone nodale) $= 0.29$ cm^2/cm .... Condition Verified ✓

A_t/s (zone courante) $= 0.14$ cm^2/cm .... Condition Verified ✓

7. Serviceability Limit State Stress Verification

   - Concrete Compression Limit State – CBA93 Art. A.5.4.2 The allowable compressive stress in concrete is:

   $$\sigma_{\text{adm}} = 0.6 \cdot f_{c28} \tag{6.31}$$

   The compressive stress in concrete is calculated by the following formula:

   $$\sigma_{bc} = \frac{M_{\text{ser}} \cdot Y}{I} \tag{6.32}$$

Table 6.44: Concrete serviceability compressive stress verification.

σ_{bc} (MPa)	σ_{adm} (MPa)	Condition
5.21	15	Condition Verified ✓

- Crack Width Limit State – CBA93 Art. A.5.4.3

  Cracking: Non-prejudicial The tensile stress in the steel is calculated by the following formula:

$$\sigma_{st} = \frac{M_{\text{ser}}}{I}(d - y) \tag{6.33}$$

Table 6.45: Steel serviceability tensile stress verification.

σ_{st} (MPa)	$\sigma_{st\text{-adm}}$ (MPa)	Condition
233.87	500	Condition Verified ✓

8. Shear Stress Verification – CBA93 Article A.5

- Verification of Ultimate Shear Stress Limit – CBA93 Article A.5.1.21 $\tau_u < \tau_{\text{adm}}$

τ_u (MPa)	τ_{adm} (MPa)	Condition
0.43	3.33	Condition Verified ✓

- Verification of Compressive Stress – CBA93 Article A.5.1.313

$$V_u < 0.267 \cdot b \cdot a \cdot f_{c28} \tag{6.34}$$

V_u (N)	$0.267 \times b \times a \times f_{c28}$ (N)	Condition
57.86	923.18	Condition Verified ✓

- Verification of Bottom Support Reinforcement – CBA93 Article A.5.1.312

$$A_{s1} \geq \frac{V_u}{f_e/\gamma_s} \tag{6.35}$$

Table 6.46: Support reinforcement verification under ultimate shear force.

A_{s1} (cm^2)	$V_u/(f_e/\gamma_s)$ (cm^2)	Condition
4.62	1.33	Condition Verified ✓

- Verification of Average Compressive Stress – CBA93 Article A.5.1.322

$$\sigma_{mb} < \frac{1.3 \cdot f_{c28}}{\gamma_b} \tag{6.36}$$

σ_{mb} (MPa)	$1.3 \times f_{c28}/\gamma_b$ (MPa)	Condition
1.29	21.68	Condition Verified ✓

Conclusion and Results

This chapter has presented the complete design of the reinforced concrete beams for all structural blocks of the proximity sports complex at El Alia El Hadjira, Wilaya of Touggourt. The calculations were carried out in accordance with BAEL 91 revised 99 for the dimensioning of longitudinal and transverse reinforcement under gravity load combinations, and with the Algerian $\leq$ Regulations RPA 2024 (DTR BC 2.48) for the seismic detailing requirements.

Three beam cross-sections were designed to accommodate the varying load levels and span conditions across the three structural blocks. In all cases, the longitudinal reinforcement computed from bending analysis is smaller than the minimum area imposed by RPA 2024 (0.5% of the gross cross-sectional area). The adopted reinforcement is therefore governed by the RPA 2024 minimum rather than by strength demand, which is characteristic of low-seismicity zones (Zone I, $A = 0.07$ g). The summary of results is presented in the table below.

Table 6.47: Comprehensive summary of beam design parameters and compliance verifications.

Parameter	**PP** 30×40	**PS** 30×30	**PS** 30×50
Block	A & B (locker rooms)	A & B (locker rooms)	Sports Hall
Section $b \times h$	30 cm $\times$ 40 cm	30 cm $\times$ 30 cm	30 cm $\times$ 50 cm
Steel grade	FeE 400	FeE 500	FeE 500
M_u support (ELU)	-84.10 kN $\cdot$ m	-6.56 kN $\cdot$ m	-59.83 kN $\cdot$ m
V_u support (ELU)	111.12 kN	10.96 kN	57.86 kN
A_{s1} support	3 HA 14 — 4.62 cm^2	3 HA 12 — 3.39 cm^2	3 HA 14 — 4.62 cm^2
A_{s2} support	3 HA 14 + 3 HA 12 — 8.01 cm^2	3 HA 12 — 3.39 cm^2	3 HA 14 — 4.62 cm^2
A_s span (both faces)	3 HA 14 — 4.62 cm^2	3 HA 12 — 3.39 cm^2	3 HA 14 — 4.62 cm^2
Stirrups ϕ_t	ϕ8 mm — 4 legs	ϕ8 mm — 4 legs	ϕ8 mm — 4 legs
Nodal spacing	7 cm $\leq$ 7.2 cm ✓	7 cm $\leq$ 7.2 cm ✓	7 cm $\leq$ 8.4 cm ✓
Current spacing	14 cm $\leq$ 14.4 cm ✓	14 cm $\leq$ 14.4 cm ✓	15 cm $\leq$ 16.8 cm ✓
τ_u (MPa)	$1.03 \leq 3.33$ ✓	$0.14 \leq 3.33$ ✓	$0.43 \leq 3.33$ ✓
σ_{bc} ELS (MPa)	$8.34 \leq 15.0$ ✓	$1.43 \leq 15.0$ ✓	$5.21 \leq 15.0$ ✓
All checks	✓ **Compliant**	✓ **Compliant**	✓ **Compliant**

All shear stress verifications are satisfied with comfortable margins. The maximum shear stress ratio is recorded for the PP 30×40 beam ($\tau_u = 1.03$ MPa versus $\tau_{\text{adm}} = 3.33$ MPa), which remains well within the allowable limit. The serviceability limit state verifications confirm that concrete compressive stresses and steel tensile stresses are within the CBA 93 limits under the quasi-permanent load combination.

The transverse reinforcement (stirrups ϕ8 mm, 4 legs) is uniform across all three beam types. The selected spacings — 7 cm in the nodal zone and 14 cm or 15 cm in the current zone — satisfy the RPA 2024 limits in all cases and also verify the minimum transverse reinforcement condition $A_t \geq 0.003 \cdot s \cdot b$ per RPA 2024 Art. 7.5.2.

In conclusion, all beam designs comply fully with the requirements of BAEL 91 revised 99 and RPA 2024. The adopted sections and reinforcement arrangements are retained for the structural execution drawings.

All verifications are COMPLIANT with BAEL 91 revised 99 and RPA 2024.

6.2 Dimensioning and Verification of Steel Members and Connections

This chapter presents the regulatory verification of all steel members and connections of the sports hall structure. The analysis was carried out using Robot Structural Analysis Professional 2024, in accordance with Eurocode 3 (EN 1993-1-1 and EN 1993-1-8). The verification covers two main aspects :

- Cross-section resistance and overall member stability under Ultimate Limit State (ULS) loading;
- Connection resistance: rigid rafter-to-column frame joint, ridge joint, bracing gusset plate, and pinned column base.

6.2.1 Member Verification — Cross-Section and Stability (ULS)

6.2.1.1 Applicable Standards and Verification Methodology

All member verifications comply with Eurocode 3 (NF EN 1993-1-1:2005/NA:2013/A1:2014). Two levels of verification are performed:

- **Cross-section resistance (Clause 6.2):** verification against axial force, bending moment, and shear force;
- **Overall member stability (Clause 6.3):** verification against flexural buckling, lateral-torsional buckling, and combined bending-compression interaction (interaction formulae 6.3.3).

Note: Robot Structural Analysis performs these checks automatically for each defined load combination, and retains the critical (maximum) utilisation ratio across all combinations.

6.2.1.2 Material Properties and Load Combinations

The steel grade used is E24 (equivalent to S235), with a yield strength $f_y = 235$ MPa and an elastic modulus $E = 210,000$ MPa.

The governing ULS load combination applied is:

$$1.35 \cdot G + 1.35 \cdot Q + 1.35 \cdot S \tag{6.37}$$

where G denotes permanent loads, Q imposed (live) loads, and S sand loads in accordance with RNV 2013 (Touggourt region, Zone III).

6.2.1.3 Verification Results — Summary Table

The Table 6.48 summarises the verification results for all member families. The utilisation ratio must be strictly less than 1.00 for the member to be compliant.

Table 6.48: Summary of structural steel member verifications and utilisation ratios.

Member	Section	Governing Comb.	Ratio	Result
Columns	HEA 400	$1.35G + 1.35Q + 1.35S$	0.25	OK ✓
Rafters	IPE 400	$1.35G + 1.35Q + 1.35S$	0.44	OK ✓
Purlins	IPE 140	$1.35G + 1.35Q + 1.35S$	0.44	OK ✓
Eave beams	HEA 140	$1.35G + 1.35Q + 1.35S$	0.10	OK ✓
Wall girts	UPN 100	$1.35G + 1.35Q + 1.35S$	0.10	OK ✓
Bracing bars	CAE 60x6	$1.35G + 1.35Q + 1.35S$	0.10	OK ✓

Overall result: All members exhibit a utilisation ratio below 1.00. The steel structure fully complies with the requirements of Eurocode 3 at the Ultimate Limit State.

6.2.1.4 Commentary on Results

The columns (HEA 400) and rafters (IPE 400) show the highest utilisation ratios (0.25 and 0.44 respectively), indicating that the design of the rigid portal frames is governed by bending and lateral-torsional buckling rather than by axial compression alone.

The bracing bars (CAE 60x6) exhibit a very low utilisation ratio (0.10), confirming that these tension-only members are more than adequate to resist the horizontal forces induced by wind and seismic actions. Full detailed verification outputs from Robot Structural Analysis are provided in Appendix C.

6.2.2 Connection Verification

All connections were verified in accordance with Eurocode 3, Part 1-8 (NF EN 1993-1-8:2005/NA:2007/AC:2009), using the connection design module integrated in Robot Structural Analysis. Four representative connections were studied.

6.2.2.1 Summary Table of Connections

Overall result: All four connections satisfy the normative requirements. The highest utilisation ratio is recorded for the column base (0.95), which requires special attention during construction.

Table 6.49: Summary of structural steel connection verifications and utilisation ratios.

Connection	Standard	Sections	Ratio	Result	
Rafter-to-Column (Rigid)	EC3 EN 1993-1-8	HEA 400 / IPE 400	0.38	Satisfactory	✓
Rafter-to-Rafter (Ridge)	EC3 EN 1993-1-8	IPE 400 / IPE 400	0.06	Satisfactory	✓
Gusset — Bracing	EC3 EN 1993-1-8	CAE 60x6	0.09	Satisfactory	✓
Column Base (Pinned)	EC3-1-8 + CEB	HEA 400	0.95	Satisfactory	✓

6.2.2.2 Rafter-to-Column Rigid Connection (Connection No. 2)

This connection is the most heavily loaded joint in the structure. It ensures the rigidity of the portal frame and the transfer of bending moments between the IPE 400 rafter and the HEA 400 column. The joint is realised by means of a bolted end plate with column web stiffeners.

Parameter	Value
Column section	HEA 400 — Steel E24 (S235)
Rafter section	IPE 400 — Steel E24 (S235)
Number of bolts	6 rows $\times$ 2 = 12 bolts
Bolt grade	HR 10.9
Bolt diameter	ϕ 18 mm
End plate thickness	$e_p = 15$ mm — Steel E24
Web weld size	$a_w = 7$ mm
Flange weld size	$a_f = 10$ mm
Design moment resistance	$M_{j,\text{Rd}} = 449$ kN $\cdot$ m
Verification ratio	$0.38 < 1.00$

Interpretation: A utilisation ratio of 0.38 indicates satisfactory resistance with a significant reserve capacity. The connection is therefore well suited to the actions transmitted by the rigid portal frame.

6.2.2.3 Rafter-to-Rafter Connection at Ridge (Connection No. 3)

This connection is located at the ridge, at the junction of two opposing rafter segments. It primarily resists shear force and a low bending moment. The joint is achieved by a bolted end plate without column web stiffeners.

The verification ratio obtained is 0.06, confirming that this connection is very generously proportioned. This low utilisation is explained by the symmetry of the applied forces at this point, which largely counterbalance each other.

6.2.2.4 Gusset Plate Connection — Bracing System (Connection No. 4)

This connection links the bracing bars (CAE 60x6) to the main structure. The joint is realised by grade 8.8 bolts of diameter 14 mm, connected through a gusset plate welded to the structural members.

The utilisation ratio is 0.09, confirming that the bolts and gusset plate comfortably resist the tensile forces generated by wind and seismic actions. This low ratio is consistent with the low seismic hazard of the site (Zone I, $A = 0.07$g).

6.2.2.5 Pinned Column Base (Connection No. 5)

The column base is modelled as a pin (hinge), consistent with the structural assumptions adopted in the Robot model. It transfers axial force and shear force from the HEA 400 column to the reinforced concrete foundation, with no bending moment transmitted. The connection consists of a base plate anchored to the concrete column head by hooked anchor bolts.

Parameter	**Value**
Column section	HEA 400 — Steel E24 (S235)
Base plate dimensions	$L = 700$ mm — $B = 400$ mm
Base plate thickness	$t_p = 20$ mm
Anchor bolts	$4 \times \phi$ 20 mm — Grade 8.8
Concrete class	C25/30 — $f_{ck} = 25$ MPa
Grouting mortar	$t_g = 30$ mm — $f_{ck,g} = 12$ MPa
Axial force	$N_{\text{Ed}} = 73.78$ kN
Shear force	$V_{\text{Ed}} = 174.67$ kN
Verification ratio	$0.95 < 1.00$

Warning: Robot Structural Analysis reports two technical remarks for this connection:

The bend radius of the anchor bolt is below the minimum specified value: 75 mm $<$ 90 mm (CEB).

The length of segment L_4 of the hooked anchor bolt is insufficient: 60 mm < 150 mm.

These points must be corrected when preparing the detailed construction drawings.

Despite these remarks, the overall utilisation ratio is $0.95 < 1.00$: the connection is satisfactory with respect to the applicable standard. It is, however, the most critically loaded connection in the structure, owing to the high shear force transferred by the rigid portal frames under wind loading.

The detailed calculations and verifications of the steel structural members and connections are provided in Appendix B 7.7, which contains direct output sheets extracted from Robot Structural Analysis Professional 2024 (Steel Structure Calculation — Calcul des Structures Acier), reproduced in their original French interface as generated by the software.

Chapter 7

Foundation Calculation and Verification

7.1 Introduction

The footing system consists of isolated reinforced concrete footings (semelles isolées) designed per BAEL 91 revised 99, based on reactions extracted from Robot Structural Analysis Professional 2024. Three footing types are addressed: S02 for Bloc A and B, S01 for the Sports Hall, and SJ02 at the construction joint between Blocs A and B.

7.2 Design Basis

7.2.1 Geotechnical Parameters

Table 7.1: Geotechnical engineering properties and site classification.

Parameter	Value
Site category (RPA 2024)	S3 — Medium dense sand
Chemical aggressiveness	XA1 (NA 16002 / NA 778)
Recommended cement	HTS — High sulfate resistance
Substructure concrete	C30/37, $f_{c28} = 30$ MPa, $E/C \leq 0.50$
Foundation type	Isolated (*Semelles isolées*)
Anchorage depth D_f	1.20 m
Allowable soil pressure σ_{sol}	1.50 bar $= 150$ kPa
Soil unit weight γ_s	18.00 kN/m^3

7.2.2 Materials and Load Combinations

Table 7.2: Material strengths and design load combinations.

Parameter	Value
Concrete: f_{c28}	30 MPa
Steel: f_e	500 MPa — FeE 500
ULS (ELU)	$1.35G + 1.5Q \quad (\gamma_b = 1.50,\ \gamma_s = 1.15)$
SLS (ELS)	$G + Q$
Accidental (Seismic)	$G + \psi Q \pm E \quad (\gamma_b = 1.20,\ \gamma_s = 1.00)$

7.3 Design Methodology

The structural design of the isolated footings follows a rigorous verification path, comprising geometric sizing, soil pressure distribution checks, punching shear verification, and reinforcement calculation:

- **Pre-dimensioning:** The base area of the footing is initially determined using the serviceability vertical load:

$$A \times B \geq \frac{N_{\text{ser}}}{\sigma_{\text{sol}}} \tag{7.1}$$

- **Soil stress verification:** Under eccentric loading, the edge pressures are calculated using the Navier formula. The maximum pressure $\sigma_{\max}$ must satisfy:

$$\sigma_{\max} = \frac{N}{A \cdot B}\left(1 + \frac{6e}{A}\right) \leq 1.33\sigma_{\text{sol}} \text{ (at ULS/ELU), and } \leq \sigma_{\text{sol}} \text{ (at SLS/ELS)} \tag{7.2}$$

- **Punching shear resistance:** The concrete section must resist punching without shear reinforcement, satisfying the following limit:

$$P_u \leq 0.045 \cdot U_c \cdot h \cdot \frac{f_{c28}}{\gamma_b} \tag{7.3}$$

- **Reinforcement calculation:** The required steel area is determined using the strut-and-tie method or standard bending theory:

$$A_s = \frac{M_u}{0.9 \cdot d \cdot \frac{f_e}{\gamma_s}} \tag{7.4}$$

The eccentricity condition $e < A/6$ ensures a fully compressive (trapezoidal) stress diagram, preventing any soil-footing detachment. All footings satisfy this condition.

7.4 Footing S02 — Bloc A (Girls' Locker Room) & Bloc B (Boys' Locker Room)

7.4.0.1 Node Layout and Governing Reactions

Node designation is retrieved directly from the Robot Structural Analysis model (Bloc A). The governing vertical reaction $F_{Z,\max} = 198.78$ kN occurs at node 13 under the ULS combination (Case 06).

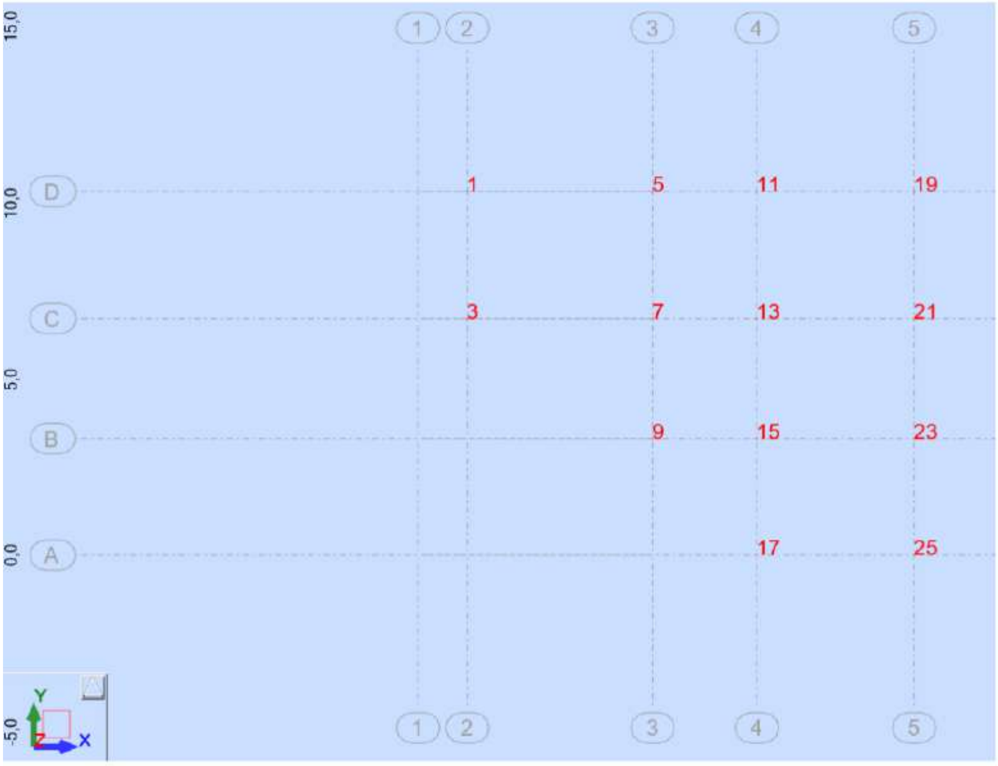

Figure 7.1: Bloc A node layout (Robot RSA 2024).

7.4.1 Foundation Reactions — CAS 06 ELU (excerpt)

7.4.2 Design Results — Footing S02

Punching shear verification:

$$U_c = 2(0.30 + 0.30) + 2(0.30 + 0.30) = 2.40 \text{ m} \implies P_u = 198.78 \text{ kN} \leq \text{capacity} \tag{7.5}$$

Note: The same footing configuration (S02) is adopted for all structural columns in Bloc A and Bloc B.

Table 7.3: Bloc A reactions CAS 06 ELU (governing node highlighted).

Node/Case	F_X (kN)	F_Y (kN)	F_Z (kN)	M_X (kNm)	M_Y (kNm)	M_Z (kNm)
1/ 6(C)	7.29	-1.74	137.02	1.85	8.83	-0.01
7/ 6(C)	-3.60	-0.15	159.91	0.17	-2.92	-0.01
13/ 6(C)	**8.88**	**0.07**	**198.78**	**-0.04**	**10.52**	**-0.01** $\leftarrow$ **MAX**
17/ 6(C)	11.85	1.53	77.32	-1.61	13.67	-0.01
21/ 6(C)	-13.46	0.19	120.21	-0.13	-13.53	-0.01
25/ 6(C)	-9.51	1.30	74.32	-1.33	-9.33	-0.01

Table 7.4: Input parameters and geometric design for Footing S02.

Parameter	Value
Input N (ELU / ELS)	198.78 kN / 145.68 kN
Moments M_0, M_y (ELU)	$10.52\ \mathrm{kN \cdot m}\ /\ -0.04\ \mathrm{kN \cdot m}$
Column section $a \times b$	0.30 m $\times$ 0.30 m
Adopted dimensions $A \times B \times H$	1.20 m $\times$ 1.20 m $\times$ 0.30 m
Eccentricity e_y	0.053 m $\leq A/6 = 0.200$ m ✓

Table 7.5: Soil stress verification — S02

Combo	Diagram	σ_{mean} (bar)	Check
ELU — Sens X	Trapezoidal	$1.86 \leq 2.00$	OK
ELS — Sens X	Trapezoidal	$1.44 \leq 1.50$	OK
ELU — Sens Y	Trapezoidal	$1.68 \leq 2.00$	OK
ELS — Sens Y	Trapezoidal	$1.31 \leq 1.50$	OK

Table 7.6: Reinforcement — S02 | Same footing adopted for all columns in Bloc A and Bloc B.

Direction	$A_{s,\text{calc}}$ (cm^2)	Adopted	Spacing
A // X	2.57 cm^2	8 HA 12 — 9.04 cm^2	$e = 15$ cm
A // Y	2.31 cm^2	8 HA 12 — 9.04 cm^2	$e = 15$ cm

7.5 Footing S01 — Sports Hall Block

7.5.0.1 Node Layout and Governing Reactions

The governing vertical reaction $F_{Z,\text{max}} = 267.02$ kN occurs at node 332 under the ULS combination (Case 22). Large bending moments $M_Y = \pm 165$ kN · m arise from the structural steel portal frames.

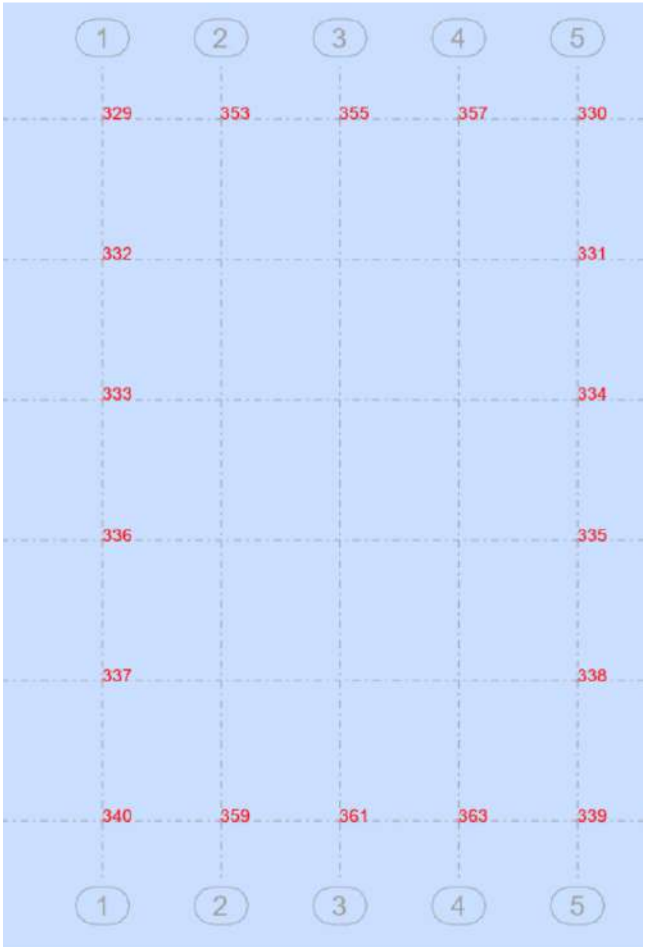

Figure 7.2: Sports Hall node layout (Robot RSA 2024)

7.5.1 Foundation Reactions — CAS 06 ELU (excerpt)

7.5.2 Design Results — Footing S01

Punching shear verification:

$$U_c = 2(0.70 + 0.65) + 2(0.40 + 0.65) = 4.80 \text{ m} \implies P_u = 267.02 \text{ kN} \leq \text{capacity} \tag{7.6}$$

Table 7.7: Sports Hall isolated footing nodal reactions under CAS 06 ELU (governing node highlighted).

Node/Case	F_X (kN)	F_Y (kN)	F_Z (kN)	M_X (kNm)	M_Y (kNm)	M_Z (kNm)
329/ 22(C)	4.51	-9.70	234.56	11.36	5.39	8.80
331/ 22(C)	-39.73	0.69	266.87	-0.78	-165.19	-7.70
332/ 22(C)	**39.71**	**0.69**	**267.02**	**-0.78**	**165.21**	**7.70** $\leftarrow$ **MAX**
334/ 22(C)	-44.90	-0.09	264.44	0.11	-186.50	0.65
337/ 22(C)	39.71	-0.69	267.02	0.78	165.21	-7.70
340/ 22(C)	4.51	9.70	234.56	-11.36	5.39	-8.80

Table 7.8: Sports Hall reactions CAS 06 ELU (governing node highlighted).

Parameter	Value
Input N (ELU / ELS)	267.02 kN / 196.10 kN
Moments M_y, M_0 (ELU)	$165.21\ \text{kN} \cdot \text{m}\ /\ -0.78\ \text{kN} \cdot \text{m}$
Column section $a \times b$	$0.70\ \text{m} \times 0.40\ \text{m}$
Eccentricity e_y	$165.21/267.02 = 0.619\ \text{m} \rightarrow$ governs footing length A
Adopted dimensions $A \times B \times H$	$3.00\ \text{m} \times 1.90\ \text{m} \times 0.65\ \text{m}$

Table 7.9: Soil stress verification — S01.

Combo	Diagram	σ_{mean} (bar)	Check
ELU — Sens X	Trapezoidal	$1.14 \leq 2.00$	OK
ELS — Sens X	Trapezoidal	$0.93 \leq 1.50$	OK
ELU — Sens Y	Trapezoidal	$0.85 \leq 2.00$	OK
ELS — Sens Y	Trapezoidal	$0.73 \leq 1.50$	OK

Table 7.10: Reinforcement selection and bar spacing for Footing S01.

Direction	$A_{s,\text{calc}}$ (cm^2)	Adopted	Spacing
$A\ /\!/\ X$	7.35 cm^2	HA 14 — 10.28 cm^2	$e = 15$ cm
$A\ /\!/\ Y$	3.59 cm^2	HA 14 — 10.28 cm^2	$e = 15$ cm

7.6 Footing SJ02 — Construction Joint (Bloc A / Bloc B)

A single shared footing receives the combined reactions of two adjacent columns at the construction joint separating Bloc A and Bloc B.

A single shared footing receives the combined reactions of two adjacent columns at the construction joint separating Bloc A and Bloc B.

Table 7.11: Input parameters and geometric design for Joint Footing SJ02.

Parameter	Value
Input N (ELU / ELS)	208.40 kN / 153.08 kN
Moments M_y, M_0 (ELU)	-13.53 kN · m / -0.13 kN · m
Column section (each)	0.30 m × 0.30 m
Eccentricity e_y	$13.53/208.40 = 0.065$ m $\leq B/6 = 0.167$ m ✓
Adopted dimensions $A \times B \times H$	1.50 m × 1.00 m × 0.35 m

Table 7.12: Soil stress verification under joint loading — SJ02.

Combo	Diagram	σ_{mean} (bar)	Check
ELU — Sens X	Trapezoidal	$1.88 \leq 2.00$	OK
ELS — Sens X	Trapezoidal	$1.46 \leq 1.50$	OK
ELU — Sens Y	Trapezoidal	$1.70 \leq 2.00$	OK
ELS — Sens Y	Trapezoidal	$1.33 \leq 1.50$	OK

Punching shear verification:

$$U_c = 2(0.30 + 0.35) + 2(0.30 + 0.35) = 2.60 \text{ m} \implies P_u = 208.40 \text{ kN} \leq \text{capacity} \tag{7.7}$$

Table 7.13: Reinforcement selection and bar spacing for Footing SJ02.

Direction	$A_{s,\text{calc}}$ (cm^2)	Adopted Reinforcement	Spacing
$A \parallel X$	3.09 cm^2	HA 12 — 7.54 cm^2	$e = 15$ cm
$A \parallel Y$	1.63 cm^2	HA 12 — 7.54 cm^2	$e = 15$ cm

7.7 Conclusion

This chapter presents the complete isolated footing design for the sports complex at El Alia El Hadjira (Wilaya of Touggourt), in accordance with BAEL 91 revised 99. All reactions were extracted from Robot RSA 2024 and the governing load combination for each footing type was identified. The soil aggressiveness (XA1) requires C30/37 concrete with HTS cement and $E/C \leq 0.50$. The results are summarised below.

Table 7.14: Summary of footing design results and compliance verifications.

Parameter	S02 — Bloc A & B	S01 — Sports Hall	SJ02 — A/B Joint
Column section	30×30 cm	40×70 cm	30×30 cm
N (ELU)	198.78 kN	267.02 kN	208.40 kN
Footing $A \times B \times H$	$1.20 \times 1.20 \times 0.30$ m	$3.00 \times 1.90 \times 0.65$ m	$1.50 \times 1.00 \times 0.35$ m
σ_{max} ELU (bar)	$1.86 \leq 2.00$ ✓	$1.14 \leq 2.00$ ✓	$1.88 \leq 2.00$ ✓
Punching check	✓ Verified	✓ Verified	✓ Verified
Steel X	HA 12 — $e = 15$ cm	HA 14 — $e = 15$ cm	HA 12 — $e = 15$ cm
Steel Y	HA 12 — $e = 15$ cm	HA 14 — $e = 15$ cm	HA 12 — $e = 15$ cm
All checks	✓ **Compliant**	✓ **Compliant**	✓ **Compliant**

All soil bearing stress, punching, and flexural reinforcement verifications are satisfied for both ULS and SLS. The adopted reinforcement exceeds the computed demand in all cases. The footing dimensions and steel layouts defined in this chapter are retained for the structural drawings and bill of quantities.

All verifications COMPLIANT with BAEL 91 revised 99 and RPA 2024.

General Conclusion

Synthesis

This work presented a structural study of a sports complex comprising a steel sports hall and two reinforced concrete blocks dedicated to changing rooms, located in El Alia, Hadjira, Wilaya of Touggourt. The study was carried out in fulfillment of the requirements for the Master's degree in Civil Engineering.

The following tasks were successfully completed throughout this study:

- **Seismic site classification:** The Wilaya of Touggourt was classified in Seismic Zone I according to the provisions of RPA 2024, with a zone acceleration coefficient (A = 0.07) and a soil category (S3). This classification corresponds to a relatively low seismicity environment while still imposing specific structural design requirements that must be respected.
- **Load evaluation:** Permanent and live loads were determined for both the reinforced concrete and steel structural systems using the load transfer method. Appropriate design load combinations at the Ultimate Limit State (ULS) and Serviceability Limit State (SLS) were established for subsequent structural verification.
- **Preliminary dimensioning of structural elements:** Initial dimensions were determined for slabs, beams, and columns of Blocks A and B, as well as for the steel sports hall structure, in accordance with the applicable technical regulations, namely BAEL 91 Revised 99 for reinforced concrete structures and g g s Rprovisions for steel structures.
- **Column design and verification:** Reinforced concrete columns were designed and verified according to BAEL 91 requirements while considering the seismic provisions of RPA 2024 for Seismic Zone I. A cross-section of 30×30 cm was adopted for the columns of Blocks A and B, whereas a cross-section of 40×70 cm was retained for the sports hall columns. All sections were verified under the governing

load combinations.

Perspectives

This work opens the way for several future developments. A complete seismic analysis and three-dimensional structural modeling of the facility using specialized software such as SAP2000 or Robot Structural Analysis is recommended as a direct continuation of the present study. Such an analysis would allow a more comprehensive evaluation of the dynamic behavior of the structure under seismic loading.

Subsequent work should include the detailed design of all structural elements, including reinforcement detailing for reinforced concrete members, design of steel connections, and foundation sizing. Furthermore, the preparation of complete execution drawings and a comparative economic study assessing alternative structural solutions would provide valuable extensions to the project.

This project has constituted a rich scientific and practical experience, enabling the application of theoretical knowledge to real-world structural engineering challenges. It has also contributed to the development of professional skills in the analysis and design of structures in accordance with Algerian standards and regulations.

Bibliography

[1] Salim Ouahmed and Mohamed Younes Mahmoudi. Conception et étude d'une salle de sport. Master's thesis, Université Abou Bekr Belkaïd Tlemcen, Tlemcen, Algeria, 2021. Supervised by Mme F. Korso and Mr B. Ghennani.

[2] SCI (Steel Construction Institute). *Steel Designers' Manual*. John Wiley & Sons Ltd, Chichester, United Kingdom, 7 edition, 2016. ISBN 9781119249863.

[3] Serine Abdelouahab and Lyna-Nour Mahmouche. Étude d'un hangar en charpente métallique équipé d'un pont roulant de capacité de levage de 10 tonnes. Master's thesis, École Nationale Supérieure des Travaux Publics (ENSTP), Algiers, Algeria, 2024. Supervised by Mme N. Tefrat and Mme M. Oumoussa.

[4] Mustansiriyah University. Title of the lecture notes, 2022. URL `https://uomustansiriyah.edu.iq/media/lectures/5/5_2022_03_21!10_36_12_PM.pdf`. Lecture notes.

[5] Mohamed Moussaoui and Abdelmounaim Beddouda. Étude d'un bâtiment (r+4) en charpente métallique selon l'eurocode 3. Master's thesis, Université Kasdi Merbah Ouargla, Ouargla, Algeria, 2014. Supervised by Mr. L. Rouag.

[6] Règles parasismiques algériennes rpa 2024. Document Technique Réglementaire DTR BC 2.48, Centre National de Recherche Appliquée en Génie Parasismique (CGS), Alger, Algeria, 2024.

[7] Règlement neige et vent (rnv 2013). Document Technique Réglementaire DTR C 2-47, Centre National d'Études et de Recherches Intégrées du Bâtiment (CNERIB), Alger, Algeria, 2013.

[8] Règles techniques de conception et de calcul des ouvrages et constructions en béton armé suivant la méthode des États limites (bael 91 révisé 99). Code de calcul, Association Française de Génie Civil (AFGC), Paris, France, 1999.

Appendix A (Architectural plans for the project)

BLOC : salle specailisee

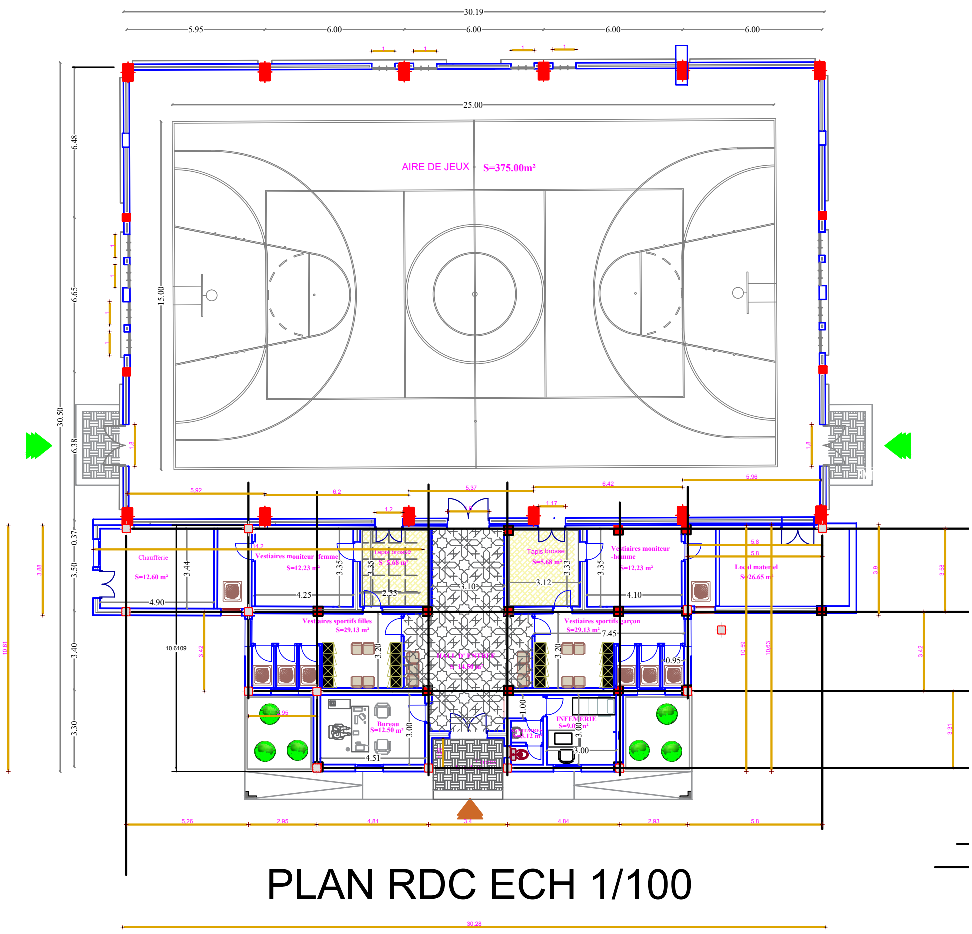

PLAN RDC ECH 1/100

Appendix B

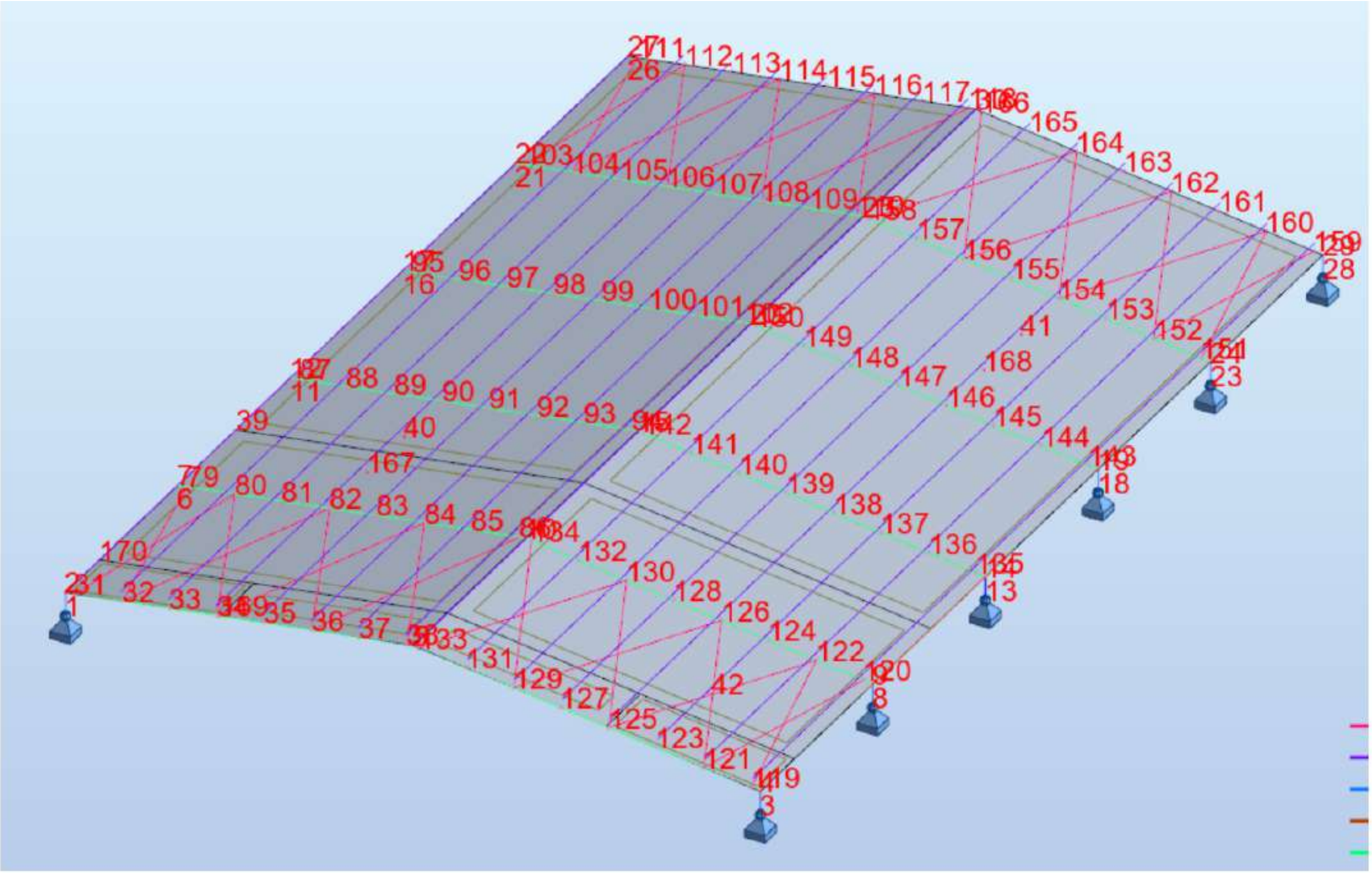

Numérotation des nœuds et de barres de la structure

Application des différents cas de charges

1 - Charges permanentes G

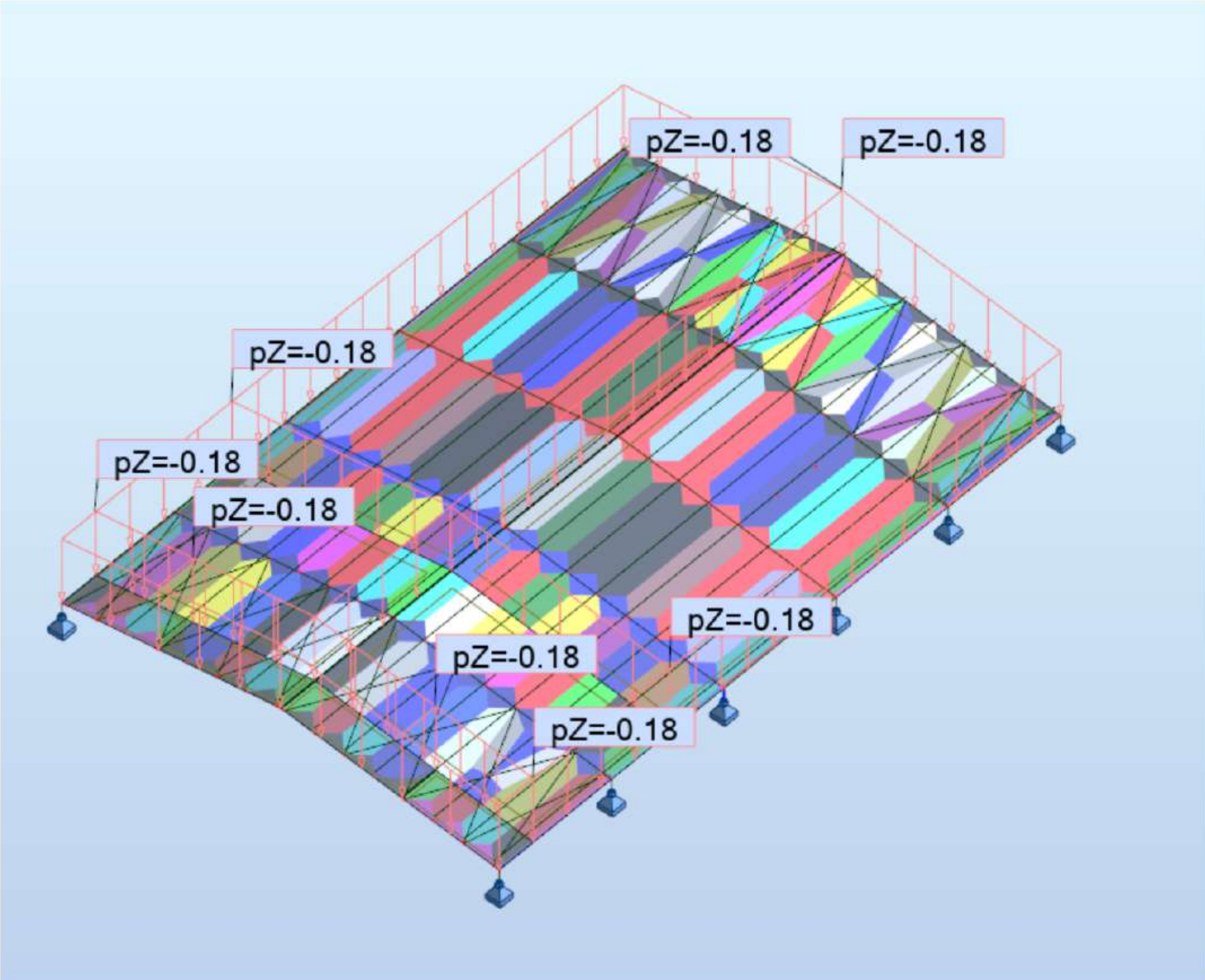

2 - Charges d'exploitation Q

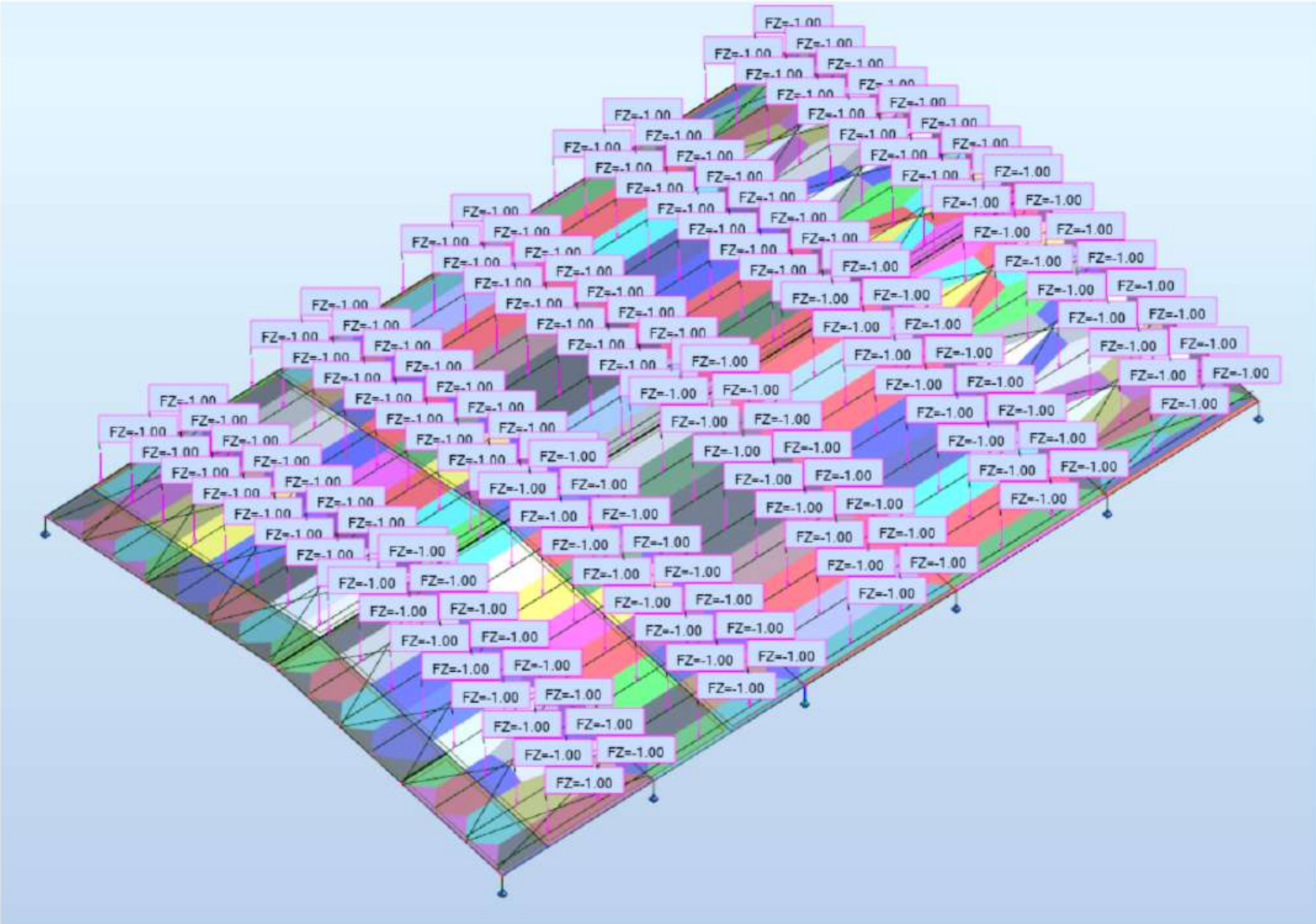

3 - Charge de sable D

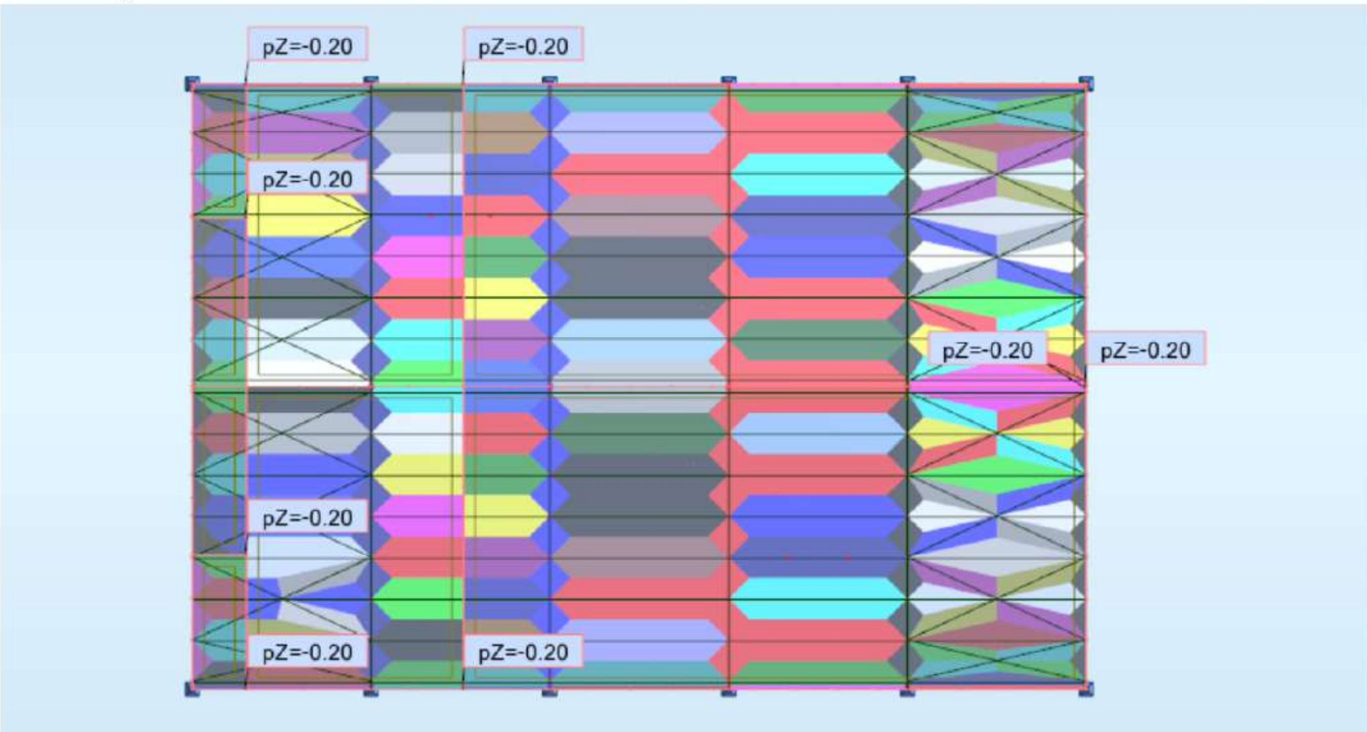

4 - Charge de vent

Vent W1

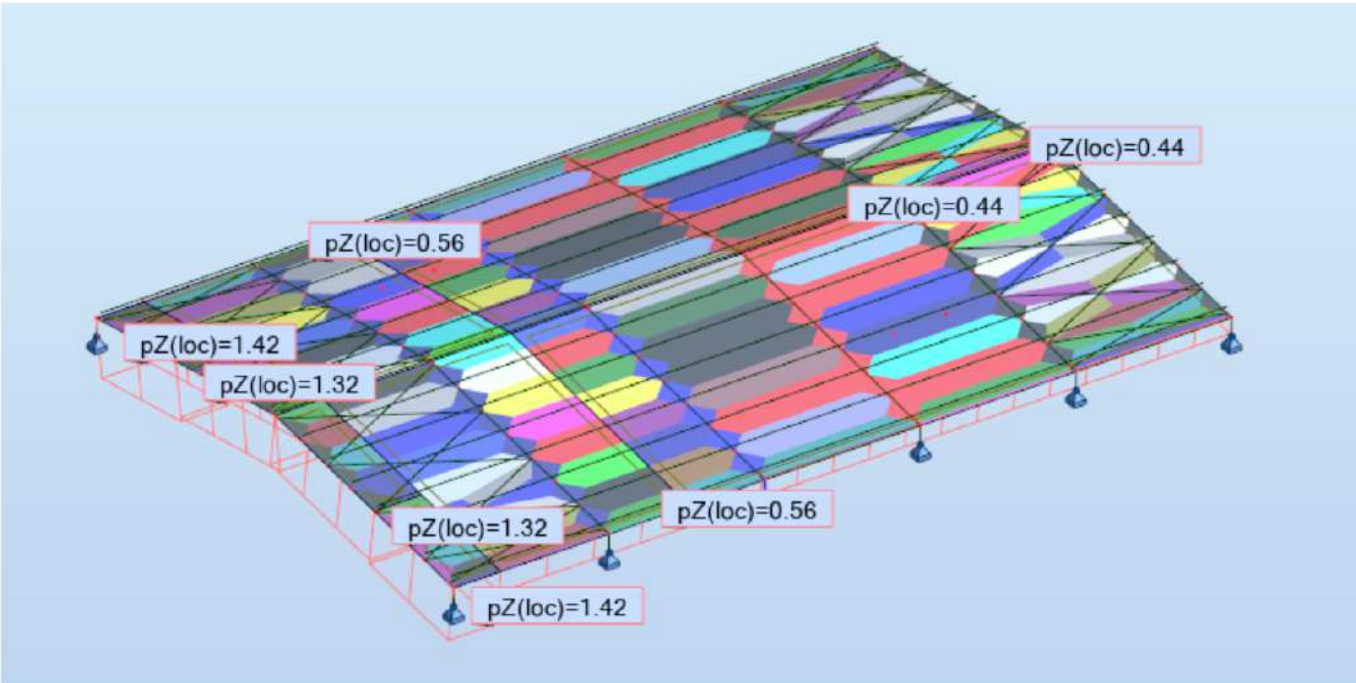

Vent W2

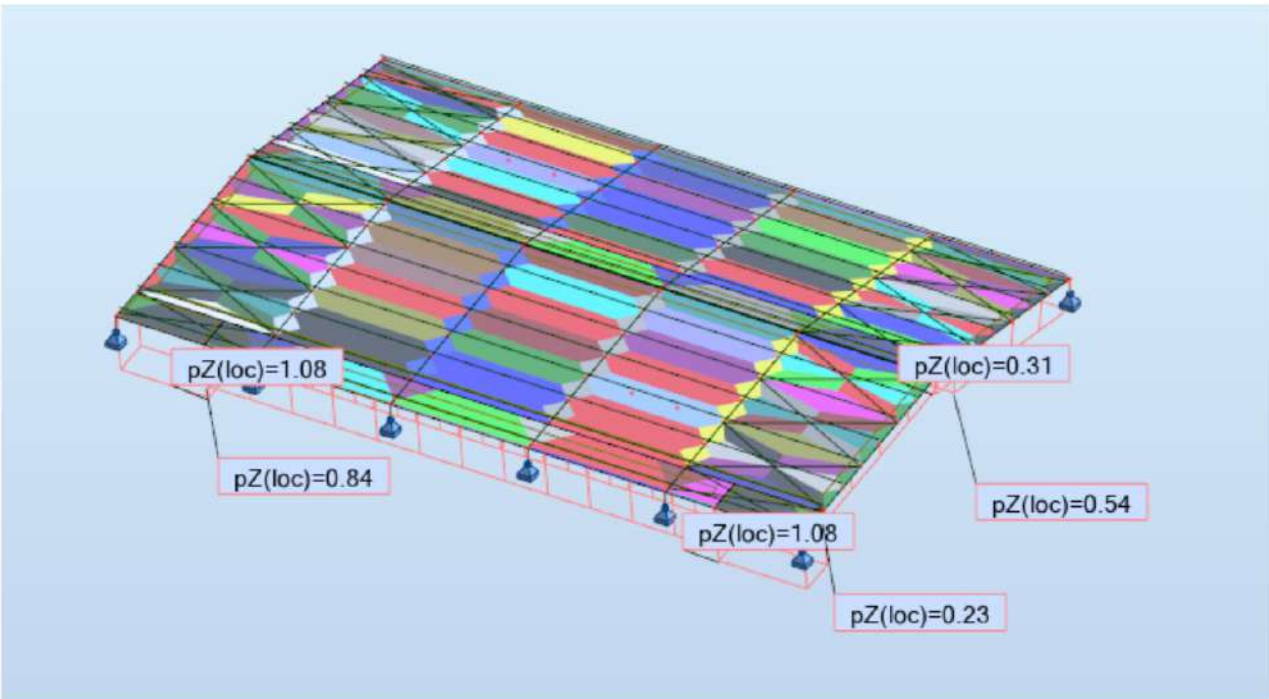

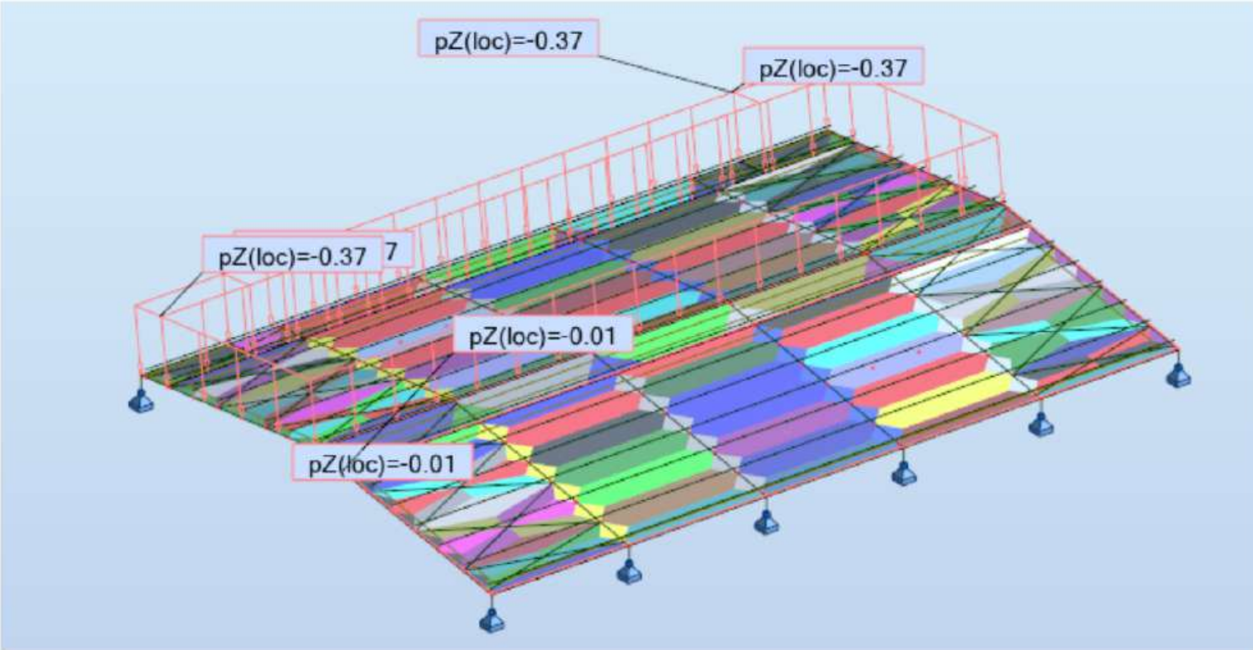

Vent W(+)

Appendix C

CALCUL DES STRUCTURES ACIER

NORME: *NF EN 1993-1-1:2005/NA:2013/A1:2014, Eurocode 3: Design of steel structures.*
TYPE D'ANALYSE: Dimensionnement des familles

FAMILLE: 3 POTEAUX
PIECE: 6 PoteauCM01_6 **POINT:** 7 **COORDONNEE:** x = 1.00 L = 0.70 m

---

CHARGEMENTS:
Cas de charge décisif: 11 1.35G+1.35Q+1.35S (1+2+3+4)*1.35

MATERIAU:
ACIER E24 fy = 235.00 MPa

PARAMETRES DE LA SECTION: POTEAUX HEA400

h=39.0 cm	gM0=1.10	gM1=1.10	
b=30.0 cm	Ay=126.20 cm2	Az=57.33 cm2	Ax=158.98 cm2
tw=1.1 cm	Iy=45069.40 cm4	Iz=8563.83 cm4	Ix=189.76 cm4
tf=1.9 cm	Wply=2561.80 cm3	Wplz=872.86 cm3	

EFFORTS INTERNES ET RESISTANCES ULTIMES:

N,Ed = 73.78 kN	My,Ed = -122.27 kN*m	Mz,Ed = 0.04 kN*m	Vy,Ed = -0.06 kN
Nc,Rd = 3396.39 kN	My,Ed,max = -122.27 kN*m		Mz,Ed,max = 0.04 kN*m
	Vy,c,Rd = 1556.59 kN		
Nb,Rd = 3396.39 kN	My,c,Rd = 547.29 kN*m	Mz,c,Rd = 186.47 kN*m	Vz,Ed = -174.67 kN
	MN,y,Rd = 547.29 kN*m	MN,z,Rd = 186.47 kN*m	Vz,c,Rd = 707.13 kN
	Mb,Rd = 547.29 kN*m		
			Classe de la section = 1

PARAMETRES DE DEVERSEMENT:

z = 0.00	Mcr = 120089.66 kN*m	Courbe,LT -	XLT = 1.00
Lcr,low=0.70 m	Lam_LT = 0.07	fi,LT = 0.46	XLT,mod = 1.00

PARAMETRES DE FLAMBEMENT:

en y:		en z:	
Ly = 0.70 m	Lam_y = 0.03	Lz = 0.70 m	Lam_z = 0.10
Lcr,y = 0.49 m	Xy = 1.00	Lcr,z = 0.70 m	Xz = 1.00
Lamy = 2.91	kyy = 0.79	Lamz = 9.54	kyz = 0.54

FORMULES DE VERIFICATION:
Contrôle de la résistance de la section:
N,Ed/Nc,Rd = 0.02 < 1.00 (6.2.4.(1))
My,Ed/MN,y,Rd = 0.22 < 1.00 (6.2.9.1.(2))
Mz,Ed/MN,z,Rd = 0.00 < 1.00 (6.2.9.1.(2))
(My,Ed/MN,y,Rd)^ 2.00 + (Mz,Ed/MN,z,Rd)^1.00 = 0.05 < 1.00 (6.2.9.1.(6))
Vy,Ed/Vy,c,Rd = 0.00 < 1.00 (6.2.6.(1))
Vz,Ed/Vz,c,Rd = 0.25 < 1.00 (6.2.6.(1))

CALCUL DES STRUCTURES ACIER

NORME: *NF EN 1993-1-1:2005/NA:2013/A1:2014, Eurocode 3: Design of steel structures.*
TYPE D'ANALYSE: Dimensionnement des familles

FAMILLE: 1 TRAVERSSES
PIECE: 8 TRAVERSES CM01_8 **POINT:** 1 **COORDONNEE:** x = 0.00 L = 0.00 m

CHARGEMENTS:
Cas de charge décisif: 11 1.35G+1.35Q+1.35S (1+2+3+4)*1.35

MATERIAU:
ACIER E24 fy = 235.00 MPa

PARAMETRES DE LA SECTION: TRVERSSE IPE40

h=40.0 cm	gM0=1.10	gM1=1.10	
b=18.0 cm	Ay=55.99 cm2	Az=42.69 cm2	Ax=84.46 cm2
tw=0.9 cm	Iy=23128.40 cm4	Iz=1317.82 cm4	Ix=51.33 cm4
tf=1.4 cm	Wply=1307.15 cm3	Wplz=229.00 cm3	

EFFORTS INTERNES ET RESISTANCES ULTIMES:

N,Ed = 182.80 kN	My,Ed = -122.27 kN*m	Mz,Ed = 0.02 kN*m	Vy,Ed = 0.73 kN
Nc,Rd = 1804.37 kN	My,Ed,max = -122.27 kN*m		Mz,Ed,max = 1.31 kN*m
	Vy,T,Rd = 690.24 kN		
Nb,Rd = 703.41 kN	My,c,Rd = 279.25 kN*m	Mz,c,Rd = 48.92 kN*m	Vz,Ed = 46.90 kN
	MN,y,Rd = 279.25 kN*m	MN,z,Rd = 48.92 kN*m	Vz,T,Rd = 526.37 kN
	Mb,Rd = 204.45 kN*m		Tt,Ed = -0.01 kN*m
			Classe de la section = 1

PARAMETRES DE DEVERSEMENT:

z = 1.00	Mcr = 406.55 kN*m	Courbe,LT -	XLT = 0.70
Lcr,low=5.12 m	Lam_LT = 0.87	fi,LT = 0.98	XLT,mod = 0.73

PARAMETRES DE FLAMBEMENT:

en y:		en z:	
Ly = 10.25 m	Lam_y = 0.33	Lz = 10.25 m	Lam_z = 1.38

Lcr,y = 5.12 m	Xy = 0.97	Lcr,z = 5.12 m	Xz = 0.39
Lamy = 30.96	kyy = 1.18	Lamz = 129.69	kyz = 1.35

FORMULES DE VERIFICATION:
Contrôle de la résistance de la section:
N,Ed/Nc,Rd = 0.10 < 1.00 (6.2.4.(1))
My,Ed/MN,y,Rd = 0.44 < 1.00 (6.2.9.1.(2))
Mz,Ed/MN,z,Rd = 0.00 < 1.00 (6.2.9.1.(2))
(My,Ed/MN,y,Rd)^ 2.00 + (Mz,Ed/MN,z,Rd)^1.00 = 0.19 < 1.00 (6.2.9.1.(6))
Vy,Ed/Vy,T,Rd = 0.00 < 1.00 (6.2.6-7)
Vz,Ed/Vz,T,Rd = 0.09 < 1.00 (6.2.6-7)
Tau,ty,Ed/(fy/(sqrt(3)*gM0)) = 0.00 < 1.00 (6.2.6)
Tau,tz,Ed/(fy/(sqrt(3)*gM0)) = 0.00 < 1.00 (6.2.6)
Contrôle de la stabilité globale de la barre:
Lambda,y = 30.96 < Lambda,max = 210.00 Lambda,z = 129.69 < Lambda,max = 210.00 STABLE
My,Ed,max/Mb,Rd = 0.60 < 1.00 (6.3.2.1.(1))
N,Ed/(Xy*N,Rk/gM1) + kyy*My,Ed,max/(XLT*My,Rk/gM1) + kyz*Mz,Ed,max/(Mz,Rk/gM1) = 0.85 < 1.00 (6.3.3.(4))
N,Ed/(Xz*N,Rk/gM1) + kzy*My,Ed,max/(XLT*My,Rk/gM1) + kzz*Mz,Ed,max/(Mz,Rk/gM1) = 0.66 < 1.00 (6.3.3.(4))

Profil correct !!!

CALCUL DES STRUCTURES ACIER

NORME: *NF EN 1993-1-1:2005/NA:2013/A1:2014, Eurocode 3: Design of steel structures.*
TYPE D'ANALYSE: Dimensionnement des familles

FAMILLE: 2 PANNES
PIECE: 48 **POINT:** 4 **COORDONNEE:** x = 0.50 L = 3.00 m

CHARGEMENTS:
Cas de charge décisif: 11 1.35G+1.35Q+1.35S (1+2+3+4)*1.35

MATERIAU:
ACIER E24 fy = 235.00 MPa

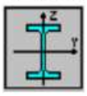

PARAMETRES DE LA SECTION: PANNES

h=14.0 cm	gM0=1.10	gM1=1.10	
b=7.3 cm	Ay=11.16 cm2	Az=7.65 cm2	Ax=16.43 cm2
tw=0.5 cm	Iy=541.22 cm4	Iz=44.92 cm4	Ix=2.46 cm4
tf=0.7 cm	Wply=88.34 cm3	Wplz=19.25 cm3	

EFFORTS INTERNES ET RESISTANCES ULTIMES:

N,Ed = 0.25 kN	My,Ed = 6.58 kN*m	Mz,Ed = 0.92 kN*m	Vy,Ed = -0.00 kN
Nc,Rd = 351.00 kN	My,Ed,max = 6.58 kN*m	Mz,Ed,max = 0.92 kN*m	Vy,c,Rd = 137.61 kN
Nb,Rd = 351.00 kN	My,c,Rd = 18.87 kN*m	Mz,c,Rd = 4.11 kN*m	Vz,Ed = 0.00 kN
	MN,y,Rd = 18.87 kN*m	MN,z,Rd = 4.11 kN*m	Vz,c,Rd = 94.31 kN
	Mb,Rd = 12.80 kN*m		
			Classe de la section = 1

FORMULES DE VERIFICATION:

Contrôle de la résistance de la section:

N,Ed/Nc,Rd = 0.00 < 1.00 (6.2.4.(1))
My,Ed/MN,y,Rd = 0.35 < 1.00 (6.2.9.1.(2))
Mz,Ed/MN,z,Rd = 0.22 < 1.00 (6.2.9.1.(2))
(My,Ed/MN,y,Rd)^ 2.00 + (Mz,Ed/MN,z,Rd)^1.00 = 0.35 < 1.00 (6.2.9.1.(6))
Vy,Ed/Vy,c,Rd = 0.00 < 1.00 (6.2.6.(1))
Vz,Ed/Vz,c,Rd = 0.00 < 1.00 (6.2.6.(1))

Contrôle de la stabilité globale de la barre:

My,Ed,max/Mb,Rd = 0.51 < 1.00 (6.3.2.1.(1))
N,Ed/(Xy*N,Rk/gM1) + kyy*My,Ed,max/(XLT*My,Rk/gM1) + kyz*Mz,Ed,max/(Mz,Rk/gM1) = 0.74 < 1.00 (6.3.3.(4))
N,Ed/(Xz*N,Rk/gM1) + kzy*My,Ed,max/(XLT*My,Rk/gM1) + kzz*Mz,Ed,max/(Mz,Rk/gM1) = 0.74 < 1.00 (6.3.3.(4))

Profil correct !!!

CALCUL DES STRUCTURES ACIER

NORME: *NF EN 1993-1-1:2005/NA:2013/A1:2014, Eurocode 3: Design of steel structures.*
TYPE D'ANALYSE: Dimensionnement des familles

FAMILLE: 5 SABLIERES
PIECE: 107 **POINT:** 7 **COORDONNEE:** x = 1.00 L = 6.00 m

CHARGEMENTS:
Cas de charge décisif: 8 1.35G+1.5S (1+2)*1.35+4*1.50

MATERIAU:
ACIER E24 fy = 235.00 MPa

PARAMETRES DE LA SECTION: SABLIERE

h=13.3 cm	gM0=1.10	gM1=1.10	
b=14.0 cm	Ay=26.36 cm2	Az=10.13 cm2	Ax=31.42 cm2
tw=0.6 cm	Iy=1033.13 cm4	Iz=389.32 cm4	Ix=8.16 cm4
tf=0.9 cm	Wply=173.50 cm3	Wplz=84.85 cm3	

EFFORTS INTERNES ET RESISTANCES ULTIMES:

N,Ed = 1.16 kN	My,Ed = -1.24 kN*m	Mz,Ed = -0.03 kN*m	Vy,Ed = 0.01 kN
Nc,Rd = 671.25 kN	My,Ed,max = -1.24 kN*m	Mz,Ed,max = 0.04 kN*m	Vy,T,Rd = 325.10 kN
Nb,Rd = 155.25 kN	My,c,Rd = 37.07 kN*m	Mz,c,Rd = 18.13 kN*m	Vz,Ed = -1.21 kN
	MN,y,Rd = 37.07 kN*m	MN,z,Rd = 18.13 kN*m	Vz,T,Rd = 124.91 kN
			Tt,Ed = -0.00 kN*m
			Classe de la section = 1

PARAMETRES DE DEVERSEMENT:

PARAMETRES DE FLAMBEMENT:

en y:		en z:	
Ly = 6.00 m	Lam_y = 1.11	Lz = 6.00 m	Lam_z = 1.81
Lcr,y = 6.00 m	Xy = 0.53	Lcr,z = 6.00 m	Xz = 0.23
Lamy = 104.63	kyy = 1.00	Lamz = 170.45	kyz = 0.44

FORMULES DE VERIFICATION:
Contrôle de la résistance de la section:
N,Ed/Nc,Rd = 0.00 < 1.00 (6.2.4.(1))
My,Ed/MN,y,Rd = 0.03 < 1.00 (6.2.9.1.(2))
Mz,Ed/MN,z,Rd = 0.00 < 1.00 (6.2.9.1.(2))
(My,Ed/MN,y,Rd)^ 2.00 + (Mz,Ed/MN,z,Rd)^1.00 = 0.00 < 1.00 (6.2.9.1.(6))
Vy,Ed/Vy,T,Rd = 0.00 < 1.00 (6.2.6-7)
Vz,Ed/Vz,T,Rd = 0.01 < 1.00 (6.2.6-7)
Tau,ty,Ed/(fy/(sqrt(3)*gM0)) = 0.00 < 1.00 (6.2.6)
Tau,tz,Ed/(fy/(sqrt(3)*gM0)) = 0.00 < 1.00 (6.2.6)
Contrôle de la stabilité globale de la barre:
Lambda,y = 104.63 < Lambda,max = 210.00 Lambda,z = 170.45 < Lambda,max = 210.00 STABLE
N,Ed/(Xy*N,Rk/gM1) + kyy*My,Ed,max/(XLT*My,Rk/gM1) + kyz*Mz,Ed,max/(Mz,Rk/gM1) = 0.04 < 1.00 (6.3.3.(4))
N,Ed/(Xz*N,Rk/gM1) + kzy*My,Ed,max/(XLT*My,Rk/gM1) + kzz*Mz,Ed,max/(Mz,Rk/gM1) = 0.03 < 1.00

(6.3.3.(4))

Profil correct !!!

CALCUL DES STRUCTURES ACIER

NORME: *NF EN 1993-1-1:2005/NA:2013/A1:2014, Eurocode 3: Design of steel structures.*
TYPE D'ANALYSE: Dimensionnement des familles

FAMILLE: 4 CNTRVT
PIECE: 172 CVT HZ_172 **POINT:** 1 **COORDONNEE:** x = 0.00 L = 0.00 m

---

CHARGEMENTS:
Cas de charge décisif: 11 1.35G+1.35Q+1.35S (1+2+3+4)*1.35

MATERIAU:
ACIER E24 fy = 235.00 MPa

PARAMETRES DE LA SECTION: CNTRV HRZ

h=6.0 cm	gM0=1.10	gM1=1.10	
b=6.0 cm	Ay=3.60 cm2	Az=3.60 cm2	Ax=6.91 cm2
tw=0.6 cm	Iy=22.79 cm4	Iz=22.79 cm4	Ix=0.82 cm4
tf=0.6 cm	Wely=5.29 cm3	Welz=5.29 cm3	

EFFORTS INTERNES ET RESISTANCES ULTIMES:
N,Ed = 1.51 kN
Nc,Rd = 147.62 kN
Nb,Rd = 32.60 kN

Classe de la section = 3

PARAMETRES DE DEVERSEMENT:

PARAMETRES DE FLAMBEMENT:

en y:		en z:	
Ly = 3.31 m	Lam_y = 1.94	Lz = 3.31 m	Lam_z = 1.94
Lcr,y = 3.31 m	Xy = 0.22	Lcr,z = 3.31 m	Xz = 0.22
Lamy = 182.29		Lamz = 182.29	

FORMULES DE VERIFICATION:
Contrôle de la résistance de la section:
N,Ed/Nc,Rd = 0.01 < 1.00 (6.2.4.(1))
Contrôle de la stabilité globale de la barre:
Lambda,y = 182.29 < Lambda,max = 210.00 Lambda,z = 182.29 < Lambda,max = 210.00 STABLE
N,Ed/Nb,Rd = 0.05 < 1.00 (6.3.1.1.(1))

Profil correct !!!

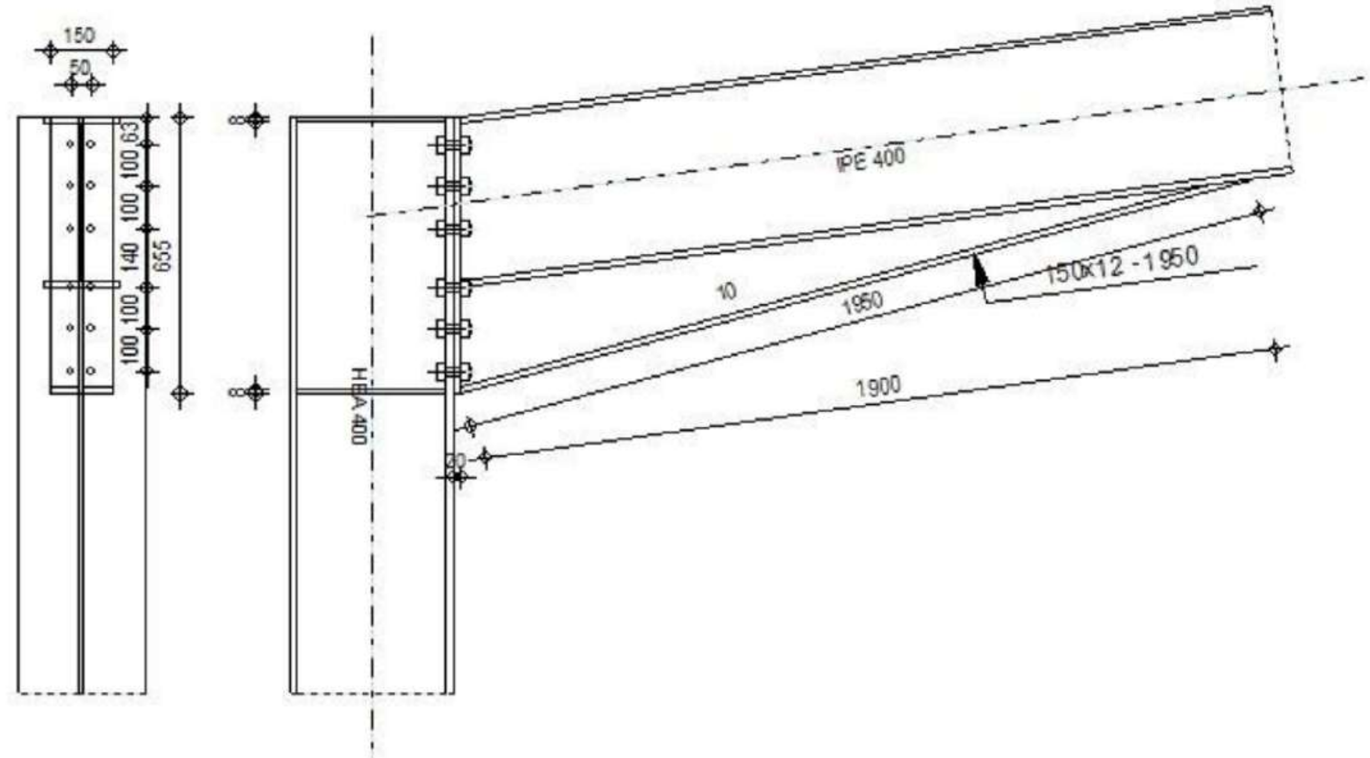

GÉNÉRAL

Assemblage N°: 2
Nom de l'assemblage: Angle de portique
Noeud de la structure: 2
Barres de la structure: 1, 3

GÉOMÉTRIE

POTEAU

Profilé: HEA 400
Barre N°: 1

α =	-90,0	[Deg]	Angle d'inclinaison
h_c =	390	[mm]	Hauteur de la section du poteau
b_{fc} =	300	[mm]	Largeur de la section du poteau
t_{wc} =	11	[mm]	Epaisseur de l'âme de la section du poteau
t_{fc} =	19	[mm]	Epaisseur de l'aile de la section du poteau
r_c =	27	[mm]	Rayon de congé de la section du poteau
A_c =	158,98	[cm^2]	Aire de la section du poteau
I_{xc} =	45069,40	[cm^4]	Moment d'inertie de la section du poteau

Matériau: ACIER E24

f_{yc} =	235,00	[MPa]	Résistance

POUTRE

Profilé: IPE 400

Barre N°: 3

α =	7,8	[Deg]	Angle d'inclinaison
h_b =	400	[mm]	Hauteur de la section de la poutre
b_f =	180	[mm]	Largeur de la section de la poutre
t_{wb} =	9	[mm]	Epaisseur de l'âme de la section de la poutre
t_{fb} =	14	[mm]	Epaisseur de l'aile de la section de la poutre
r_b =	21	[mm]	Rayon de congé de la section de la poutre
r_b =	21	[mm]	Rayon de congé de la section de la poutre
A_b =	84,46	[cm^2]	Aire de la section de la poutre
I_{xb} =	23128,40	[cm^4]	Moment d'inertie de la poutre

Matériau: ACIER E24

f_{yb} =	235,00	[MPa]	Résistance

BOULONS

Le plan de cisaillement passe par la partie NON FILETÉE du boulon

d =	20	[mm]	Diamètre du boulon
Classe =	HR 10.9		Classe du boulon
F_{tRd} =	176,40	[kN]	Résistance du boulon à la traction
n_h =	2		Nombre de colonnes des boulons
n_v =	6		Nombre de rangéss des boulons
h_1 =	63	[mm]	Pince premier boulon-extrémité supérieure de la platine d'about

Ecartement e_i = 50 [mm]

Entraxe p_i = 100;100;140;100;100 [mm]

PLATINE

h_p =	655	[mm]	Hauteur de la platine
b_p =	150	[mm]	Largeur de la platine
t_p =	20	[mm]	Epaisseur de la platine

Matériau: ACIER E24

f_{yp} =	235,00	[MPa]	Résistance

JARRET INFÉRIEUR

w_d =	150	[mm]	Largeur de la platine
t_{fd} =	12	[mm]	Epaisseur de l'aile
h_d =	251	[mm]	Hauteur de la platine
t_{wd} =	10	[mm]	Epaisseur de l'âme
l_d =	1900	[mm]	Longueur de la platine
α =	15,2	[Deg]	Angle d'inclinaison

Matériau: ACIER E24

f_{ybu} =	235,00	[MPa]	Résistance

RAIDISSEUR POTEAU

Supérieur

h_{su} =	352	[mm]	Hauteur du raidisseur
b_{su} =	144	[mm]	Largeur du raidisseur
t_{hu} =	8	[mm]	Epaisseur du raidisseur

a_w =	7	[mm]	Soudure âme
a_f =	10	[mm]	Soudure semelle
a_s =	7	[mm]	Soudure du raidisseur
a_{fd} =	5	[mm]	Soudure horizontale

COEFFICIENTS DE MATÉRIAU

γ_{M0} =	1,00	Coefficient de sécurité partiel	[2.2]
γ_{M1} =	1,00	Coefficient de sécurité partiel	[2.2]
γ_{M2} =	1,25	Coefficient de sécurité partiel	[2.2]
γ_{M3} =	1,10	Coefficient de sécurité partiel	[2.2]

EFFORTS

Etat limite: ultime

Cas: 11: 1.35G+1.35Q+1.35S (1+2+3+4)*1.35

$M_{b1,Ed}$ =	72,05	[kN*m]	Moment fléchissant dans la poutre droite
$V_{b1,Ed}$ =	41,72	[kN]	Effort tranchant dans la poutre droite
$N_{b1,Ed}$ =	-102,91	[kN]	Effort axial dans la poutre droite
$M_{c1,Ed}$ =	72,05	[kN*m]	Moment fléchissant dans le poteau inférieur
$V_{c1,Ed}$ =	102,93	[kN]	Effort tranchant dans le poteau inférieur
$N_{c1,Ed}$ =	-42,89	[kN]	Effort axial dans le poteau inférieur

RÉSULTATS

RÉSISTANCES DE LA POUTRE

COMPRESSION

A_b = 84,46 [cm²] Aire de la section EN1993-1-1:[6.2.4]

$N_{cb,Rd} = A_b f_{yb} / \gamma_{M0}$

$N_{cb,Rd}$ = 1984,81 [kN] Résistance de calcul de la section à la compression EN1993-1-1:[6.2.4]

CISAILLEMENT

A_{vb} = 67,79 [cm²] Aire de la section au cisaillement EN1993-1-1:[6.2.6.(3)]

$V_{cb,Rd} = A_{vb} (f_{yb} / \sqrt{3}) / \gamma_{M0}$

$V_{cb,Rd}$ = 919,77 [kN] Résistance de calcul de la section au cisaillement EN1993-1-1:[6.2.6.(2)]

$V_{b1,Ed} / V_{cb,Rd} \le 1,0$ 0,05 < 1,00 vérifié (0,05)

FLEXION - MOMENT PLASTIQUE (SANS RENFORTS)

W_{plb} = 1307,15 [cm³] Facteur plastique de la section EN1993-1-1:[6.2.5.(2)]

$M_{b,pl,Rd} = W_{plb} f_{yb} / \gamma_{M0}$

$M_{b,pl,Rd}$ = 307,18 [kN*m] Résistance plastique de la section à la flexion (sans renforts) EN1993-1-1:[6.2.5.(2)]

FLEXION AU CONTACT DE LA PLAQUE AVEC L'ELEMENT ASSEMBLE

W_{pl} = 1909,49 [cm³] Facteur plastique de la section EN1993-1-1:[6.2.5]

$M_{cb,Rd} = W_{pl} f_{yb} / \gamma_{M0}$

γ =	15,2	[Deg]	Angle d'inclinaison du renfort	
$b_{eff,c,wb}$ =	295	[mm]	Largeur efficace de l'âme à la compression	[6.2.6.2.(1)]
A_{vb} =	42,69	[cm^2]	Aire de la section au cisaillement	EN1993-1-1:[6.2.6.(3)]
ω =	0,83		Coefficient réducteur pour l'interaction avec le cisaillement	[6.2.6.2.(1)]
$\sigma_{com,Ed}$ =	63,74	[MPa]	Contrainte de compression maximale dans l'âme	[6.2.6.2.(2)]
k_{wc} =	1,00		Coefficient réducteur dû aux contraintes de compression	[6.2.6.2.(2)]

$F_{c,wb,Rd1} = [\omega\ k_{wc}\ b_{eff,c,wb}\ t_{wb}\ f_{yb} / \gamma_{M0}] \cos(\gamma) / \sin(\gamma - \beta)$

$F_{c,wb,Rd1}$ =	3735,28	[kN]	Résistance de l'âme de la poutre	[6.2.6.2.(1)]

Flambement:

d_{wb} =	331	[mm]	Hauteur de l'âme comprimée	[6.2.6.2.(1)]
λ_p =	1,13		Elancement de plaque	[6.2.6.2.(1)]
ρ =	0,73		Coefficient réducteur pour le flambement de l'élément	[6.2.6.2.(1)]

$F_{c,wb,Rd2} = [\omega\ k_{wc}\ \rho\ b_{eff,c,wb}\ t_{wb}\ f_{yb} / \gamma_{M1}] \cos(\gamma) / \sin(\gamma - \beta)$

$F_{c,wb,Rd2}$ =	2715,52	[kN]	Résistance de l'âme de la poutre	[6.2.6.2.(1)]

Résistance de l'aile du renfort

$F_{c,wb,Rd3} = b_b\ t_b\ f_{yb} / (0.8 * \gamma_{M0})$

$F_{c,wb,Rd3}$ =	634,50	[kN]	Résistance de l'aile du renfort	[6.2.6.7.(1)]

Résistance finale:

$F_{c,wb,Rd,low} = \mathrm{Min}\ (F_{c,wb,Rd1}\ ,\ F_{c,wb,Rd2}\ ,\ F_{c,wb,Rd3})$

$F_{c,wb,Rd,low}$ =	634,50	[kN]	Résistance de l'âme de la poutre	[6.2.6.2.(1)]

RÉSISTANCES DU POTEAU

PANNEAU D'AME EN CISAILLEMENT

$M_{b1,Ed}$ =	72,05	[kN*m]	Moment fléchissant dans la poutre droite	[5.3.(3)]
$M_{b2,Ed}$ =	0,00	[kN*m]	Moment fléchissant dans la poutre gauche	[5.3.(3)]
$V_{c1,Ed}$ =	102,93	[kN]	Effort tranchant dans le poteau inférieur	[5.3.(3)]
$V_{c2,Ed}$ =	0,00	[kN]	Effort tranchant dans le poteau supérieur	[5.3.(3)]
z =	536	[mm]	Bras de levier	[6.2.5]

$V_{wp,Ed} = (M_{b1,Ed} - M_{b2,Ed}) / z - (V_{c1,Ed} - V_{c2,Ed}) / 2$

$V_{wp,Ed}$ =	83,07	[kN]	Panneau d'âme en cisaillement	[5.3.(3)]
A_{vs} =	57,33	[cm^2]	Aire de cisaillement de l'âme du poteau	EN1993-1-1:[6.2.6.(3)]
A_{vc} =	57,33	[cm^2]	Aire de la section au cisaillement	EN1993-1-1:[6.2.6.(3)]
d_s =	647	[mm]	Distance entre les centres de gravités des raidisseurs	[6.2.6.1.(4)]
$M_{pl,fc,Rd}$ =	6,36	[kN*m]	Résistance plastique de l'aile du poteau en flexion	[6.2.6.1.(4)]
$M_{pl,stu,Rd}$ =	1,13	[kN*m]	Résistance plastique du raidisseur transversal supérieur en flexion	[6.2.6.1.(4)]
$M_{pl,stl,Rd}$ =	1,13	[kN*m]	Résistance plastique du raidisseur transversal inférieur en flexion	[6.2.6.1.(4)]

$V_{wp,Rd} = 0.9\ (A_{vs} * f_{y,wc}) / (\sqrt{3}\ \gamma_{M0}) + \mathrm{Min}(4\ M_{pl,fc,Rd} / d_s\ ,\ (2\ M_{pl,fc,Rd} + M_{pl,stu,Rd} + M_{pl,stl,Rd}) / d_s)$

$V_{wp,Rd}$ =	723,22	[kN]	Résistance du panneau d'âme au cisaillement	[6.2.6.1]
$V_{wp,Ed} / V_{wp,Rd} \leq 1,0$	0,11 < 1,00		vérifié	(0,11)

AME EN COMPRESSION TRANSVERSALE - NIVEAU DE L'AILE INFERIEURE DE LA POUTRE

Pression diamétrale:

t_{wc} =	11	[mm]	Epaisseur efficace de l'âme du poteau	[6.2.6.2.(6)]
$b_{eff,c,wc}$ =	311	[mm]	Largeur efficace de l'âme à la compression	[6.2.6.2.(1)]

d_{wc} = 298 [mm] Hauteur de l'âme comprimée [6.2.6.2.(1)]

λ_p =	0,86		Elancement de plaque	[6.2.6.2.(1)]
ρ =	0,89		Coefficient réducteur pour le flambement de l'élément	[6.2.6.2.(1)]
λ_s =	3,38		Elancement du raidisseur	EN1993-1-1:[6.3.1.2]
χ_s =	1,00		Coefficient de flambement du raidisseur	EN1993-1-1:[6.3.1.2]

$F_{c,wc,Rd2} = \omega\ k_{wc}\ \rho\ b_{eff,c,wc}\ t_{wc}\ f_{yc} / \gamma_{M1} + A_s\ \chi_s\ f_{ys} / \gamma_{M1}$

$F_{c,wc,Rd2}$ = 1052,59 [kN] Résistance de l'âme du poteau [6.2.6.2.(1)]

Résistance finale:

$F_{c,wc,Rd,low} = \text{Min}\ (F_{c,wc,Rd1}\ ,\ F_{c,wc,Rd2})$

$F_{c,wc,Rd}$ = 1052,59 [kN] Résistance de l'âme du poteau [6.2.6.2.(1)]

AME EN TRACTION TRANSVERSALE - NIVEAU DE L'AILE INFERIEURE DE LA POUTRE

Pression diamétrale:

t_{wc} =	11	[mm]	Epaisseur efficace de l'âme du poteau	[6.2.6.2.(6)]
$b_{eff,c,wc}$ =	312	[mm]	Largeur efficace de l'âme à la compression	[6.2.6.2.(1)]
A_{vc} =	57,33	[cm²]	Aire de la section au cisaillement	EN1993-1-1:[6.2.6.(3)]
ω =	0,83		Coefficient réducteur pour l'interaction avec le cisaillement	[6.2.6.2.(1)]
$\sigma_{com,Ed}$ =	26,52	[MPa]	Contrainte de compression maximale dans l'âme	[6.2.6.2.(2)]
k_{wc} =	1,00		Coefficient réducteur dû aux contraintes de compression	[6.2.6.2.(2)]
A_s =	19,62	[cm²]	Aire de la section du raidisseur renforçant l'âme	EN1993-1-1:[6.2.4]

$F_{c,wc,Rd1} = \omega\ k_{wc}\ b_{eff,c,wc}\ t_{wc}\ f_{yc} / \gamma_{M0} + A_s\ f_{ys} / \gamma_{M0}$

$F_{c,wc,Rd1}$ = 1127,01 [kN] Résistance de l'âme du poteau [6.2.6.2.(1)]

Flambement:

d_{wc} =	298	[mm]	Hauteur de l'âme comprimée	[6.2.6.2.(1)]
λ_p =	0,86		Elancement de plaque	[6.2.6.2.(1)]
ρ =	0,89		Coefficient réducteur pour le flambement de l'élément	[6.2.6.2.(1)]
λ_s =	3,38		Elancement du raidisseur	EN1993-1-1:[6.3.1.2]
χ_s =	1,00		Coefficient de flambement du raidisseur	EN1993-1-1:[6.3.1.2]

$F_{c,wc,Rd2} = \omega\ k_{wc}\ \rho\ b_{eff,c,wc}\ t_{wc}\ f_{yc} / \gamma_{M1} + A_s\ \chi_s\ f_{ys} / \gamma_{M1}$

$F_{c,wc,Rd2}$ = 1053,35 [kN] Résistance de l'âme du poteau [6.2.6.2.(1)]

Résistance finale:

$F_{c,wc,Rd,upp} = \text{Min}\ (F_{c,wc,Rd1}\ ,\ F_{c,wc,Rd2})$

$F_{c,wc,Rd,upp}$ = 1053,35 [kN] Résistance de l'âme du poteau [6.2.6.2.(1)]

PARAMÈTRES GÉOMÉTRIQUES DE L'ASSEMBLAGE

LONGUEURS EFFICACES ET PARAMETRES - SEMELLE DU POTEAU

Nr	m	m_x	e	e_x	p	$l_{eff,cp}$	$l_{eff,nc}$	$l_{eff,1}$	$l_{eff,2}$	$l_{eff,cp,g}$	$l_{eff,nc,g}$	$l_{eff,1,g}$	$l_{eff,2,g}$
1	-2	-	125	-	100	-13	-17	-17	-17	93	-41	-41	-41
2	-2	-	125	-	100	-13	148	-13	148	200	100	100	100
3	-2	-	125	-	120	-13	148	-13	148	240	120	120	120
4	-2	-	125	-	120	-13	148	-13	148	240	120	120	120
5	-2	-	125	-	100	-13	148	-13	148	200	100	100	100
6	-2	-	125	-	100	-13	-17	-17	-17	93	-41	-41	-41

LONGUEURS EFFICACES ET PARAMETRES - PLATINE D'ABOUT

Nr	m	m_x	e	e_x	p	$l_{eff,cp}$	$l_{eff,nc}$	$l_{eff,1}$	$l_{eff,2}$	$l_{eff,cp,g}$	$l_{eff,nc,g}$	$l_{eff,1,g}$	$l_{eff,2,g}$
1	13	–	50	–	100	80	102	80	102	140	95	95	95
2	13	–	50	–	100	80	114	80	114	200	100	100	100
3	13	–	50	–	120	80	114	80	114	240	120	120	120
4	13	–	50	–	120	80	114	80	114	240	120	120	120
5	13	–	50	–	100	80	114	80	114	200	100	100	100
6	13	–	50	–	100	80	114	80	114	140	107	107	107

m – Distance du boulon de l'âme
m_x – Distance du boulon de l'aile de la poutre
e – Pince entre le boulon et le bord extérieur
e_x – Pince entre le boulon et le bord extérieur horizontal
p – Entraxe des boulons
$l_{eff,cp}$ – Longueur effective pour une seule ligne de boulons dans les mécanismes circulaires
$l_{eff,nc}$ – Longueur effective pour une seule ligne de boulons dans les mécanismes non circulaires
$l_{eff,1}$ – Longueur effective pour une seule ligne de boulons pour le mode 1
$l_{eff,2}$ – Longueur effective pour une seule ligne de boulons pour le mode 2
$l_{eff,cp,g}$ – Longueur effective pour un groupe de boulons dans les mécanismes circulaires
$l_{eff,nc,g}$ – Longueur effective pour un groupe de boulons dans les mécanismes non circulaires
$l_{eff,1,g}$ – Longueur effective pour un groupe de boulons pour le mode 1
$l_{eff,2,g}$ – Longueur effective pour un groupe de boulons pour le mode 2

RÉSISTANCE DE L'ASSEMBLAGE À LA COMPRESSION

$N_{j,Rd} = \text{Min} (N_{cb,Rd} 2 F_{c,wb,Rd,low} , 2 F_{c,wc,Rd,low} , 2 F_{c,wc,Rd,upp})$

$N_{j,Rd} =$ 1269,00 [kN] Résistance de l'assemblage à la compression [6.2]

$N_{b1,Ed} / N_{j,Rd} \leq 1,0$ 0,08 < 1,00 vérifié (0,08)

RÉSISTANCE DE L'ASSEMBLAGE À LA FLEXION

$F_{t,Rd} =$ 176,40 [kN] Résistance du boulon à la traction [Tableau 3.4]
$B_{p,Rd} =$ 313,73 [kN] Résistance du boulon au cisaillement au poinçonnement [Tableau 3.4]

$F_{t,fc,Rd}$ – résistance de la semelle du poteau à la flexion
$F_{t,wc,Rd}$ – résistance de l'âme du poteau à la traction
$F_{t,ep,Rd}$ – résistance de la platine fléchie à la flexion
$F_{t,wb,Rd}$ – résistance de l'âme à la traction

$F_{t,fc,Rd} = \text{Min} (F_{T,1,fc,Rd} , F_{T,2,fc,Rd} , F_{T,3,fc,Rd})$ [6.2.6.4] , [Tab.6.2]
$F_{t,wc,Rd} = \omega \, b_{eff,t,wc} \, t_{wc} \, f_{yc} / \gamma_{M0}$ [6.2.6.3.(1)]
$F_{t,ep,Rd} = \text{Min} (F_{T,1,ep,Rd} , F_{T,2,ep,Rd} , F_{T,3,ep,Rd})$ [6.2.6.5] , [Tab.6.2]
$F_{t,wb,Rd} = b_{eff,t,wb} \, t_{wb} \, f_{yb} / \gamma_{M0}$ [6.2.6.8.(1)]

RESISTANCE DE LA RANGEE DE BOULONS N° 1

$F_{t1,Rd,comp}$ - Formule	$F_{t1,Rd,comp}$	Composant
$F_{t1,Rd} = \text{Min} (F_{t1,Rd,comp})$	162,29	Résistance d'une rangée de boulon
$F_{t,fc,Rd(1)} = 346,82$	346,82	Aile du poteau - traction
$F_{t,ep,Rd(1)} = 352,80$	352,80	Platine d'about - traction
$F_{t,wb,Rd(1)} = 162,29$	162,29	Ame de la poutre - traction
$B_{p,Rd} = 627,46$	627,46	Boulons au cisaillement/poinçonnement
$V_{wp,Rd}/\beta = 723,22$	723,22	Panneau d'âme - compression
$F_{c,wc,Rd} = 1052,59$	1052,59	Ame du poteau - compression
$F_{c,fb,Rd} = 699,23$	699,23	Aile de la poutre - compression
$F_{c,wb,Rd} = 634,50$	634,50	Ame de la poutre - compression

RESISTANCE DE LA RANGEE DE BOULONS N° 2

$F_{t2,Rd,comp}$ - Formule	$F_{t2,Rd,comp}$	Composant

$F_{t2,Rd,comp}$ - Formule	$F_{t2,Rd,comp}$	Composant
$F_{t2,Rd} = Min (F_{t2,Rd,comp})$	162,29	Résistance d'une rangée de boulon
$F_{t,ep,Rd(2)} = 352,80$	352,80	Platine d'about - traction
$F_{t,wb,Rd(2)} = 162,29$	162,29	Ame de la poutre - traction
$B_{p,Rd} = 627,46$	627,46	Boulons au cisaillement/poinçonnement
$V_{wp,Rd}/\beta - \sum_1^1 F_{ti,Rd} = 723,22 - 162,29$	560,93	Panneau d'âme - compression
$F_{c,wc,Rd} - \sum_1^1 F_{tj,Rd} = 1052,59 - 162,29$	890,30	Ame du poteau - compression
$F_{c,fb,Rd} - \sum_1^1 F_{tj,Rd} = 699,23 - 162,29$	536,94	Aile de la poutre - compression
$F_{c,wb,Rd} - \sum_1^1 F_{tj,Rd} = 634,50 - 162,29$	472,21	Ame de la poutre - compression
$F_{t,wc,Rd(2+1)} - \sum_1^1 F_{tj,Rd} = 151,95 - 162,29$	-10,34	Ame du poteau - traction - groupe
$F_{t,ep,Rd(2+1)} - \sum_1^1 F_{tj,Rd} = 705,60 - 162,29$	543,31	Platine d'about - traction - groupe
$F_{t,wb,Rd(2+1)} - \sum_1^1 F_{tj,Rd} = 394,97 - 162,29$	232,68	Ame de la poutre - traction - groupe

RESISTANCE DE LA RANGEE DE BOULONS N° 3

$F_{t3,Rd,comp}$ - Formule	$F_{t3,Rd,comp}$	Composant
$F_{t3,Rd} = Min (F_{t3,Rd,comp})$	106,85	Résistance d'une rangée de boulon
$F_{t,ep,Rd(3)} = 352,80$	352,80	Platine d'about - traction
$F_{t,wb,Rd(3)} = 162,29$	162,29	Ame de la poutre - traction
$B_{p,Rd} = 627,46$	627,46	Boulons au cisaillement/poinçonnement
$V_{wp,Rd}/\beta - \sum_1^2 F_{ti,Rd} = 723,22 - 324,58$	398,64	Panneau d'âme - compression
$F_{c,wc,Rd} - \sum_1^2 F_{tj,Rd} = 1052,59 - 324,58$	728,01	Ame du poteau - compression
$F_{c,fb,Rd} - \sum_1^2 F_{tj,Rd} = 699,23 - 324,58$	374,65	Aile de la poutre - compression
$F_{c,wb,Rd} - \sum_1^2 F_{tj,Rd} = 634,50 - 324,58$	309,92	Ame de la poutre - compression
$F_{t,wc,Rd(3+2)} - \sum_2^2 F_{tj,Rd} = 512,44 - 162,29$	350,15	Ame du poteau - traction - groupe
$F_{t,wc,Rd(3+2+1)} - \sum_2^1 F_{tj,Rd} = 431,43 - 324,58$	106,85	Ame du poteau - traction - groupe
$F_{t,ep,Rd(3+2)} - \sum_2^2 F_{tj,Rd} = 705,60 - 162,29$	543,31	Platine d'about - traction - groupe
$F_{t,wb,Rd(3+2)} - \sum_2^2 F_{tj,Rd} = 444,62 - 162,29$	282,33	Ame de la poutre - traction - groupe
$F_{t,ep,Rd(3+2+1)} - \sum_2^1 F_{tj,Rd} = 1058,40 - 324,58$	733,82	Platine d'about - traction - groupe
$F_{t,wb,Rd(3+2+1)} - \sum_2^1 F_{tj,Rd} = 637,49 - 324,58$	312,91	Ame de la poutre - traction - groupe

RESISTANCE DE LA RANGEE DE BOULONS N° 4

$F_{t4,Rd,comp}$ - Formule	$F_{t4,Rd,comp}$	Composant
$F_{t4,Rd} = Min (F_{t4,Rd,comp})$	162,29	Résistance d'une rangée de boulon
$F_{t,ep,Rd(4)} = 352,80$	352,80	Platine d'about - traction
$F_{t,wb,Rd(4)} = 162,29$	162,29	Ame de la poutre - traction
$B_{p,Rd} = 627,46$	627,46	Boulons au cisaillement/poinçonnement
$V_{wp,Rd}/\beta - \sum_1^3 F_{ti,Rd} = 723,22 - 431,43$	291,79	Panneau d'âme - compression
$F_{c,wc,Rd} - \sum_1^3 F_{tj,Rd} = 1052,59 - 431,43$	621,16	Ame du poteau - compression
$F_{c,fb,Rd} - \sum_1^3 F_{tj,Rd} = 699,23 - 431,43$	267,80	Aile de la poutre - compression
$F_{c,wb,Rd} - \sum_1^3 F_{tj,Rd} = 634,50 - 431,43$	203,07	Ame de la poutre - compression
$F_{t,wc,Rd(4+3)} - \sum_3^3 F_{tj,Rd} = 549,29 - 106,85$	442,44	Ame du poteau - traction - groupe
$F_{t,wc,Rd(4+3+2)} - \sum_3^2 F_{tj,Rd} = 705,21 - 269,14$	436,07	Ame du poteau - traction - groupe
$F_{t,wc,Rd(4+3+2+1)} - \sum_3^1 F_{tj,Rd} = 647,24 - 431,43$	215,81	Ame du poteau - traction - groupe
$F_{t,ep,Rd(4+3)} - \sum_3^3 F_{tj,Rd} = 705,60 - 106,85$	598,75	Platine d'about - traction - groupe
$F_{t,wb,Rd(4+3)} - \sum_3^3 F_{tj,Rd} = 485,04 - 106,85$	378,19	Ame de la poutre - traction - groupe
$F_{t,ep,Rd(4+3+2)} - \sum_3^2 F_{tj,Rd} = 1058,40 - 269,14$	789,26	Platine d'about - traction - groupe
$F_{t,wb,Rd(4+3+2)} - \sum_3^2 F_{tj,Rd} = 687,14 - 269,14$	418,00	Ame de la poutre - traction - groupe
$F_{t,ep,Rd(4+3+2+1)} - \sum_3^1 F_{tj,Rd} = 1411,20 - 431,43$	979,77	Platine d'about - traction - groupe
$F_{t,wb,Rd(4+3+2+1)} - \sum_3^1 F_{tj,Rd} = 880,01 - 431,43$	448,58	Ame de la poutre - traction - groupe

Réduction supplémentaire de la résistance d'une rangée de boulons

$F_{t4,Rd} = F_{t2,Rd} h_4/h_2$

$F_{t4,Rd} =$ 82,07 [kN] Résistance réduite d'une rangée de boulon [6.2.7.2.(9)]FRA

RESISTANCE DE LA RANGEE DE BOULONS N° 5

$F_{t5,Rd,comp}$ - Formule	$F_{t5,Rd,comp}$	Composant
$F_{t5,Rd} = Min (F_{t5,Rd,comp})$	120,99	Résistance d'une rangée de boulon
$F_{t,ep,Rd(5)} = 352,80$	352,80	Platine d'about - traction
$F_{t,wb,Rd(5)} = 162,29$	162,29	Ame de la poutre - traction
$B_{p,Rd} = 627,46$	627,46	Boulons au cisaillement/poinçonnement
$V_{wp,Rd}/\beta - \sum_1^4 F_{ti,Rd} = 723,22 - 513,51$	209,71	Panneau d'âme - compression
$F_{c,wc,Rd} - \sum_1^4 F_{tj,Rd} = 1052,59 - 513,51$	539,09	Ame du poteau - compression
$F_{c,fb,Rd} - \sum_1^4 F_{tj,Rd} = 699,23 - 513,51$	185,73	Aile de la poutre - compression
$F_{c,wb,Rd} - \sum_1^4 F_{tj,Rd} = 634,50 - 513,51$	120,99	Ame de la poutre - compression
$F_{t,wc,Rd(5+4)} - \sum_4^4 F_{tj,Rd} = 512,44 - 82,07$	430,36	Ame du poteau - traction - groupe
$F_{t,wc,Rd(5+4+3)} - \sum_4^3 F_{tj,Rd} = 705,21 - 188,93$	516,28	Ame du poteau - traction - groupe
$F_{t,wc,Rd(5+4+3+2)} - \sum_4^2 F_{tj,Rd} = 819,45 - 351,22$	468,23	Ame du poteau - traction - groupe
$F_{t,wc,Rd(5+4+3+2+1)} - \sum_4^1 F_{tj,Rd} = 777,34 - 513,51$	263,83	Ame du poteau - traction - groupe
$F_{t,ep,Rd(5+4)} - \sum_4^4 F_{tj,Rd} = 705,60 - 82,07$	623,53	Platine d'about - traction - groupe
$F_{t,wb,Rd(5+4)} - \sum_4^4 F_{tj,Rd} = 444,62 - 82,07$	362,55	Ame de la poutre - traction - groupe
$F_{t,ep,Rd(5+4+3)} - \sum_4^3 F_{tj,Rd} = 1058,40 - 188,93$	869,47	Platine d'about - traction - groupe
$F_{t,wb,Rd(5+4+3)} - \sum_4^3 F_{tj,Rd} = 687,14 - 188,93$	498,21	Ame de la poutre - traction - groupe
$F_{t,ep,Rd(5+4+3+2)} - \sum_4^2 F_{tj,Rd} = 1411,20 - 351,22$	1059,98	Platine d'about - traction - groupe
$F_{t,wb,Rd(5+4+3+2)} - \sum_4^2 F_{tj,Rd} = 889,24 - 351,22$	538,02	Ame de la poutre - traction - groupe
$F_{t,ep,Rd(5+4+3+2+1)} - \sum_4^1 F_{tj,Rd} = 1764,00 - 513,51$	1250,49	Platine d'about - traction - groupe
$F_{t,wb,Rd(5+4+3+2+1)} - \sum_4^1 F_{tj,Rd} = 1082,11 - 513,51$	568,60	Ame de la poutre - traction - groupe

Réduction supplémentaire de la résistance d'une rangée de boulons

$F_{t5,Rd} = F_{t2,Rd}\ h_5/h_2$

$F_{t5,Rd} =$ 48,65 [kN] Résistance réduite d'une rangée de boulon [6.2.7.2.(9)]FRA

RESISTANCE DE LA RANGEE DE BOULONS N° 6

$F_{t6,Rd,comp}$ - Formule	$F_{t6,Rd,comp}$	Composant
$F_{t6,Rd} = Min (F_{t6,Rd,comp})$	72,34	Résistance d'une rangée de boulon
$F_{t,fc,Rd(6)} = 346,82$	346,82	Aile du poteau - traction
$F_{t,ep,Rd(6)} = 352,80$	352,80	Platine d'about - traction
$F_{t,wb,Rd(6)} = 162,29$	162,29	Ame de la poutre - traction
$B_{p,Rd} = 627,46$	627,46	Boulons au cisaillement/poinçonnement
$V_{wp,Rd}/\beta - \sum_1^5 F_{ti,Rd} = 723,22 - 562,16$	161,06	Panneau d'âme - compression
$F_{c,wc,Rd} - \sum_1^5 F_{tj,Rd} = 1052,59 - 562,16$	490,44	Ame du poteau - compression
$F_{c,fb,Rd} - \sum_1^5 F_{tj,Rd} = 699,23 - 562,16$	137,08	Aile de la poutre - compression
$F_{c,wb,Rd} - \sum_1^5 F_{tj,Rd} = 634,50 - 562,16$	72,34	Ame de la poutre - compression
$F_{t,wc,Rd(6+5)} - \sum_5^5 F_{tj,Rd} = 151,95 - 48,65$	103,30	Ame du poteau - traction - groupe
$F_{t,wc,Rd(6+5+4)} - \sum_5^4 F_{tj,Rd} = 431,43 - 130,72$	300,71	Ame du poteau - traction - groupe
$F_{t,wc,Rd(6+5+4+3)} - \sum_5^3 F_{tj,Rd} = 647,24 - 237,58$	409,67	Ame du poteau - traction - groupe
$F_{t,wc,Rd(6+5+4+3+2)} - \sum_5^2 F_{tj,Rd} = 777,34 - 399,87$	377,47	Ame du poteau - traction - groupe
$F_{t,wc,Rd(6+5+4+3+2+1)} - \sum_5^1 F_{tj,Rd} = 729,27 - 562,16$	167,11	Ame du poteau - traction - groupe
$F_{t,ep,Rd(6+5)} - \sum_5^5 F_{tj,Rd} = 705,60 - 48,65$	656,95	Platine d'about - traction - groupe
$F_{t,wb,Rd(6+5)} - \sum_5^5 F_{tj,Rd} = 417,96 - 48,65$	369,31	Ame de la poutre - traction - groupe
$F_{t,ep,Rd(6+5+4)} - \sum_5^4 F_{tj,Rd} = 1058,40 - 130,72$	927,68	Platine d'about - traction - groupe
$F_{t,wb,Rd(6+5+4)} - \sum_5^4 F_{tj,Rd} = 660,48 - 130,72$	529,76	Ame de la poutre - traction - groupe
$F_{t,ep,Rd(6+5+4+3)} - \sum_5^3 F_{tj,Rd} = 1411,20 - 237,58$	1173,62	Platine d'about - traction - groupe
$F_{t,wb,Rd(6+5+4+3)} - \sum_5^3 F_{tj,Rd} = 903,00 - 237,58$	665,43	Ame de la poutre - traction - groupe
$F_{t,ep,Rd(6+5+4+3+2)} - \sum_5^2 F_{tj,Rd} = 1764,00 - 399,87$	1364,13	Platine d'about - traction - groupe
$F_{t,wb,Rd(6+5+4+3+2)} - \sum_5^2 F_{tj,Rd} = 1105,10 - 399,87$	705,24	Ame de la poutre - traction - groupe
$F_{t,ep,Rd(6+5+4+3+2+1)} - \sum_5^1 F_{tj,Rd} = 2116,80 - 562,16$	1554,64	Platine d'about - traction - groupe
$F_{t,wb,Rd(6+5+4+3+2+1)} - \sum_5^1 F_{tj,Rd} = 1297,97 - 562,16$	735,82	Ame de la poutre - traction - groupe

Réduction supplémentaire de la résistance d'une rangée de boulons

$F_{t6,Rd} = F_{t2,Rd}\ h_6/h_2$

$F_{t6,Rd}$ = 15,23 [kN] Résistance réduite d'une rangée de boulon [6.2.7.2.(9)]FRA

TABLEAU RECAPITULATIF DES EFFORTS

Nr	h_j	$F_{tj,Rd}$	$F_{t,fc,Rd}$	$F_{t,wc,Rd}$	$F_{t,ep,Rd}$	$F_{t,wb,Rd}$	$F_{t,Rd}$	$B_{p,Rd}$
1	586	162,29	346,82	-	352,80	162,29	352,80	627,46
2	486	162,29	-	-	352,80	162,29	352,80	627,46
3	386	106,85	-	-	352,80	162,29	352,80	627,46
4	246	82,07	-	-	352,80	162,29	352,80	627,46
5	146	48,65	-	-	352,80	162,29	352,80	627,46
6	46	15,23	346,82	-	352,80	162,29	352,80	627,46

RESISTANCE DE L'ASSEMBLAGE A LA FLEXION $M_{j,Rd}$

$M_{j,Rd} = \sum h_j F_{tj,Rd}$

$M_{j,Rd}$ = 242,96 [kN*m] Résistance de l'assemblage à la flexion [6.2]

$M_{b1,Ed} / M_{j,Rd} \leq 1,0$ 0,30 < 1,00 vérifié (0,30)

VÉRIFICATION DE L'INTERACTION M+N

$M_{b1,Ed} / M_{j,Rd} + N_{b1,Ed} / N_{j,Rd} \leq 1$ [6.2.5.1.(3)]

$M_{b1,Ed} / M_{j,Rd} + N_{b1,Ed} / N_{j,Rd}$ 0,38 < 1,00 vérifié (0,38)

RÉSISTANCE DE L'ASSEMBLAGE AU CISAILLEMENT

α_v = 0,60 Coefficient pour le calcul de $F_{v,Rd}$ [Tableau 3.4]

β_{Lf} = 0,94 Coefficient réducteur pour les assemblages longs [3.8]

$F_{v,Rd}$ = 141,75 [kN] Résistance d'un boulon au cisaillement [Tableau 3.4]

$F_{t,Rd,max}$ = 176,40 [kN] Résistance d'un boulon à la traction [Tableau 3.4]

$F_{b,Rd,int}$ = 164,42 [kN] Résistance du boulon intérieur en pression diamétrale [Tableau 3.4]

$F_{b,Rd,ext}$ = 135,78 [kN] Résistance du boulon de rive en pression diamétrale [Tableau 3.4]

Nr	$F_{tj,Rd,N}$	$F_{tj,Ed,N}$	$F_{tj,Rd,M}$	$F_{tj,Ed,M}$	$F_{tj,Ed}$	$F_{vj,Rd}$
1	352,80	-17,15	162,29	48,13	30,98	265,72
2	352,80	-17,15	162,29	48,13	30,98	265,72
3	352,80	-17,15	106,85	31,69	14,54	275,15
4	352,80	-17,15	82,07	24,34	7,19	279,37
5	352,80	-17,15	48,65	14,43	-2,72	283,50
6	352,80	-17,15	15,23	4,52	-12,64	283,50

$F_{tj,Rd,N}$ – Résistance d'une rangée de boulons à la traction pure

$F_{tj,Ed,N}$ – Effort dans une rangée de boulons dû à l'effort axial

$F_{tj,Rd,M}$ – Résistance d'une rangée de boulons à la flexion pure

$F_{tj,Ed,M}$ – Effort dans une rangée de boulons dû au moment

$F_{tj,Ed}$ – Effort de traction maximal dans la rangée de boulons

$F_{vj,Rd}$ – Résistance réduite d'une rangée de boulon

$F_{tj,Ed,N} = N_{j,Ed}\ F_{tj,Rd,N} / N_{j,Rd}$

$F_{tj,Ed,M} = M_{j,Ed}\ F_{tj,Rd,M} / M_{j,Rd}$

$F_{tj,Ed} = F_{tj,Ed,N} + F_{tj,Ed,M}$

$F_{vj,Rd} = \mathrm{Min}\ (n_h F_{v,Ed} / (1 - F_{tj,Ed} / (1.4\ n_h F_{t,Rd,max})),\ n_h F_{v,Rd}\ ,\ n_h F_{b,Rd})$

$V_{j,Rd} = n_h \sum_1^n F_{vj,Rd}$ [Tableau 3.4]

$V_{j,Rd}$ = 1652,96 [kN] Résistance de l'assemblage au cisaillement [Tableau 3.4]

$V_{b1,Ed} / V_{j,Rd} \leq 1,0$ 0,03 < 1,00 vérifié (0,03)

RÉSISTANCE DES SOUDURES

A_w = 125,26 [cm^2] Aire de toutes les soudures [4.5.3.2(2)]

A_{wy} = 45,08 [cm^2] Aire des soudures horizontales [4.5.3.2(2)]

$\sigma_{\perp} \leq 0.9*f_u/\gamma_{M2}$	43,16 < 262,80	vérifié	(0,16)

RIGIDITÉ DE L'ASSEMBLAGE

t_{wash} =	4	[mm]	Epaisseur de la plaquette	[6.2.6.3.(2)]
h_{head} =	14	[mm]	Hauteur de la tête du boulon	[6.2.6.3.(2)]
h_{nut} =	20	[mm]	Hauteur de l'écrou du boulon	[6.2.6.3.(2)]
L_b =	64	[mm]	Longueur du boulon	[6.2.6.3.(2)]
k_{10} =	6	[mm]	Coefficient de rigidité des boulons	[6.3.2.(1)]

RIGIDITES DES RANGEES DE BOULONS

Nr	hj	k_3	k_4	k_5	$k_{eff,j}$	$k_{eff,j}\ h_j$	$k_{eff,j}\ h_j^2$
					Somme	-6,30	-276,35
1	586	-0	11198	277	-0	-2,29	-134,25
2	486	-0	8795	277	-0	-1,47	-71,50
3	386	-0	8795	277	-0	-1,17	-45,08
4	246	-0	8795	277	-0	-0,74	-18,29
5	146	-0	8795	277	-0	-0,44	-6,43
6	46	-0	11198	277	-0	-0,18	-0,81

$k_{eff,j} = 1 / (\sum_3^5 (1 / k_{i,j}))$ [6.3.3.1.(2)]

$z_{eq} = \sum_j k_{eff,j}\ h_j^2 / \sum_j k_{eff,j}\ h_j$

z_{eq} = 439 [mm] Bras de levier équivalent [6.3.3.1.(3)]

$k_{eq} = \sum_j k_{eff,j}\ h_j / z_{eq}$

k_{eq} = -1 [mm] Coefficient de rigidité équivalent du système de boulons [6.3.3.1.(1)]

A_{vc} =	57,33	[cm²]	Aire de la section au cisaillement	EN1993-1-1:[6.2.6.(3)]
β =	1,00		Paramètre de transformation	[5.3.(7)]
z =	439	[mm]	Bras de levier	[6.2.5]
k_1 =	5	[mm]	Coefficient de rigidité du panneau d'âme du poteau en cisaillement	[6.3.2.(1)]
k_2 =	∞		Coefficient de rigidité du panneau d'âme du poteau en compression	[6.3.2.(1)]

$S_{j,ini} = E\ z_{eq}^2 / \sum_i (1 / k_1 + 1 / k_2 + 1 / k_{eq})$ [6.3.1.(4)]

$S_{j,ini}$ = ∞ Rigidité en rotation initiale [6.3.1.(4)]

μ = 1,00 Coefficient de rigidité de l'assemblage [6.3.1.(6)]

$S_j = S_{j,ini} / \mu$ [6.3.1.(4)]

S_j = ∞ Rigidité en rotation finale [6.3.1.(4)]

Classification de l'assemblage par rigidité.

$S_{j,rig}$ =	118510,82	[kN*m]	Rigidité de l'assemblage rigide	[5.2.2.5]
$S_{j,pin}$ =	2370,22	[kN*m]	Rigidité de l'assemblage articulé	[5.2.2.5]

$S_{j,ini} \geq S_{j,rig}$ RIGIDE

COMPOSANT LE PLUS FAIBLE:

AME DE LA POUTRE OU AILE DE LA CONTREPLAQUE EN COMPRESSION

REMARQUES

NF EN 1993-1-8:2005/NA:2007/AC:2009

Ratio
0,06

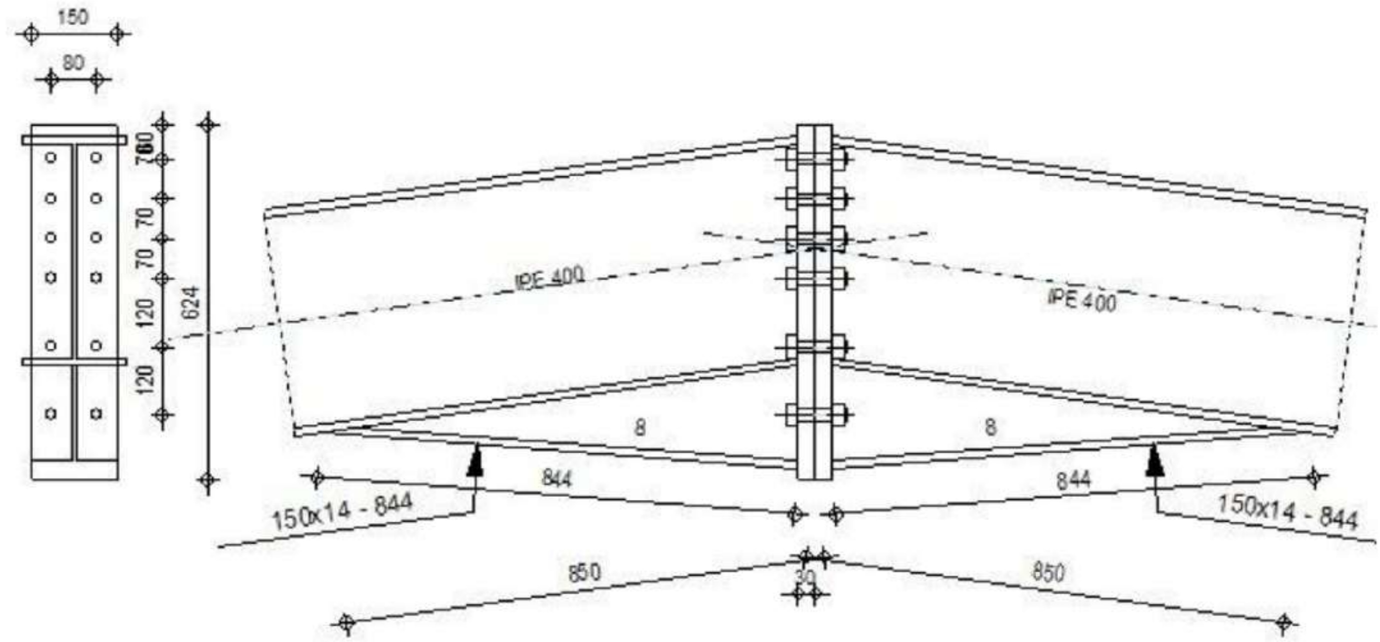

GÉNÉRAL

Assemblage N°: 3
Nom de l'assemblage: Poutre - poutre
Noeud de la structure: 5
Barres de la structure: 3, 4

GÉOMÉTRIE

GAUCHE

POUTRE

Profilé: IPE 400
Barre N°: 3

α =	-172,2	[Deg]	Angle d'inclinaison
h_{bl} =	400	[mm]	Hauteur de la section de la poutre
b_{fbl} =	180	[mm]	Largeur de la section de la poutre
t_{wbl} =	9	[mm]	Epaisseur de l'âme de la section de la poutre
t_{fbl} =	14	[mm]	Epaisseur de l'aile de la section de la poutre
r_{bl} =	21	[mm]	Rayon de congé de la section de la poutre

α = -172,2 [Deg] Angle d'inclinaison
A_{bl} = 84,46 [cm^2] Aire de la section de la poutre
I_{xbl} = 23128,40 [cm^4] Moment d'inertie de la poutre
Matériau: ACIER E24
f_{yb} = 235,00 [MPa] Résistance

DROITE

POUTRE

Profilé: IPE 400
Barre N°: 4
α = -7,8 [Deg] Angle d'inclinaison
h_{br} = 400 [mm] Hauteur de la section de la poutre
b_{fbr} = 180 [mm] Largeur de la section de la poutre
t_{wbr} = 9 [mm] Epaisseur de l'âme de la section de la poutre
t_{fbr} = 14 [mm] Epaisseur de l'aile de la section de la poutre
r_{br} = 21 [mm] Rayon de congé de la section de la poutre
A_{br} = 84,46 [cm^2] Aire de la section de la poutre
I_{xbr} = 23128,40 [cm^4] Moment d'inertie de la poutre
Matériau: ACIER E24
f_{yb} = 235,00 [MPa] Résistance

BOULONS

Le plan de cisaillement passe par la partie NON FILETÉE du boulon
d = 20 [mm] Diamètre du boulon
Classe = HR 10.9 Classe du boulon
F_{tRd} = 176,40 [kN] Résistance du boulon à la traction
n_h = 2 Nombre de colonnes des boulons
n_v = 6 Nombre de rangéss des boulons
h_1 = 60 [mm] Pince premier boulon-extrémité supérieure de la platine d'about
Ecartement e_i = 80 [mm]
Entraxe p_i = 70;70;70;120;120 [mm]

PLATINE

h_{pr} = 624 [mm] Hauteur de la platine
b_{pr} = 150 [mm] Largeur de la platine
t_{pr} = 30 [mm] Epaisseur de la platine
Matériau: ACIER E24
f_{ypr} = 235,00 [MPa] Résistance

JARRET INFÉRIEUR

w_{rd} = 150 [mm] Largeur de la platine
t_{frd} = 14 [mm] Epaisseur de l'aile
h_{rd} = 180 [mm] Hauteur de la platine
t_{wrd} = 8 [mm] Epaisseur de l'âme
l_{rd} = 850 [mm] Longueur de la platine
α_d = 4,3 [Deg] Angle d'inclinaison
Matériau: ACIER E24
f_{ybu} = 235,00 [MPa] Résistance

SOUDURES D'ANGLE

a_w =	7	[mm]	Soudure âme	
a_f =	10	[mm]	Soudure semelle	
a_{fd} =	5	[mm]	Soudure horizontale	

COEFFICIENTS DE MATÉRIAU

γ_{M0} =	1,00	Coefficient de sécurité partiel	[2.2]
γ_{M1} =	1,00	Coefficient de sécurité partiel	[2.2]
γ_{M2} =	1,25	Coefficient de sécurité partiel	[2.2]
γ_{M3} =	1,10	Coefficient de sécurité partiel	[2.2]

EFFORTS

Etat limite: ultime

Cas: 11: 1.35G+1.35Q+1.35S (1+2+3+4)*1.35

$M_{b1,Ed}$ =	2,19	[kN*m]	Moment fléchissant dans la poutre droite
$N_{b1,Ed}$ =	-100,27	[kN]	Effort axial dans la poutre droite

RÉSULTATS

RÉSISTANCES DE LA POUTRE

COMPRESSION

A_b = 84,46 [cm²] Aire de la section EN1993-1-1:[6.2.4]

$N_{cb,Rd} = A_b\ f_{yb} / \gamma_{M0}$

$N_{cb,Rd}$ = 1984,81 [kN] Résistance de calcul de la section à la compression EN1993-1-1:[6.2.4]

FLEXION - MOMENT PLASTIQUE (SANS RENFORTS)

W_{plb} = 1307,15 [cm³] Facteur plastique de la section EN1993-1-1:[6.2.5.(2)]

$M_{b,pl,Rd} = W_{plb}\ f_{yb} / \gamma_{M0}$

$M_{b,pl,Rd}$ = 307,18 [kN*m] Résistance plastique de la section à la flexion (sans renforts) EN1993-1-1:[6.2.5.(2)]

FLEXION AU CONTACT DE LA PLAQUE AVEC L'ELEMENT ASSEMBLE

W_{el} = 1627,42 [cm³] Facteur élastique de la section EN1993-1-1:[6.2.5]

$M_{cb,Rd} = W_{el}\ f_{yb} / \gamma_{M0}$

$M_{cb,Rd}$ = 382,44 [kN*m] Résistance de calcul de la section à la flexion EN1993-1-1:[6.2.5]

FLEXION AVEC EFFORT AXIAL AU CONTACT DE LA PLAQUE AVEC L'ELEMENT ASSEMBLE

n = 0,05 Rapport de l'effort axial à la résistance de la section EN1993-1-1:[6.2.9.1.(5)]

$M_{Nb,Rd} = M_{cb,Rd}\ (1 - n)$

$M_{Nb,Rd}$ = 363,12 [kN*m] Résistance réduite (effort axial) de la section à la flexion EN1993-1-1:[6.2.9.2.(1)]

AILE ET AME EN COMPRESSION

$M_{cb,Rd}$ = 382,44 [kN*m] Résistance de calcul de la section à la flexion EN1993-1-1:[6.2.5]

h_f = 570 [mm] Distance entre les centres de gravité des ailes [6.2.6.7.(1)]

$F_{c,fb,Rd} = M_{cb,Rd} / h_f$

$F_{c,fb,Rd}$ = 671,02 [kN] Résistance de l'aile et de l'âme comprimées [6.2.6.7.(1)]

AME OU AILE DU RENFORT EN COMPRESSION - NIVEAU DE L'AILE INFERIEURE DE LA POUTRE

Pression diamétrale:

β =	7,8	[Deg]	Angle entre la platine d'about et la poutre	
γ =	4,3	[Deg]	Angle d'inclinaison du renfort	
$b_{eff,c,wb}$ =	267	[mm]	Largeur efficace de l'âme à la compression	[6.2.6.2.(1)]
A_{vb} =	42,69	[cm²]	Aire de la section au cisaillement	EN1993-1-1:[6.2.6.(3)]
ω =	0,85		Coefficient réducteur pour l'interaction avec le cisaillement	[6.2.6.2.(1)]
$\sigma_{com,Ed}$ =	13,44	[MPa]	Contrainte de compression maximale dans l'âme	[6.2.6.2.(2)]
k_{wc} =	1,00		Coefficient réducteur dû aux contraintes de compression	[6.2.6.2.(2)]

$F_{c,wb,Rd1} = [\omega\ k_{wc}\ b_{eff,c,wb}\ t_{wb}\ f_{yb} / \gamma_{M0}] \cos(\gamma) / \sin(\gamma - \beta)$

$F_{c,wb,Rd,low}$ = 1641,68 [kN] Résistance de l'âme de la poutre [6.2.6.2.(1)]

PARAMÈTRES GÉOMÉTRIQUES DE L'ASSEMBLAGE

LONGUEURS EFFICACES ET PARAMETRES - PLATINE D'ABOUT

Nr	m	m_x	e	e_x	p	$l_{eff,cp}$	$l_{eff,nc}$	$l_{eff,1}$	$l_{eff,2}$	$l_{eff,cp,g}$	$l_{eff,nc,g}$	$l_{eff,1,g}$	$l_{eff,2,g}$
1	28	–	35	–	70	175	201	175	201	157	159	157	159
2	28	–	35	–	70	175	155	155	155	140	70	70	70
3	28	–	35	–	70	175	155	155	155	140	70	70	70
4	28	–	35	–	95	175	155	155	155	190	95	95	95
5	28	–	35	–	120	175	155	155	155	240	120	120	120
6	28	–	35	–	120	175	155	155	155	207	137	137	137

m – Distance du boulon de l'âme
m_x – Distance du boulon de l'aile de la poutre
e – Pince entre le boulon et le bord extérieur
e_x – Pince entre le boulon et le bord extérieur horizontal
p – Entraxe des boulons
$l_{eff,cp}$ – Longueur effective pour une seule ligne de boulons dans les mécanismes circulaires
$l_{eff,nc}$ – Longueur effective pour une seule ligne de boulons dans les mécanismes non circulaires
$l_{eff,1}$ – Longueur effective pour une seule ligne de boulons pour le mode 1
$l_{eff,2}$ – Longueur effective pour une seule ligne de boulons pour le mode 2
$l_{eff,cp,g}$ – Longueur effective pour un groupe de boulons dans les mécanismes circulaires
$l_{eff,nc,g}$ – Longueur effective pour un groupe de boulons dans les mécanismes non circulaires
$l_{eff,1,g}$ – Longueur effective pour un groupe de boulons pour le mode 1
$l_{eff,2,g}$ – Longueur effective pour un groupe de boulons pour le mode 2

RÉSISTANCE DE L'ASSEMBLAGE À LA COMPRESSION

$N_{j,Rd} = \mathrm{Min}\ (N_{cb,Rd} 2\ F_{c,wb,Rd,low})$

$N_{j,Rd}$ = 1984,81 [kN] Résistance de l'assemblage à la compression [6.2]

$N_{b1,Ed} / N_{j,Rd} \leq 1,0$ 0,05 < 1,00 vérifié (0,05)

RÉSISTANCE DE L'ASSEMBLAGE À LA FLEXION

$F_{t,Rd}$ = 176,40 [kN] Résistance du boulon à la traction [Tableau 3.4]

$B_{p,Rd}$ = 495,37 [kN] Résistance du boulon au cisaillement au poinçonnement [Tableau 3.4]

$F_{t,fc,Rd}$ – résistance de la semelle du poteau à la flexion
$F_{t,wc,Rd}$ – résistance de l'âme du poteau à la traction
$F_{t,ep,Rd}$ – résistance de la platine fléchie à la flexion
$F_{t,wb,Rd}$ – résistance de l'âme à la traction

$F_{t,fc,Rd} = \mathrm{Min}\ (F_{T,1,fc,Rd}\ ,\ F_{T,2,fc,Rd}\ ,\ F_{T,3,fc,Rd})$ [6.2.6.4] , [Tab.6.2]

$F_{t,wc,Rd} = \omega\ b_{eff,t,wc}\ t_{wc}\ f_{yc} / \gamma_{M0}$ [6.2.6.3.(1)]

$F_{t,ep,Rd} = \mathrm{Min}\ (F_{T,1,ep,Rd}\ ,\ F_{T,2,ep,Rd}\ ,\ F_{T,3,ep,Rd})$ [6.2.6.5] , [Tab.6.2]

$F_{t,wb,Rd} = b_{eff,t,wb}\ t_{wb}\ f_{yb} / \gamma_{M0}$ [6.2.6.8.(1)]

RESISTANCE DE LA RANGEE DE BOULONS N° 1

$F_{t1,Rd,comp}$ - Formule	$F_{t1,Rd,comp}$	Composant
$F_{t1,Rd} = Min (F_{t1,Rd,comp})$	352,76	Résistance d'une rangée de boulon
$F_{t,ep,Rd(1)} = 352,80$	352,80	Platine d'about - traction
$F_{t,wb,Rd(1)} = 352,76$	352,76	Ame de la poutre - traction
$B_{p,Rd} = 990,73$	990,73	Boulons au cisaillement/poinçonnement
$F_{c,fb,Rd} = 671,02$	671,02	Aile de la poutre - compression
$F_{c,wb,Rd} = 1641,68$	1641,68	Ame de la poutre - compression

RESISTANCE DE LA RANGEE DE BOULONS N° 2

$F_{t2,Rd,comp}$ - Formule	$F_{t2,Rd,comp}$	Composant
$F_{t2,Rd} = Min (F_{t2,Rd,comp})$	110,06	Résistance d'une rangée de boulon
$F_{t,ep,Rd(2)} = 352,80$	352,80	Platine d'about - traction
$F_{t,wb,Rd(2)} = 313,00$	313,00	Ame de la poutre - traction
$B_{p,Rd} = 990,73$	990,73	Boulons au cisaillement/poinçonnement
$F_{c,fb,Rd} - \sum_1^1 F_{tj,Rd} = 671,02 - 352,76$	318,26	Aile de la poutre - compression
$F_{c,wb,Rd} - \sum_1^1 F_{tj,Rd} = 1641,68 - 352,76$	1288,92	Ame de la poutre - compression
$F_{t,ep,Rd(2+1)} - \sum_1^1 F_{tj,Rd} = 705,60 - 352,76$	352,84	Platine d'about - traction - groupe
$F_{t,wb,Rd(2+1)} - \sum_1^1 F_{tj,Rd} = 462,82 - 352,76$	110,06	Ame de la poutre - traction - groupe

RESISTANCE DE LA RANGEE DE BOULONS N° 3

$F_{t3,Rd,comp}$ - Formule	$F_{t3,Rd,comp}$	Composant
$F_{t3,Rd} = Min (F_{t3,Rd,comp})$	141,47	Résistance d'une rangée de boulon
$F_{t,ep,Rd(3)} = 352,80$	352,80	Platine d'about - traction
$F_{t,wb,Rd(3)} = 313,00$	313,00	Ame de la poutre - traction
$B_{p,Rd} = 990,73$	990,73	Boulons au cisaillement/poinçonnement
$F_{c,fb,Rd} - \sum_1^2 F_{tj,Rd} = 671,02 - 462,82$	208,20	Aile de la poutre - compression
$F_{c,wb,Rd} - \sum_1^2 F_{tj,Rd} = 1641,68 - 462,82$	1178,86	Ame de la poutre - compression
$F_{t,ep,Rd(3+2)} - \sum_2^2 F_{tj,Rd} = 628,86 - 110,06$	518,80	Platine d'about - traction - groupe
$F_{t,wb,Rd(3+2)} - \sum_2^2 F_{tj,Rd} = 282,94 - 110,06$	172,88	Ame de la poutre - traction - groupe
$F_{t,ep,Rd(3+2+1)} - \sum_2^1 F_{tj,Rd} = 1058,40 - 462,82$	595,58	Platine d'about - traction - groupe
$F_{t,wb,Rd(3+2+1)} - \sum_2^1 F_{tj,Rd} = 604,29 - 462,82$	141,47	Ame de la poutre - traction - groupe

RESISTANCE DE LA RANGEE DE BOULONS N° 4

$F_{t4,Rd,comp}$ - Formule	$F_{t4,Rd,comp}$	Composant
$F_{t4,Rd} = Min (F_{t4,Rd,comp})$	66,73	Résistance d'une rangée de boulon
$F_{t,ep,Rd(4)} = 352,80$	352,80	Platine d'about - traction
$F_{t,wb,Rd(4)} = 313,00$	313,00	Ame de la poutre - traction
$B_{p,Rd} = 990,73$	990,73	Boulons au cisaillement/poinçonnement
$F_{c,fb,Rd} - \sum_1^3 F_{tj,Rd} = 671,02 - 604,29$	66,73	Aile de la poutre - compression
$F_{c,wb,Rd} - \sum_1^3 F_{tj,Rd} = 1641,68 - 604,29$	1037,39	Ame de la poutre - compression
$F_{t,ep,Rd(4+3)} - \sum_3^3 F_{tj,Rd} = 671,15 - 141,47$	529,68	Platine d'about - traction - groupe
$F_{t,wb,Rd(4+3)} - \sum_3^3 F_{tj,Rd} = 333,47 - 141,47$	192,00	Ame de la poutre - traction - groupe
$F_{t,ep,Rd(4+3+2)} - \sum_3^2 F_{tj,Rd} = 985,58 - 251,53$	734,06	Platine d'about - traction - groupe
$F_{t,wb,Rd(4+3+2)} - \sum_3^2 F_{tj,Rd} = 474,94 - 251,53$	223,41	Ame de la poutre - traction - groupe
$F_{t,ep,Rd(4+3+2+1)} - \sum_3^1 F_{tj,Rd} = 1411,20 - 604,29$	806,91	Platine d'about - traction - groupe
$F_{t,wb,Rd(4+3+2+1)} - \sum_3^1 F_{tj,Rd} = 796,29 - 604,29$	192,00	Ame de la poutre - traction - groupe

RESISTANCE DE LA RANGEE DE BOULONS N° 5

$F_{t5,Rd,comp}$ - Formule	$F_{t5,Rd,comp}$	Composant
$F_{t5,Rd} = Min (F_{t5,Rd,comp})$	0,00	Résistance d'une rangée de boulon
$F_{t,ep,Rd(5)} = 352,80$	352,80	Platine d'about - traction
$F_{t,wb,Rd(5)} = 313,00$	313,00	Ame de la poutre - traction
$B_{p,Rd} = 990,73$	990,73	Boulons au cisaillement/poinçonnement

$F_{t,ep,Rd(5+4+3+2+1)} - \sum_4^1 F_{tj,Rd}$ = 1764,00 - 671,02	1092,98	Platine d'about - traction - groupe
$F_{t,wb,Rd(5+4+3+2+1)} - \sum_4^1 F_{tj,Rd}$ = 1038,81 - 671,02	367,79	Ame de la poutre - traction - groupe

Les autres boulons sont inactifs (ils ne transfèrent pas de charges) car la résistance d'un des composants de l'assemblage s'est épuisée ou ces boulons sont situés au-dessous du centre de rotation.

TABLEAU RECAPITULATIF DES EFFORTS

Nr	h_j	$F_{tj,Rd}$	$F_{t,fc,Rd}$	$F_{t,wc,Rd}$	$F_{t,ep,Rd}$	$F_{t,wb,Rd}$	$F_{t,Rd}$	$B_{p,Rd}$
1	537	352,76	-	-	352,80	352,76	352,80	990,73
2	467	110,06	-	-	352,80	313,00	352,80	990,73
3	397	141,47	-	-	352,80	313,00	352,80	990,73
4	327	66,73	-	-	352,80	313,00	352,80	990,73
5	207	-	-	-	352,80	313,00	352,80	990,73
6	87	-	-	-	352,80	313,00	352,80	990,73

RESISTANCE DE L'ASSEMBLAGE A LA FLEXION $M_{j,Rd}$

$M_{j,Rd} = \sum h_j F_{tj,Rd}$

$M_{j,Rd}$ =	318,65	[kN*m]	Résistance de l'assemblage à la flexion	[6.2]
$M_{b1,Ed} / M_{j,Rd} \le 1,0$	0,01 < 1,00		vérifié	(0,01)

VÉRIFICATION DE L'INTERACTION M+N

$M_{b1,Ed} / M_{j,Rd} + N_{b1,Ed} / N_{j,Rd} \le 1$			[6.2.5.1.(3)]
$M_{b1,Ed} / M_{j,Rd} + N_{b1,Ed} / N_{j,Rd}$	0,06 < 1,00	vérifié	(0,06)

RÉSISTANCE DES SOUDURES

A_w =	145,49	[cm^2]	Aire de toutes les soudures	[4.5.3.2(2)]
A_{wy} =	75,48	[cm^2]	Aire des soudures horizontales	[4.5.3.2(2)]
A_{wz} =	70,01	[cm^2]	Aire des soudures verticales	[4.5.3.2(2)]
I_{wy} =	62660,64	[cm^4]	Moment d'inertie du système de soudures par rapport à l'axe horiz.	[4.5.3.2(5)]
$\sigma_{\perp max}=\tau_{\perp max}$ =	-9,07	[MPa]	Contrainte normale dans la soudure	[4.5.3.2(6)]
$\sigma_{\perp}=\tau_{\perp}$ =	-8,78	[MPa]	Contraintes dans la soudure verticale	[4.5.3.2(5)]
τ_{II} =	0,00	[MPa]	Contrainte tangentielle	[4.5.3.2(5)]
β_w =	0,80		Coefficient de corrélation	[4.5.3.2(7)]

$\sqrt{[\sigma_{\perp max}^2 + 3*(\tau_{\perp max}^2)]} \le f_u/(\beta_w*\gamma_{M2})$	18,14 < 365,00	vérifié	(0,05)
$\sqrt{[\sigma_{\perp}^2 + 3*(\tau_{\perp}^2+\tau_{II}^2)]} \le f_u/(\beta_w*\gamma_{M2})$	17,56 < 365,00	vérifié	(0,05)
$\sigma_{\perp} \le 0.9*f_u/\gamma_{M2}$	9,07 < 262,80	vérifié	(0,03)

RIGIDITÉ DE L'ASSEMBLAGE

t_{wash} =	4	[mm]	Epaisseur de la plaquette	[6.2.6.3.(2)]
h_{head} =	14	[mm]	Hauteur de la tête du boulon	[6.2.6.3.(2)]
h_{nut} =	20	[mm]	Hauteur de l'écrou du boulon	[6.2.6.3.(2)]
L_b =	68	[mm]	Longueur du boulon	[6.2.6.3.(2)]
k_{10} =	6	[mm]	Coefficient de rigidité des boulons	[6.3.2.(1)]

RIGIDITES DES RANGEES DE BOULONS

Nr	hj	k_3	k_4	k_5	$k_{eff,j}$	$k_{eff,j}\ h_j$	$k_{eff,j}\ h_j^2$
					Somme	104,49	4244,15
1	537	∞	∞	178	5	28,86	1549,26
2	467	∞	∞	79	5	23,34	1089,56
3	397	∞	∞	79	5	19,84	787,26
4	327	∞	∞	108	5	16,90	552,30
5	207	∞	∞	136	5	10,91	225,64
6	87	∞	∞	156	5	4,62	40,12

$k_{eff,j} = 1 / (\sum_3^5 (1 / k_{i,j}))$ [6.3.3.1.(2)]

$z_{eq} = \sum_j k_{eff,j}\ h_j^2 / \sum_j k_{eff,j}\ h_j$

$z_{eq} =$ 406 [mm] Bras de levier équivalent [6.3.3.1.(3)]

$k_{eq} = \sum_j k_{eff,j}\ h_j / z_{eq}$

$k_{eq} =$ 26 [mm] Coefficient de rigidité équivalent du système de boulons [6.3.3.1.(1)]

$S_{j,ini} = E\ z_{eq}^2\ k_{eq}$ [6.3.1.(4)]

$S_{j,ini} =$ 891270,55 [kN*m] Rigidité en rotation initiale [6.3.1.(4)]

$\mu =$ 1,00 Coefficient de rigidité de l'assemblage [6.3.1.(6)]

$S_j = S_{j,ini} / \mu$ [6.3.1.(4)]

$S_j =$ 891270,55 [kN*m] Rigidité en rotation finale [6.3.1.(4)]

Classification de l'assemblage par rigidité.

$S_{j,rig} =$ 118510,82 [kN*m] Rigidité de l'assemblage rigide [5.2.2.5]

$S_{j,pin} =$ 2370,22 [kN*m] Rigidité de l'assemblage articulé [5.2.2.5]

$S_{j,ini} \geq S_{j,rig}$ RIGIDE

COMPOSANT LE PLUS FAIBLE:

POUTRE EN COMPRESSION

REMARQUES

Boulon face à la semelle ou trop proche de la semelle. 6 [mm] < 10 [mm]

Epaisseur de l'âme de la contreplaque inférieure à l'épaisseur de l'âme de la poutre 8 [mm] < 9 [mm]

Assemblage satisfaisant vis à vis de la Norme Ratio 0,06

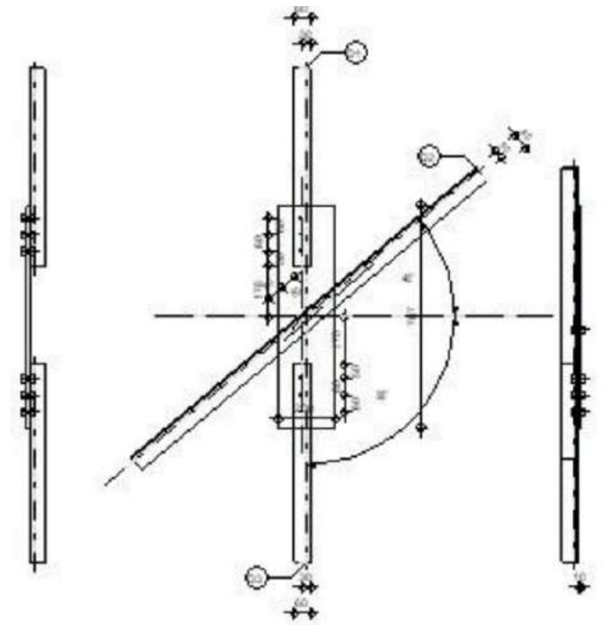

Général

Assemblage N°: 4
Nom de l'assemblage: Gousset - contreventement
Noeud de la structure: 42
Barres de la structure: 139, 141, 140, 142,

Géométrie

Barres

		Barre 1	Barre 2-4	Barre 3			
Barre N°:		139	141	140			
Profilé:		CAE 60x6	CAE 60x6	CAE 60x6			
	h	60	60	60			mm
	b_f	60	60	60			mm
	t_w	6	6	6			mm
	t_f	6	6	6			mm
	r	8	8	8			mm
	A	6,91	6,91	6,91			cm2
Matériau:		ACIER E24	ACIER E24	ACIER E24			
	f_y	235,00	235,00	235,00			MPa
	f_u	365,00	365,00	365,00			MPa
Angle	α	90,0	40,0	90,0			Deg

		Barre 1	Barre 2-4	Barre 3			
Longueur	l	0,00	0,00	0,00			m

BOULONS

Barre 1

Le plan de cisaillement passe par la partie NON FILETÉE du boulon

Classe = 8.8 Classe du boulon

d = 14 [mm] Diamètre du boulon

d_0 = 15 [mm] Diamètre du trou de boulon

A_s = 1,15 [cm^2] Aire de la section efficace du boulon

A_v = 1,54 [cm^2] Aire de la section du boulon

f_{yb} = 550,00 [MPa] Limite de plasticité

f_{ub} = 800,00 [MPa] Résistance du boulon à la traction

n = 3 Nombre de colonnes des boulons

Espacement des boulons 60;60 [mm]

e_1 = 50 [mm] Distance du centre de gravité du premier boulon de l'extrémité de la barre

e_2 = 30 [mm] Distance de l'axe des boulons du bord de la barre

e_c = 178 [mm] Distance de l'extrémité de la barre du point d'intersection des axes des barres

Barre 2-4

Le plan de cisaillement passe par la partie NON FILETÉE du boulon

Classe = 8.8 Classe du boulon

d = 14 [mm] Diamètre du boulon

d_0 = 15 [mm] Diamètre du trou de boulon

A_s = 1,15 [cm^2] Aire de la section efficace du boulon

A_v = 1,54 [cm^2] Aire de la section du boulon

f_{yb} = 550,00 [MPa] Limite de plasticité

f_{ub} = 800,00 [MPa] Résistance du boulon à la traction

n = 1 Nombre de colonnes des boulons

Espacement des boulons [mm]

e_2 = 30 [mm] Distance de l'axe des boulons du bord de la barre

Barre 3

Le plan de cisaillement passe par la partie NON FILETÉE du boulon

Classe = 8.8 Classe du boulon

d = 14 [mm] Diamètre du boulon

d_0 = 15 [mm] Diamètre du trou de boulon

A_s = 1,15 [cm^2] Aire de la section efficace du boulon

A_v = 1,54 [cm^2] Aire de la section du boulon

f_{yb} = 550,00 [MPa] Limite de plasticité

f_{ub} = 800,00 [MPa] Résistance du boulon à la traction

n = 3 Nombre de colonnes des boulons

Espacement des boulons 60;60 [mm]

e_1 = 50 [mm] Distance du centre de gravité du premier boulon de l'extrémité de la barre

e_2 = 30 [mm] Distance de l'axe des boulons du bord de la barre

e_c = 170 [mm] Distance de l'extrémité de la barre du point d'intersection des axes des barres

GOUSSET

l_p = 200 [mm] Longueur de la platine

h_p = 787 [mm] Hauteur de la platine

t_p = 10 [mm] Epaisseur de la platine

Paramètres

h_1 = 0 [mm] Grugeage

v_1 = 0 [mm] Grugeage

h_1 =	0	[mm]	Grugeage
h_2 =	0	[mm]	Grugeage
v_2 =	0	[mm]	Grugeage
h_3 =	0	[mm]	Grugeage
v_3 =	0	[mm]	Grugeage
h_4 =	0	[mm]	Grugeage
v_4 =	0	[mm]	Grugeage

Centre de gravité de la tôle par rapport au centre de gravité des barres (0;-1)

e_V = 394 [mm] Distance verticale de l'extrémité du gousset du point d'intersection des axes des barres

e_H = 100 [mm] Distance horizontale de l'extrémité du gousset du point d'intersection des axes des barres

Matériau: ACIER E24

f_y = 235,00 [MPa] Résistance

COEFFICIENTS DE MATÉRIAU

γ_{M0} =	1,00	Coefficient de sécurité partiel	[2.2]
γ_{M2} =	1,25	Coefficient de sécurité partiel	[2.2]

EFFORTS

Cas: 11: 1.35G+1.35Q+1.35S (1+2+3+4)*1.35

$N_{b1,Ed}$ =	-1,38	[kN]	Effort axial
$N_{b2,Ed}$ =	0,73	[kN]	Effort axial
$N_{b3,Ed}$ =	-0,79	[kN]	Effort axial
$N_{b4,Ed}$ =	0,40	[kN]	Effort axial

RÉSULTATS

BARRE 1

RÉSISTANCE DES BOULONS

$F_{v,Rd}$ = 59,11 [kN] Résistance de la tige d'un boulon au cisaillement $F_{v,Rd}= 0.6*f_{ub}*A_v*m/\gamma_{M2}$

Pression du boulon sur la barre

Direction x

k_{1x} = 2,50	Coefficient pour le calcul de $F_{b,Rd}$		$k_{1x}=\min[2.8*(e_2/d_0)-1.7, 2.5]$
$k_{1x} > 0.0$	2,50 > 0,00	vérifié	
α_{bx} = 1,00	Coefficient dépendant de l'espacement des boulons		$\alpha_{bx}=\min[e_1/(3*d_0), p_1/(3*d_0)-0.25, f_{ub}/f_u, 1]$
$\alpha_{bx} > 0.0$	1,00 > 0,00	vérifié	
$F_{b,Rd1x}$ = 61,32 [kN]	Résistance de calcul à l'état limite de plastification de la paroi du trou		$F_{b,Rd1x}=k_{1x}*\alpha_{bx}*f_u*d*t_i/\gamma_{M2}$

Direction z

k_{1z} = 2,50	Coefficient pour le calcul de $F_{b,Rd}$		$k_{1z}=\min[2.8*(e_1/d_0)-1.7, 1.4*(p_1/d_0)-1.7, 2.5]$
$k_{1z} > 0.0$	2,50 > 0,00	vérifié	
α_{bz} = 0,67	Coefficient pour le calcul de $F_{b,Rd}$		$\alpha_{bz}=\min[e_2/(3*d_0), f_{ub}/f_u, 1]$
$\alpha_{bz} > 0.0$	0,67 > 0,00	vérifié	
$F_{b,Rd1z}$ = 40,88 [kN]	Résistance d'un boulon en pression diamétrale		$F_{b,Rd1z}=k_{1z}*\alpha_{bz}*f_u*d*t_i/\gamma_{M2}$

Pression du boulon sur la platine

Direction x

k_{1x} = 2,50	Coefficient pour le calcul de $F_{b,Rd}$		$k_1=\min[2.8*(e_2/d_0)-1.7, 2.5]$
$k_{1x} > 0.0$	2,50 > 0,00	vérifié	
α_{bx} = 1,00	Coefficient dépendant de l'espacement des boulons		$\alpha_{bx}=\min[e_1/(3*d_0), p_1/(3*d_0)-0.25, f_{ub}/f_u, 1]$
$\alpha_{bx} > 0.0$	1,00 > 0,00	vérifié	

$F_{b,Rd2x}$ = 102,20 [kN]	Résistance de calcul à l'état limite de plastification de la paroi du trou		$F_{b,Rd2x}=k_1*\alpha_b*f_u*d*t_i/\gamma_{M2}$
Direction z			
k_{1z} = 2,50	Coefficient pour le calcul de $F_{b,Rd}$		$k_{1z}=\min[2.8*(e_1/d_0)-1.7, 1.4*(p_1/d_0)-1.7, 2.5]$
$k_{1z} > 0.0$	2,50 > 0,00	vérifié	
α_{bz} = 1,00	Coefficient pour le calcul de $F_{b,Rd}$		$\alpha_{bz}=\min[e_2/(3*d_0), f_{ub}/f_u, 1]$
$\alpha_{bz} > 0.0$	1,00 > 0,00	vérifié	
$F_{b,Rd2z}$ = 102,20 [kN]	Résistance d'un boulon en pression diamétrale		$F_{b,Rd2z}=k_{1z}*\alpha_{bz}*f_u*d*t_i/\gamma_{M2}$

VÉRIFICATION DE L'ASSEMBLAGE POUR LES EFFORTS AGISSANT SUR LES BOULONS

cisaillement des boulons

e =	13	[mm]	Excentricité de l'effort axial par rapport à l'axe des boulons	
M_0 =	-0,02	[kN*m]	Moment fléchissant réel	$M_0=N_{b1,Ed}*e$
F_{NSd} =	-0,46	[kN]	Force résultante dans le boulon due à l'influence de l'effort axial	$F_{NSd} = N_{b1,Ed}/n$
F_{MSd} =	-0,15	[kN]	Effort composant dans le boulon dû à l'influence du moment	$F_{MSd}=M_0*x_{max}/\Sigma x_i^2$
$F_{x,Ed}$ =	-0,46	[kN]	Effort de calcul total dans le boulon sur la direction x	$F_{x,Ed} = F_{NSd}$
$F_{z,Ed}$ =	-0,15	[kN]	Effort de calcul total dans le boulon sur la direction z	$F_{z,Ed} = F_{MSd}$
F_{Ed} =	0,48	[kN]	Effort tranchant résultant dans le boulon	$F_{Ed} = \sqrt{(F_{x,Ed}^2 + F_{z,Ed}^2)}$
F_{Rdx} =	61,32	[kN]	Résistance résultante de calcul du boulon sur la direction x	$F_{Rdx}=\min(F_{bRd1x}, F_{bRd2x})$
F_{Rdz} =	40,88	[kN]	Résistance résultante de calcul du boulon sur la direction z	$F_{Rdz}=\min(F_{bRd1z}, F_{bRd2z})$

$\lvert F_{x,Ed}\rvert \le F_{Rdx}$	|-0,46| < 61,32	vérifié	(0,01)
$\lvert F_{z,Ed}\rvert \le F_{Rdz}$	|-0,15| < 40,88	vérifié	(0,00)
$F_{Ed} \le F_{vRd}$	0,48 < 59,11	vérifié	(0,01)

VÉRIFICATION DE LA SECTION DE LA POUTRE AFFAIBLIE PAR LES TROUS

β_3 =	0,62		Coefficient de réduction	[Tableau 3.8]
A_{net} =	6,01	[cm²]	Aire de la section nette	$A_{net} = A - d_0*t_{f1}$
$N_{u,Rd}$ =	108,81	[kN]	Résistance de calcul de la section nette	$N_{u,Rd} = (\beta_3*A_{net}*f_{u1})/\gamma_{M2}$
$N_{pl,Rd}$ =	146,15	[kN]	Résistance de calcul plastique de la section brute	$N_{pl,Rd} = (0.9*A*f_{y1})/\gamma_{M2}$

$\lvert N_{b1,Ed}\rvert \le N_{u,Rd}$	|-1,38| < 108,81	vérifié	(0,01)
$\lvert N_{b1,Ed}\rvert \le N_{pl,Rd}$	|-1,38| < 146,15	vérifié	(0,01)

VÉRIFICATION DE LA BARRE POUR LE CISAILLEMENT DE BLOC

A_{nt} =	1,35	[cm²]	Aire nette de la zone de la section en traction	
A_{nv} =	7,95	[cm²]	Aire de la zone de la section en traction	
V_{effRd} =	127,57	[kN]	Résistance de calcul de la section affaiblie par les trous	$V_{effRd}=0.5*f_u*A_{nt}/\gamma_{M2} + (1/\sqrt{3})*f_y*A_{nv}/\gamma_{M0}$

$\lvert N_{b1,Ed}\rvert \le V_{effRd}$	|-1,38| < 127,57	vérifié	(0,01)

BARRE 2-4

RÉSISTANCE DES BOULONS

$F_{v,Rd}$ = 59,11 [kN]	Résistance de la tige d'un boulon au cisaillement		$F_{v,Rd}= 0.6*f_{ub}*A_v*m/\gamma_{M2}$

Pression du boulon sur la barre

Direction x			
k_{1x} = 2,50	Coefficient pour le calcul de $F_{b,Rd}$		$k_{1x}=\min[2.8*(e_2/d_0)-1.7, 2.5]$
$k_{1x} > 0.0$	2,50 > 0,00	vérifié	
α_{bx} = 0,89	Coefficient dépendant de l'espacement des boulons		$\alpha_{bx}=\min[e_1/(3*d_0), f_{ub}/f_u, 1]$
$\alpha_{bx} > 0.0$	0,89 > 0,00	vérifié	
$F_{b,Rd1x}$ = 54,51 [kN]	Résistance de calcul à l'état limite de plastification de la paroi du trou		$F_{b,Rd1x}=k_{1x}*\alpha_{bx}*f_u*d*t_i/\gamma_{M2}$
Direction z			
k_{1z} = 2,50	Coefficient pour le calcul de $F_{b,Rd}$		$k_{1z}=\min[2.8*(e_1/d_0)-1.7, 2.5]$
$k_{1z} > 0.0$	2,50 > 0,00	vérifié	

$F_{b,Rd2x}$ = 3,64	[kN]	Résistance de calcul à l'état limite de plastification de la paroi du trou		$F_{b,Rd2x}=k_1*\alpha_b*f_u*d*t_i/\gamma_{M2}$

Direction z

k_{1z} =	0,08		Coefficient pour le calcul de $F_{b,Rd}$		$k_{1z}=\min[2.8*(e_1/d_0)-1.7, 2.5]$
k_{1z} > 0.0			0,08 > 0,00	vérifié	
α_{bz} =	0,25		Coefficient pour le calcul de $F_{b,Rd}$		$\alpha_{bz}=\min[e_2/(3*d_0), f_{ub}/f_u, 1]$
α_{bz} > 0.0			0,25 > 0,00	vérifié	
$F_{b,Rd2z}$ =	0,80	[kN]	Résistance d'un boulon en pression diamétrale		$F_{b,Rd2z}=k_{1z}*\alpha_{bz}*f_u*d*t_i/\gamma_{M2}$

VÉRIFICATION DE L'ASSEMBLAGE POUR LES EFFORTS AGISSANT SUR LES BOULONS

cisaillement des boulons

e =	13	[mm]	Excentricité de l'effort axial par rapport à l'axe des boulons		
M_0 =	0,00	[kN*m]	Moment fléchissant réel		$M_0=N_{b2,Ed}*e$
F_{NSd} =	0,32	[kN]	Force résultante dans le boulon due à l'influence de l'effort axial		$F_{NSd} = N_{b2,Ed}/n$
F_{MSd} =	0,00	[kN]	Effort composant dans le boulon dû à l'influence du moment		$F_{MSd}=M_0*x_{max}/\Sigma x_i^2$
$F_{x,Ed}$ =	0,32	[kN]	Effort de calcul total dans le boulon sur la direction x		$F_{x,Ed} = F_{NSd}$
$F_{z,Ed}$ =	0,00	[kN]	Effort de calcul total dans le boulon sur la direction z		$F_{z,Ed} = F_{MSd}$
F_{Ed} =	0,32	[kN]	Effort tranchant résultant dans le boulon		$F_{Ed} = \sqrt{(F_{x,Ed}^2 + F_{z,Ed}^2)}$
F_{Rdx} =	3,64	[kN]	Résistance résultante de calcul du boulon sur la direction x		$F_{Rdx}=\min(F_{bRd1x}, F_{bRd2x})$
F_{Rdz} =	0,80	[kN]	Résistance résultante de calcul du boulon sur la direction z		$F_{Rdz}=\min(F_{bRd1z}, F_{bRd2z})$
$\lvert F_{x,Ed}\rvert \le F_{Rdx}$			|0,32| < 3,64	vérifié	(0,09)
$\lvert F_{z,Ed}\rvert \le F_{Rdz}$			|0,00| < 0,80	vérifié	(0,00)
$F_{Ed} \le F_{vRd}$			0,32 < 59,11	vérifié	(0,01)

VÉRIFICATION DE LA SECTION DE LA POUTRE AFFAIBLIE PAR LES TROUS

$N_{u,Rd}$ =	78,84	[kN]	Résistance de calcul de la section nette		$N_{u,Rd} = [2*(e_2-0.5*d_0)*t_{f2}*f_{u2}]/\gamma_{M2}$
$N_{pl,Rd}$ =	146,15	[kN]	Résistance de calcul plastique de la section brute		$N_{pl,Rd} = (0.9*A*f_{y2})/\gamma_{M2}$
$\lvert N_{b2,Ed}\rvert \le N_{u,Rd}$			|0,32| < 78,84	vérifié	(0,00)
$\lvert N_{b2,Ed}\rvert \le N_{pl,Rd}$			|0,32| < 146,15	vérifié	(0,00)

VÉRIFICATION DE LA BARRE POUR LE CISAILLEMENT DE BLOC

A_{nt} =	1,35	[cm^2]	Aire nette de la zone de la section en traction		
A_{nv} =	1,95	[cm^2]	Aire de la zone de la section en traction		
V_{effRd} =	46,17	[kN]	Résistance de calcul de la section affaiblie par les trous		$V_{effRd}=0.5*f_u*A_{nt}/\gamma_{M2} + (1/\sqrt{3})*f_y*A_{nv}/\gamma_{M0}$
$\lvert N_{b2,Ed}\rvert \le V_{effRd}$			|0,32| < 46,17	vérifié	(0,01)

BARRE 3

RÉSISTANCE DES BOULONS

$F_{v,Rd}$ =	59,11	[kN]	Résistance de la tige d'un boulon au cisaillement	$F_{v,Rd}= 0.6*f_{ub}*A_v*m/\gamma_{M2}$

Pression du boulon sur la barre

Direction x

k_{1x} =	2,50	Coefficient pour le calcul de $F_{b,Rd}$	$k_{1x}=\min[2.8*(e_2/d_0)-1.7, 2.5]$

$F_{b,Rd1z}$ =	40,88	[kN]	Résistance d'un boulon en pression diamétrale	$F_{b,Rd1z}=k_{1z}*\alpha_{bz}*f_u*d*t_i/\gamma_{M2}$

Pression du boulon sur la platine

Direction x

k_{1x} =	2,50		Coefficient pour le calcul de $F_{b,Rd}$	$k_1=\min[2.8*(e_2/d_0)-1.7, 2.5]$
$k_{1x} > 0.0$		2,50 > 0,00	vérifié	
α_{bx} =	1,00		Coefficient dépendant de l'espacement des boulons	$\alpha_{bx}=\min[e_1/(3*d_0), p_1/(3*d_0)-0.25, f_{ub}/f_u, 1]$
$\alpha_{bx} > 0.0$		1,00 > 0,00	vérifié	
$F_{b,Rd2x}$ =	102,20	[kN]	Résistance de calcul à l'état limite de plastification de la paroi du trou	$F_{b,Rd2x}=k_1*\alpha_b*f_u*d*t_i/\gamma_{M2}$

Direction z

k_{1z} =	2,50		Coefficient pour le calcul de $F_{b,Rd}$	$k_{1z}=\min[2.8*(e_1/d_0)-1.7, 1.4*(p_1/d_0)-1.7, 2.5]$
$k_{1z} > 0.0$		2,50 > 0,00	vérifié	
α_{bz} =	1,00		Coefficient pour le calcul de $F_{b,Rd}$	$\alpha_{bz}=\min[e_2/(3*d_0), f_{ub}/f_u, 1]$
$\alpha_{bz} > 0.0$		1,00 > 0,00	vérifié	
$F_{b,Rd2z}$ =	102,20	[kN]	Résistance d'un boulon en pression diamétrale	$F_{b,Rd2z}=k_{1z}*\alpha_{bz}*f_u*d*t_i/\gamma_{M2}$

VÉRIFICATION DE L'ASSEMBLAGE POUR LES EFFORTS AGISSANT SUR LES BOULONS

cisaillement des boulons

e =	13	[mm]	Excentricité de l'effort axial par rapport à l'axe des boulons	
M_0 =	-0,01	[kN*m]	Moment fléchissant réel	$M_0=N_{b3,Ed}*e$
F_{NSd} =	-0,26	[kN]	Force résultante dans le boulon due à l'influence de l'effort axial	$F_{NSd} = N_{b3,Ed}/n$
F_{MSd} =	-0,09	[kN]	Effort composant dans le boulon dû à l'influence du moment	$F_{MSd}=M_0*x_{max}/\Sigma x_i^2$
$F_{x,Ed}$ =	-0,26	[kN]	Effort de calcul total dans le boulon sur la direction x	$F_{x,Ed} = F_{NSd}$
$F_{z,Ed}$ =	-0,09	[kN]	Effort de calcul total dans le boulon sur la direction z	$F_{z,Ed} = F_{MSd}$
F_{Ed} =	0,28	[kN]	Effort tranchant résultant dans le boulon	$F_{Ed} = \sqrt{(F_{x,Ed}^2 + F_{z,Ed}^2)}$
F_{Rdx} =	61,32	[kN]	Résistance résultante de calcul du boulon sur la direction x	$F_{Rdx}=\min(F_{bRd1x}, F_{bRd2x})$
F_{Rdz} =	40,88	[kN]	Résistance résultante de calcul du boulon sur la direction z	$F_{Rdz}=\min(F_{bRd1z}, F_{bRd2z})$
$\lvert F_{x,Ed}\rvert \le F_{Rdx}$		|-0,26| < 61,32	vérifié	(0,00)
$\lvert F_{z,Ed}\rvert \le F_{Rdz}$		|-0,09| < 40,88	vérifié	(0,00)
$F_{Ed} \le F_{vRd}$		0,28 < 59,11	vérifié	(0,00)

VÉRIFICATION DE LA SECTION DE LA POUTRE AFFAIBLIE PAR LES TROUS

β_3 =	0,62		Coefficient de réduction	[Tableau 3.8]
A_{net} =	6,01	[cm²]	Aire de la section nette	$A_{net} = A - d_0*t_{f3}$
$N_{u,Rd}$ =	108,81	[kN]	Résistance de calcul de la section nette	$N_{u,Rd} = (\beta_3*A_{net}*f_{u3})/\gamma_{M2}$
$N_{pl,Rd}$ =	146,15	[kN]	Résistance de calcul plastique de la section brute	$N_{pl,Rd} = (0.9*A*f_{y3})/\gamma_{M2}$
$\lvert N_{b3,Ed}\rvert \le N_{u,Rd}$		|-0,79| < 108,81	vérifié	(0,01)
$\lvert N_{b3,Ed}\rvert \le N_{pl,Rd}$		|-0,79| < 146,15	vérifié	(0,01)

VÉRIFICATION DE LA BARRE POUR LE CISAILLEMENT DE BLOC

A_{nt} =	1,35	[cm²]	Aire nette de la zone de la section en traction	
A_{nv} =	7,95	[cm²]	Aire de la zone de la section en traction	
V_{effRd} =	127,57	[kN]	Résistance de calcul de la section affaiblie par les trous	$V_{effRd}=0.5*f_u*A_{nt}/\gamma_{M2} + (1/\sqrt{3})*f_y*A_{nv}/\gamma_{M0}$
$\lvert N_{b3,Ed}\rvert \le V_{effRd}$		|-0,79| < 127,57	vérifié	(0,01)

REMARQUES

Entraxe des boulons sur la barre 2 trop faible 0 [mm] < 33 [mm]
Boulon hors de la platine pour la barre 2
Boulon hors de la platine pour la barre 4

Assemblage satisfaisant vis à vis de la Norme Ratio 0,09

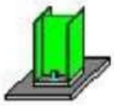

Robot Structural Analysis Professional 2024

Calcul du Pied de Poteau articulé

Eurocode 3: NF EN 1993-1-8:2005/NA:2007/AC:2009 + CEB

Design Guide: Design of fastenings in concrete

OK

Ratio
0,95

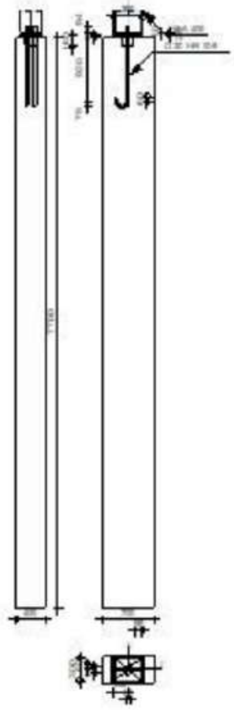

GÉNÉRAL

Assemblage N°:	6
Nom de l'assemblage:	Pied de poteau articulé
Noeud de la structure:	13
Barres de la structure:	11

GÉOMÉTRIE

POTEAU

Profilé: HEA 400
Barre N°: 11

L_c =	0,70	[m]	Longueur du poteau
α =	0,0	[Deg]	Angle d'inclinaison
h_c =	390	[mm]	Hauteur de la section du poteau

PLATINE DE PRESCELLEMENT

l_{pd} =	390	[mm]	Longueur
b_{pd} =	300	[mm]	Largeur
t_{pd} =	25	[mm]	Epaisseur
Matériau:	ACIER E24		
f_{ypd} =	235,00	[MPa]	Résistance
f_{upd} =	365,00	[MPa]	Résistance ultime du matériau

ANCRAGE

Le plan de cisaillement passe par la partie NON FILETÉE du boulon

Classe =	HR 10.9		Classe de tiges d'ancrage
f_{yb} =	900,00	[MPa]	Limite de plasticité du matériau du boulon
f_{ub} =	1000,00	[MPa]	Résistance du matériau du boulon à la traction
d =	30	[mm]	Diamètre du boulon
A_s =	5,61	[cm^2]	Aire de la section efficace du boulon
A_v =	7,07	[cm^2]	Aire de la section du boulon
n =	2		Nombre de rangéss des boulons
e_V =	104	[mm]	Entraxe

Dimensions des tiges d'ancrage

L_1 =	94	[mm]
L_2 =	920	[mm]
L_3 =	150	[mm]
L_4 =	60	[mm]

Platine

l_{wd} =	60	[mm]	Longueur
b_{wd} =	60	[mm]	Largeur
t_{wd} =	10	[mm]	Epaisseur

BÊCHE

Profilé:	HEA 160		
l_w =	160	[mm]	Longueur
Matériau:	ACIER E24		
f_{yw} =	235,00	[MPa]	Résistance

COEFFICIENTS DE MATÉRIAU

γ_{M0} =	1,00	Coefficient de sécurité partiel
γ_{M2} =	1,25	Coefficient de sécurité partiel
γ_C =	1,50	Coefficient de sécurité partiel

SEMELLE ISOLÉE

$C_{f,d}$ = 0,30 Coef. de frottement entre la plaque d'assise et le beton

SOUDURES

a_p =	7	[mm]	Plaque principale du pied de poteau
a_w =	4	[mm]	Bêche

EFFORTS

Cas: 5: W

$N_{j,Ed}$ =	27,75	[kN]	Effort axial
$V_{j,Ed,y}$ =	0,04	[kN]	Effort tranchant
$V_{j,Ed,z}$ =	-67,64	[kN]	Effort tranchant

RÉSULTATS

ZONE TENDUE

RUPTURE DU BOULON D'ANCRAGE

A_b =	5,61	[cm^2]	Aire de section efficace du boulon	[Tableau 3.4]
f_{ub} =	1000,00	[MPa]	Résistance du matériau du boulon à la traction	[Tableau 3.4]
Beta =	0,85		Coefficient de réduction de la résistance du boulon	[3.6.1.(3)]

$F_{t,Rd,s1} = beta*0.9*f_{ub}*A_b/\gamma_{M2}$

$F_{t,Rd,s1}$ =	343,33	[kN]	Résistance du boulon à la rupture	[Tableau 3.4]
γ_{Ms} =	1,20		Coefficient de sécurité partiel	CEB [3.2.3.2]
f_{yb} =	900,00	[MPa]	Limite de plasticité du matériau du boulon	CEB [9.2.2]

$F_{t,Rd,s2} = f_{yb}*A_b/\gamma_{Ms}$

$F_{t,Rd,s2}$ =	420,75	[kN]	Résistance du boulon à la rupture	CEB [9.2.2]

$F_{t,Rd,s} = \min(F_{t,Rd,s1},F_{t,Rd,s2})$

$F_{t,Rd,s}$ =	343,33	[kN]	Résistance du boulon à la rupture	

ARRACHEMENT DU BOULON D'ANCRAGE DU BETON

f_{ck} =	25,00	[MPa]	Résistance caractéristique du béton à la compression	EN 1992-1:[3.1.2]

$f_{ctd} = 0.7*0.3*f_{ck}^{2/3}/\gamma_C$

f_{ctd} =	1,20	[MPa]	Résistance de calcul à la traction	EN 1992-1:[8.4.2.(2)]
η_1 =	1,00		Coef. dépendant des conditions du bétonnage et de l'adhérence	EN 1992-1:[8.4.2.(2)]
η_2 =	1,00		Coef. dépendant du diamètre du boulon d'ancrage	EN 1992-1:[8.4.2.(2)]

$f_{bd} = 2.25*\eta_1*\eta_2*f_{ctd}$

f_{bd} =	2,69	[MPa]	Adhérence de calcul admissible	EN 1992-1:[8.4.2.(2)]
h_{ef} =	890	[mm]	Longueur effective du boulon d'ancrage	EN 1992-1:[8.4.2.(2)]

$F_{t,Rd,p} = \pi*d*h_{ef}*f_{bd}$

$F_{t,Rd,p}$ =	225,91	[kN]	Résistance de calc. pour le soulèvement	EN 1992-1:[8.4.2.(2)]

ARRACHEMENT DU CONE DE BETON

h_{ef} =	233	[mm]	Longueur effective du boulon d'ancrage	CEB [9.2.4]

$N_{Rk,c}^0 = 7.5[N^{0.5}/mm^{0.5}]*f_{ck}^{0.5}*h_{ef}^{1.5}$

$N_{Rk,c}^0 =$ 133,66 [kN] Résistance caractéristique du boulon d'ancrage CEB [9.2.4]
$s_{cr,N} =$ 700 [mm] Largeur critique du cône de béton CEB [9.2.4]
$c_{cr,N} =$ 350 [mm] Distance critique du bord de la fondation CEB [9.2.4]
$A_{c,N0} =$ 4900,00 [cm^2] Aire de surface maximale du cône CEB [9.2.4]
$A_{c,N} =$ 1400,00 [cm^2] Aire de surface réelle du cône CEB [9.2.4]
$\psi_{A,N} = A_{c,N}/A_{c,N0}$
$\psi_{A,N} =$ 0,29 Coef. dépendant de l'entraxe et de la pince des boulons d'ancrage CEB [9.2.4]
c = 148 [mm] Pince minimale boulon d'ancrage-extrémité CEB [9.2.4]
$\psi_{s,N} = 0.7 + 0.3*c/c_{cr.N} \leq 1.0$
$\psi_{s,N} =$ 0,83 Coef. dépendant du pince boulon d'ancrage-extrémité de la fondation CEB [9.2.4]
$\psi_{ec,N} =$ 1,00 Coef. dépendant de la répartition des efforts de traction dans les boulons d'ancrage CEB [9.2.4]
$\psi_{re,N} = 0.5 + h_{ef}[mm]/200 \leq 1.0$
$\psi_{re,N} =$ 1,00 Coef. dépendant de la densité du ferraillage dans la fondation CEB [9.2.4]
$\psi_{ucr,N} =$ 1,00 Coef. dépendant du degré de fissuration du béton CEB [9.2.4]
$\gamma_{Mc} =$ 2,16 Coefficient de sécurité partiel CEB [3.2.3.1]
$F_{t,Rd,c} = N_{Rk,c}^0*\psi_{A,N}*\psi_{s,N}*\psi_{ec,N}*\psi_{re,N}*\psi_{ucr,N}/\gamma_{Mc}$
$F_{t,Rd,c} =$ 14,62 [kN] Résistance de calcul du boulon d'ancrage à l'arrachement du cône de béton EN 1992-1:[8.4.2.(2)]

FENDAGE DU BETON

$h_{ef} =$ 890 [mm] Longueur effective du boulon d'ancrage CEB [9.2.5]
$N_{Rk,c}^0 = 7.5[N^{0.5}/mm^{0.5}]*f_{ck}^{0.5}*h_{ef}^{1.5}$
$N_{Rk,c}^0 =$ 995,67 [kN] Résistance de calc. pour le soulèvement CEB [9.2.5]
$s_{cr,N} =$ 1780 [mm] Largeur critique du cône de béton CEB [9.2.5]
$c_{cr,N} =$ 890 [mm] Distance critique du bord de la fondation CEB [9.2.5]
$A_{c,N0} =$ 31684,00 [cm^2] Aire de surface maximale du cône CEB [9.2.5]
$A_{c,N} =$ 1400,00 [cm^2] Aire de surface réelle du cône CEB [9.2.5]
$\psi_{A,N} = A_{c,N}/A_{c,N0}$
$\psi_{A,N} =$ 0,04 Coef. dépendant de l'entraxe et de la pince des boulons d'ancrage CEB [9.2.5]
c = 148 [mm] Pince minimale boulon d'ancrage-extrémité CEB [9.2.5]
$\psi_{s,N} = 0.7 + 0.3*c/c_{cr.N} \leq 1.0$
$\psi_{s,N} =$ 0,75 Coef. dépendant du pince boulon d'ancrage-extrémité de la fondation CEB [9.2.5]
$\psi_{ec,N} =$ 1,00 Coef. dépendant de la répartition des efforts de traction dans les boulons d'ancrage CEB [9.2.5]
$\psi_{re,N} = 0.5 + h_{ef}[mm]/200 \leq 1.0$
$\psi_{re,N} =$ 1,00 Coef. dépendant de la densité du ferraillage dans la fondation CEB [9.2.5]
$\psi_{ucr,N} =$ 1,00 Coef. dépendant du degré de fissuration du béton CEB [9.2.5]
$\psi_{h,N} = (h/(2*h_{ef}))^{2/3} \leq 1.2$
$\psi_{h,N} =$ 1,20 Coef. dépendant de la hauteur de la fondation CEB [9.2.5]
$\gamma_{M,sp} =$ 2,16 Coefficient de sécurité partiel CEB [3.2.3.1]
$F_{t,Rd,sp} = N_{Rk,c}^0*\psi_{A,N}*\psi_{s,N}*\psi_{ec,N}*\psi_{re,N}*\psi_{ucr,N}*\psi_{h,N}/\gamma_{M,sp}$
$F_{t,Rd,sp} =$ 18,33 [kN] Résistance de calcul du boulon d'ancrage au fendage du béton CEB [9.2.5]

RESISTANCE DU BOULON D'ANCRAGE A LA TRACTION

$F_{t,Rd} = \min(F_{t,Rd,s}, F_{t,Rd,p}, F_{t,Rd,c}, F_{t,Rd,sp})$
$F_{t,Rd} =$ 14,62 [kN] Résistance du boulon d'ancrage à traction

FLEXION DE LA PLAQUE DE BASE

$l_{eff,1} =$ 242 [mm] Longueur effective pour une seule ligne de boulons pour le mode 1 [6.2.6.5]
$l_{eff,2} =$ 275 [mm] Longueur effective pour une seule ligne de boulons pour le mode 2 [6.2.6.5]
m = 39 [mm] Pince boulon-bord de renforcement [6.2.6.5]
$M_{pl,1,Rd} =$ 8,90 [kN*m] Résistance plastique de la dalle pour le mode 1 [6.2.4]
$M_{pl,2,Rd} =$ 10,09 [kN*m] Résistance plastique de la dalle pour le mode 2 [6.2.4]
$F_{T,1,Rd} =$ 922,84 [kN] Résistance de la dalle pour le mode 1 [6.2.4]
$F_{T,2,Rd} =$ 221,32 [kN] Résistance de la dalle pour le mode 2 [6.2.4]
$F_{T,3,Rd} =$ 29,24 [kN] Résistance de la dalle pour le mode 3 [6.2.4]
$F_{t,pl,Rd} = \min(F_{T,1,Rd}, F_{T,2,Rd}, F_{T,3,Rd})$
$F_{t,pl,Rd} =$ 29,24 [kN] Résistance de la dalle pour le mode à la traction [6.2.4]

RESISTANCE DE L'AME DU POTEAU A LA TRACTION

t_{wc} =	11	[mm]	Epaisseur efficace de l'âme du poteau	[6.2.6.3.(8)]
$b_{eff,t,wc}$ =	242	[mm]	Largeur efficace de l'âme à la traction	[6.2.6.3.(2)]
A_{vc} =	57,33	[cm^2]	Aire de la section au cisaillement	EN1993-1-1:[6.2.6.(3)]
ω =	0,88		Coefficient réducteur pour l'interaction avec le cisaillement	[6.2.6.3.(4)]

$F_{t,wc,Rd} = \omega\ b_{eff,t,wc}\ t_{wc}\ f_{yc}\ /\ \gamma_{M0}$

$F_{t,wc,Rd}$ =	553,60	[kN]	Résistance de l'âme du poteau	[6.2.6.3.(1)]

RESISTANCES DE SEMELLE DANS LA ZONE TENDUE

$N_{j,Rd}$ =	29,24	[kN]	Résistance de la semelle à la traction axiale	[6.2.8.3]

CONTRÔLE DE LA RÉSISTANCE DE L'ASSEMBLAGE

$N_{j,Ed} / N_{j,Rd} \le 1{,}0$ (6.24)	0,95 < 1,00	vérifié	(0,95)

CISAILLEMENT

PRESSION DU BOULON D'ANCRAGE SUR LA PLAQUE D'ASSISE

Cisaillement par l'effort $V_{j,Ed,y}$

$\alpha_{d,y}$ =	0,83	Coef. d'emplacement des boulons en direction du cisaillement	[Tableau 3.4]
$\alpha_{b,y}$ =	0,83	Coef. pour les calculs de la résistance $F_{1,vb,Rd}$	[Tableau 3.4]
$k_{1,y}$ =	2,50	Coef. d'emplacement des boulons perpendiculairement à la direction du cisaillement	[Tableau 3.4]

$F_{1,vb,Rd,y} = k_{1,y}*\alpha_{b,y}*f_{up}*d*t_p\ /\ \gamma_{M2}$

$F_{1,vb,Rd,y}$ =	456,25	[kN]	Résistance du boulon d'ancrage à la pression sur la plaque d'assise	[6.2.2.(7)]

Cisaillement par l'effort $V_{j,Ed,z}$

$\alpha_{d,z}$ =	0,79	Coef. d'emplacement des boulons en direction du cisaillement	[Tableau 3.4]
$\alpha_{b,z}$ =	0,79	Coef. pour les calculs de la résistance $F_{1,vb,Rd}$	[Tableau 3.4]
$k_{1,z}$ =	2,50	Coef. d'emplacement des boulons perpendiculairement à la direction du cisaillement	[Tableau 3.4]

$F_{1,vb,Rd,z} = k_{1,z}*\alpha_{b,z}*f_{up}*d*t_p\ /\ \gamma_{M2}$

$F_{1,vb,Rd,z}$ =	433,44	[kN]	Résistance du boulon d'ancrage à la pression sur la plaque d'assise	[6.2.2.(7)]

CISAILLEMENT DU BOULON D'ANCRAGE

α_b =	0,25		Coef. pour les calculs de la résistance $F_{2,vb,Rd}$	[6.2.2.(7)]
A_{vb} =	7,07	[cm^2]	Aire de la section du boulon	[6.2.2.(7)]
f_{ub} =	1000,00	[MPa]	Résistance du matériau du boulon à la traction	[6.2.2.(7)]
γ_{M2} =	1,25		Coefficient de sécurité partiel	[6.2.2.(7)]

$F_{2,vb,Rd} = \alpha_b*f_{ub}*A_{vb}/\gamma_{M2}$

$F_{2,vb,Rd}$ =	140,24	[kN]	Résistance du boulon au cisaillement - sans bras de levier	[6.2.2.(7)]
α_M =	2,00		Coef. dépendant de l'ancrage du boulon dans la fondation	CEB [9.3.2.2]
$M_{Rk,s}$ =	3,46	[kN*m]	Résistance caractéristique de l'ancrage à la flexion	CEB [9.3.2.2]
l_{sm} =	58	[mm]	Longueur du bras de levier	CEB [9.3.2.2]
γ_{Ms} =	1,20		Coefficient de sécurité partiel	CEB [3.2.3.2]

$F_{v,Rd,sm} = \alpha_M*M_{Rk,s}/(l_{sm}*\gamma_{Ms})$

$F_{v,Rd,sm}$ =	100,30	[kN]	Résistance du boulon au cisaillement - avec bras de levier	CEB [9.3.1]

RUPTURE DU BETON PAR EFFET DE LEVIER

$N_{Rk,c}$ =	31,58	[kN]	Résistance de calc. pour le soulèvement	CEB [9.2.4]
k_3 =	2,00		Coef. dépendant de la longueur de l'ancrage	CEB [9.3.3]
γ_{Mc} =	2,16		Coefficient de sécurité partiel	CEB [3.2.3.1]

$F_{v,Rd,cp} = k_3*N_{Rk,c}/\gamma_{Mc}$

$F_{v,Rd,cp}$ =	29,24	[kN]	Résistance du béton à l'effet de levier	CEB [9.3.1]

ECRASEMENT DU BORD DU BETON

Cisaillement par l'effort $V_{j,Ed,y}$

$V_{Rk,c,y}^0$ =	63,26	[kN]	Résistance caractéristique du boulon d'ancrage	CEB [9.3.4.(a)]
$\psi_{A,V,y}$ =	0,70		Coef. dépendant de l'entraxe et de la pince des boulons d'ancrage	CEB [9.3.4]
$\psi_{h,V,y}$ =	1,00		Coef. dépendant de l'épaisseur de la fondation	CEB [9.3.4.(c)]

$V_{Rk,c,z}^0 =$	67,80	[kN]	Résistance caractéristique du boulon d'ancrage	CEB [9.3.4.(a)]
$\psi_{A,V,z} =$	0,64		Coef. dépendant de l'entraxe et de la pince des boulons d'ancrage	CEB [9.3.4]
$\psi_{h,V,z} =$	1,00		Coef. dépendant de l'épaisseur de la fondation	CEB [9.3.4.(c)]
$\psi_{s,V,z} =$	0,89		Coef. d'influence des bords parallèles à l'effort de cisaillement	CEB [9.3.4.(d)]
$\psi_{ec,V,z} =$	1,00		Coef. d'irrégularité de la répartition de l'effort tranchant sur le boulon d'ancrage	CEB [9.3.4.(e)]
$\psi_{\alpha,V,z} =$	1,00		Coef. dépendant de l'angle d'action de l'effort tranchant	CEB [9.3.4.(f)]
$\psi_{ucr,V,z} =$	1,00		Coef. dépendant du mode de ferraillage du bord de la fondation	CEB [9.3.4.(g)]
$\gamma_{Mc} =$	2,16		Coefficient de sécurité partiel	CEB [3.2.3.1]

$F_{v,Rd,c,z} = V_{Rk,c,z}^0 * \psi_{A,V,z} * \psi_{h,V,z} * \psi_{s,V,z} * \psi_{ec,V,z} * \psi_{\alpha,V,z} * \psi_{ucr,V,z} / \gamma_{Mc}$

$F_{v,Rd,c,z} =$ 17,80 [kN] Résistance du béton pour l'écrasement du bord CEB [9.3.1]

GLISSEMENT DE LA SEMELLE

$C_{f,d} =$	0,30		Coef. de frottement entre la plaque d'assise et le béton	[6.2.2.(6)]
$N_{c,Ed} =$	0,00	[kN]	Effort de compression	[6.2.2.(6)]

$F_{f,Rd} = C_{f,d} * N_{c,Ed}$

$F_{f,Rd} =$ 0,00 [kN] Résistance au glissement [6.2.2.(6)]

CONTACT DE LA CALE D'ARRET AVEC BETON

$F_{v,Rd,wg,y} = 1.4 * l_w * b_{wy} * f_{ck} / \gamma_c$

$F_{v,Rd,wg,y} =$ 373,33 [kN] Résistance au contact de la cale d'arrêt avec béton

$F_{v,Rd,wg,z} = 1.4 * l_w * b_{wz} * f_{ck} / \gamma_c$

$F_{v,Rd,wg,z} =$ 205,33 [kN] Résistance au contact de la cale d'arrêt avec béton

CONTROLE DU CISAILLEMENT

$V_{j,Rd,y} = n_b * \min(F_{1,vb,Rd,y}, F_{2,vb,Rd}, F_{v,Rd,sm}, F_{v,Rd,cp}, F_{v,Rd,c,y}) + F_{v,Rd,wg,y} + F_{f,Rd}$

$V_{j,Rd,y} =$ 410,53 [kN] Résistance de l'assemblage au cisaillement CEB [9.3.1]

$V_{j,Ed,y} / V_{j,Rd,y} \leq 1,0$	0,00 < 1,00	vérifié	(0,00)

$V_{j,Rd,z} = n_b * \min(F_{1,vb,Rd,z}, F_{2,vb,Rd}, F_{v,Rd,sm}, F_{v,Rd,cp}, F_{v,Rd,c,z}) + F_{v,Rd,wg,z} + F_{f,Rd}$

$V_{j,Rd,z} =$ 240,94 [kN] Résistance de l'assemblage au cisaillement CEB [9.3.1]

$V_{j,Ed,z} / V_{j,Rd,z} \leq 1,0$	0,28 < 1,00	vérifié	(0,28)
$V_{j,Ed,y} / V_{j,Rd,y} + V_{j,Ed,z} / V_{j,Rd,z} \leq 1,0$	0,28 < 1,00	vérifié	(0,28)

SOUDURES ENTRE LE POTEAU ET LA PLAQUE D'ASSISE

$\sigma_\perp =$	1,49	[MPa]	Contrainte normale dans la soudure	[4.5.3.(7)]
$\tau_\perp =$	1,49	[MPa]	Contrainte tengentielle perpendiculaire	[4.5.3.(7)]
$\tau_{yII} =$	0,01	[MPa]	Contrainte tengentielle parallèle à $V_{j,Ed,y}$	[4.5.3.(7)]
$\tau_{zII} =$	-13,73	[MPa]	Contrainte tengentielle parallèle à $V_{j,Ed,z}$	[4.5.3.(7)]
$\beta_W =$	0,85		Coefficient dépendant de la résistance	[4.5.3.(7)]

$\sigma_\perp / (0.9 * f_u / \gamma_{M2}) \leq 1.0$ (4.1)	0,01 < 1,00	vérifié	(0,01)
$\sqrt{(\sigma_\perp^2 + 3.0 (\tau_{yII}^2 + \tau_\perp^2))} / (f_u / (\beta_W * \gamma_{M2})) \leq 1.0$ (4.1)	0,01 < 1,00	vérifié	(0,01)
$\sqrt{(\sigma_\perp^2 + 3.0 (\tau_{zII}^2 + \tau_\perp^2))} / (f_u / (\beta_W * \gamma_{M2})) \leq 1.0$ (4.1)	0,07 < 1,00	vérifié	(0,07)

COMPOSANT LE PLUS FAIBLE:

FONDATION A L'ARRACHEMENT DU CONE DE BETON

REMARQUES

Rayon de courbure de l'ancrage trop faible.	75 [mm] < 90 [mm]
Segment L4 du boulon d'ancrage à crosse trop court.	60 [mm] < 150 [mm]

Assemblage satisfaisant vis à vis de la Norme Ratio 0,95